ARTICULAR CARTILAGE- AND SYNOVIOCYTE-BINDING SMALL MOLECULE DRUG DELIVERY SYSTEM FOR THE INTRA-ARTICULAR TREATMENT OF OSTEOARTHRITIS

A Dissertation
Presented to
The Academic Faculty

By

Lina María Mancipe Castro

In Partial Fulfillment
of the Requirements for the Degree
Doctor of Philosophy in Bioengineering

Georgia Institute of Technology

August 2020

ARTICULAR CARTILAGE- AND SYNOVIOCYTE-BINDING SMALL MOLECULE DRUG DELIVERY SYSTEM FOR THE INTRA-ARTICULAR TREATMENT OF OSTEOARTHRITIS

Approved by:

Dr. Andrés J. García, Advisor
George W. Woodruff School of Mechanical Engineering
Georgia Institute of Technology

Dr. Robert E. Guldberg, Co-advisor
Phil and Penny Knight Campus for Accelerating Scientific Impact
University of Oregon

Dr. Susan Thomas
George W. Woodruff School of Mechanical Engineering
Georgia Institute of Technology

Dr. Nick Willett
School of Medicine, Department of Orthopaedics
Emory University

Dr. James Dahlman
Wallace H. Coulter Department of Biomedical Engineering
Georgia Institute of Technology

Date Approved: July **07**, 2020

No hay mal que dure cien años, ni cuerpo que los resista

Cultura Popular

A mis padres Olga Lucía Castro y Germán Mancipe, a mi hermana Laura Mancipe y mi abuelita Fanny Burbano, quienes rieron y lloraron conmigo durante este proceso. Por el sacrificio tan grande que hicimos como familia, por todos los abrazos que no nos dimos durante 5 años, por escuchar cada noche mis historias y por siempre levantarme cada vez que caí. Todo el esfuerzo fue por ustedes, porque nunca hubiera podido lograrlo sin su amor y apoyo incondicional.

ACKNOWLEDGEMENTS

When I came to graduate school, I remember having so many expectations and dreams about the next five years and my professional life after graduating. I knew it was going to be an intellectual challenge, but what I did not know was that doing a PhD at one of the most prestigious engineering schools in the world, immersed in a completely new culture, was going to question my perception of the world and challenge me in every aspect of my life. There has been a lot of people who have shaped my path and attitude throughout this journey and it would be impossible to express in few words how grateful I am to each one of them. To family, friends, colleagues and mentors, thank you for your unconditional support.

I want to thank my advisor Dr. Robert Guldberg for believing in my potential since the first time we met. Also, I want to thank my co-advisor Dr. Andrés García for welcoming me into his lab. To Bob, Andrés and my thesis committee members, Dr. Nick Willett, Dr. Susan Thomas and Dr. James Dahlman, thank you for your support and guidance throughout the development of my thesis project. I also appreciate the help and guidance I received from my lab mates in both, Guldberg and García Labs, specially Casey Vantucci, Gilad Doron, Marissa Ruhele and Brett Klosterhoff for their help with surgeries and for keeping a united Guldberg Lab at Georgia Tech. I want to extend a special ”thank you” to those colleagues that became good friends and who were always there for me: Woojin Han, Ricardo Cruz, Rachit Agarwal, Ramesh Subbiah and Adriana Mulero.

I also want to acknowledge that nothing would have been possible without the excellent formation I received at my Alma Mater, where I learned the technical and

personal skills needed to embark in this journey. I am proud and honored to be part of the first generation of Biomedical Engineers at La Universidad de los Andes and grateful for belonging to this amazing BME family. I want to thank professors Juan Carlos Briceñ, Juan Manuel Cordovez, Mario Valderrama, Diana Marcela Tabima and Diana Gaitán for showing me how to be an excellent researcher, for sharing their passion for making Colombia a better place, for teaching me the importance of always remembering and being proud of where I came from and for making me feel I will always have a home at Uniandes-IBIO.

My experience as a graduate student was nothing like I imagined. There were way more difficulties than expected and I grew as a person more than I could have ever imagined. Having to deal with loneliness and depression, being far away from my family, adapting to a new culture, changing laboratories and research projects in the middle of my PhD, recovering form a knee surgery and realizing I need another one in the other leg, were all experiences that shaped my character and thought me that life will be constantly challenging me and offering opportunities to grow and become a better version of myself. I could have never survived to these experiences alone and I would like to show my gratitude to my family and all the friends that picked me up every time I fell.

Para mi familia, fue un sacrificio enorme estar separados solo para que yo pudiera perseguir mis sueños. Todos nuestros corazones se rompían cada vez que nos despedíamos o celebrábamos nuestros cumpleaños o logros a través de una pantalla. Hoy puedo decir que estas experiencias nos hicieron una familia más fuerte y unida. Estar lejos me hizo aprovechar al máximo los pocos días que estaba en casa, apreciar mucho más esos abrazos que no podía sentir en todo el año, valorar cada día más mi familia y reconocer que es el pilar que me sostiene.

Gracias a mis papás Olga Lucía Castro y Germán Darío Mancipe, a mi hermana Laura Daniela Mancipe y a mi abuelita Fanny Burbano por su apoyo incondicional, por siempre creer que lo podía lograr y por darme la certeza que si decidía no continuar, ellos estarían igual de orgullosos.

Quiero agradecerle a mi papá por recordarme en los momentos más difíciles que yo podía lograr todo lo que me propusiera, por hacerme ver que así como subir y bajar de la caja de archivos me daba miedo cuando era una bebé, el doctorado era igual y también iba a lograr llegar a la cima. Habría sido imposible lidiar con la soledad sin las llamadas constantes a mi mamá, quien se volvió esclava del celular para poder hablar conmigo 24/7. Gracias por acompañarme todas las mañnas camino al laboratorio y todas las noches antes de dormir. Quiero agradecerle a mi hermana por hacerme ver todo más simple de lo que parecía, por apoyarme cuando las cosas salían mal y por celebrar como propio cada uno de mis pequeños logros. Gracias por ser mi asesora de imagen y la diseñadora de todas las figuras de mis artículos (y de los que vendrán jaja). Quiero agradecerle a la vida por permitirme disfrutar de mi abuelita y hacerla parte de esta experiencia. Muchas gracias por rezar todo el día por mi, mis experimentos y mis ratas. Aunque no creo en dios, estoy convencida que toda la energía positiva que me enviabas me hizo más fuerte y resiliente.

También quiero agradecer a mi familia por ser los mejores asesores de investigación. Aunque ninguno es científico y mi hermana ni siquiera entienede la anatomía de la rodilla de un pollo, siempre se preocuparon por entender cada detalle de mis experimentos. Gracias por proponer soluciones cuando nada me salía bien, que de hecho muchas veces fueron un éxito. Muchas gracias por consentirme tanto, por llorar y celebrar conmigo mis caídas y logros, por hacerme la

mejor comida del mundo cuando iba a Colombia en navidad, por dejarme estar como un koala todo el día recargando los abrazos para el siguiente año, por el apoyo incondicional y mucho mucho más.

I also want to thank all my friends who supported me and cheered me up when I needed. I want to specially acknowledge Diana Marcela Gaitán who, despite being so far away, always understood my struggles and offered me her advice and guidance throughout the hardest times. I still have no idea what super powers she has, but she would always comfort me during every anxiety or panic attack and made me feel hopeful and capable. I am also very thankful for all the support I received from my college friends Sthephanie Colmenares, Estefany Pinto, Paula Flórez and Juliana Jaramillo.

Finally, this would not have been possible without the support of my ”Latino Gang” at Georgia Tech, I want to thank all my friends for keeping me sane, for all the happy hours and parties. I want to thank Asta (my only ”gringo” friend) for showing me the value of humility, for hosting every Colombian Independence Day celebration and for offering me such a beautiful friendship. I am specially grateful to Fernando Patiño, Oliver Giraldo and Leonardo García for being my family away from home, for helping me recover from my knee surgery and rescuing me from the darkest places every time I fell. I also want to extend my gratitude to Diego Osorio, Mónica Sierra, Jorge M. Lozano, Andrés Castro and Ana Mora for planning something fun to do every weekend, for every lunch I did not have to take in front of a computer pretending to be working and for reminding me that life is much more than work. To Fernando, for helping me overcome my fears and be a stronger woman, for believing in me, specially when I did not, and always highlighting the brightest side, thank you!

TABLE OF CONTENTS

Acknowledgments v

List of Tables xiv

List of Figures xv

List of Symbols xvii

Summary xix

Chapter 1:Introduction 1

1.1 Specific Aim 1 3

1.2 Specific Aim 2 3

1.3 Specific Aim 3 4

Chapter 2:Background 6

2.1 Osteoarthritis (OA) 6

2.1.1 Prevalence 6

2.1.2 Disease progression 6

2.2 Current clinical treatments for osteoarthritis 9

2.2.1 Non-pharmacological management 9

2.2.2 Pharmacological management 9

2.3 Novel targets for OA treatment and drug candidates 12
2.4 Intra-articular (IA) drug delivery strategies in OA 13
2.4.1 Hydrogels 13
2.4.2 Liposomes 15
2.4.3 Nanoparticles and microparticles 16
2.5 The importance of targeting for IA drug delivery 16
2.5.1 Cartilage targeting 18
2.5.2 Synovial membrane targeting 19
2.6 Poly(ethylene glycol) (PEG) microgels 21
2.7 Medial meniscus transection (MMT) rat OA model 23

Chapter 3: Designing a Strategy to Achieve Small Molecule Drug Loading and Sustained Release From PEG Microgels 25

3.1 Introduction 25
3.2 Materials and Methods 26
3.2.1 Materials 26
3.2.2 Synthesis of PLGA nanoparticles 27
3.2.3 Synthesis of PLGA-loaded PEG microgels 27
3.2.4 Small molecule release profile characterization 28
3.3 Results 29
3.3.1 PLGA nanoparticles and PEG microgels 29
3.3.2 Small molecule release profile 30
3.4 Discussion 34
3.5 Conclusions 37

Chapter 4: Engineering Synovium- and Cartilage-Binding PEG Microgels Through Active Targeting Strategies 38

4.1 Introduction 38

4.2 Materials and Methods 39

4.2.1 Materials 39

4.2.2 Synthesis of peptide-functionalized PEG microgels 40

4.2.3 Peptide-functionalized PEG microgels binding assays 41

4.3 Results 43

4.3.1 Synoviocytes targeting peptide (HAP-1) binding and specificity assays 43

4.3.2 Cartilage targeting peptide (WYR) binding and specificity assays 45

4.4 Discussion 47

4.5 Conclusions 53

Chapter 5: Evaluating the *In Vivo* Efficacy of PLGA-Loaded Peptide-Functionalized PEG Microgels as Small Molecule Drug Delivery Systems in a Rat Model of OA 54

5.1 Introduction 54

5.2 Materials and Methods 55

5.2.1 Materials 55

5.2.2 Unilateral medial meniscus transection (MMT) procedure . . 55

5.2.3 Microgels intra-articular mechanical stability 56

5.2.4 Microgels intra-articular retention and their effect on knee joint health and OA progression 56

5.2.5 Intra-articular drug retention time 58

5.2.6 *In vivo* localization of nano-composite microgels 59

5.3 Results 59

5.3.1 Microgels intra-articular mechanical Stability 59

5.3.2 Microgels intra-articular retention 60

5.3.3 Effect of microgels on knee joint health and OA progression . 63

5.3.4 Model small-molecule drug-loaded microgels intra-articular retention time 68

5.3.5 *In vivo* localization of nano-composite microgels 72

5.4 Discussion 74

5.5 Conclusions 81

Chapter 6:Future Considerations and Conclusions 82

6.1 Contributions to the field 83

6.1.1 Hydrogel microspheres for improved intra-articular retention of small molecule drugs 83

6.1.2 Intra-articular tissue-specific drug delivery 85

6.2 Future Directions 87

6.2.1 Effect of HAP-1-functionalized PEG microgels on internalization and inflammation 87

6.2.2 *In vivo* localization of WYR-functionalized PEG microgels via magnetic resonance imaging 88

6.2.3 Effect of WYR-functionalized PEG microgels on drug delivery, penetration and retention into articular cartilage 89

6.2.4 Evaluation of the efficacy of peptide-functionalized PEG microgels as intra-articular drug delivery systems for OA treatment 90

6.3 Clinical Translation 91

6.4 Conclusions 94

Appendix A: Supplementary Methods 96

A.1 Optimal cutting temperature (OCT) embedding of tissue samples containing PEG microgels 96

A.2 PLGA nanoparticles distribution in PEG microgels 97

Appendix B: Supplementary Results 102

B.1 Self-quenching effect in cyanine dyes 102

B.2 Cyanine 7 release profile 105

References 122

LIST OF TABLES

Table 2.1 Half-life of different molecules after intra-articular delivery. . . . 14

Table 3.1 PLGA NPs-loaded microgels mean size and coefficient of variance (CV%). 30

Table 4.1 Synoviocytes, cartilage and integrin-binding peptide sequences. 40

Table 6.1 Clinical trials using intra-articular drug administration. 92

LIST OF FIGURES

Figure 2.1 Signs of knee OA. 8

Figure 2.2 PEG-4MAL Chemistry. 21

Figure 2.3 Flow-focusing Microfluidic Device Design. 22

Figure 2.4 OA progression in the rat MMT model. 24

Figure 3.1 PLGA nanoparticles and PEG microgels size distribution. . . 29

Figure 3.2 PLGA nanoparticles distribution inside PEG microgels. 31

Figure 3.3 Small molecule release profile from PLGA NPs-loaded PEG microgels. 33

Figure 4.1 HAP-1 peptide-functionalized PEG microgels binding to rabbit synoviocytes. 44

Figure 4.3 WYR peptide-functionalized PEG microgels binding assays. . 45

Figure 4.2 HAP-1-functionalized PEG microgels binding to human synoviocytes. 46

Figure 4.4 WYR peptide-functionalized PEG microgels specificity assay. 48

Figure 5.1 WYR peptide-functionalized PEG microgels *in vivo* mechanical stability. 61

Figure 5.2 Peptide-functionalized PEG microgels *in vivo* retention. 64

Figure 5.3 Peptide-functionalized PEG microgels effect on cartilage degradation and osteophyte formation. 66

Figure 5.4 Peptide-functionalized PEG microgels effect on synovial membrane thickness. 67

Figure 5.5 *In vivo* localization of peptide-functionalized PEG microgels. . 69

Figure 5.6 Intra-articular cargo retention time of Cy-7-loaded peptide-functionalized PEG microgels. 70

Figure 5.7 Microgel formulations get trapped within the synovial membrane. 75

Figure A.1 PLGA nanoparticle distribution in PEG microgels: Image processing. 101

Figure B.1 Cyanine 7 self-quenching effect. 104

Figure B.2 Cyanine 7 release profile. 105

LIST OF SYMBOLS

ADAMTS: A disintegrin and metalloproteinase with thrombospondin motifs

AIC: Akaike's Information Criterion

ANOVA: Analysis of variance

β**-NGF**: Beta-nerve growth factor

BMP-2: Bone morphogenetic protein 2

BSA: Bovine serum albumin

C2C12: Mouse myoblast cell line

CAP: Cartilage affinity peptide

CV: Coefficient of variance

Cy7: Cyanine 7

DCM: Dichloromethane

DMOAD: Disease modifying osteoarthritis drugs

DTT: Dithiothreitol

ECM: Extracellular matrix

EPIC-μ**CT**:Equilibrium partitioning of an ionic contrast agent via micro-computed tomography

FBS: Fetal bovine serum

FDA: Food and drug administration

HA: Hyaluronic acid

HAP-1: Fibroblast-like synoviocyte-binding peptide (SFHQFARATLAS)

HAP-1sc: Fibroblast-like synoviocyte-binding scrambled peptide (CALSQAFRHAFTS)

HIG-82: Rabbit fibroblast-like synoviocyte cell line

IA: Intra-articular

IL-1β: Interleukin-1 beta

IL-4: Interleukin-4

IL-6: Interleukin-6

IL-15: Interleukin-15

IL-27: Interleukin-27

IV: Intra-venous

IVIS: *In vivo* imaging system

KGN: Kartogenin

MabCII: Monoclonal anti-type II collagen antibody

MAL: Maleimide

MC3T3-E1: Mouse preosteoblast cell line

MCL: Medial collateral ligament

MMP: Matrix metalloproteinases

MMT: Medial meniscus transection

NF-κB: Nuclear factor kappa B

NIR: Near infra-red

NPs: Nanoparticles

NSAID: Non-steroidal anti-inflammatory drugs

OA: Osteoarthritis

OCT: Optimal cutting temperature

PBS$^{+/+}$: Phosphate buffered saline with calcium and magnesium

PBS$^{-/-}$: Phosphate buffered saline without calcium and magnesium

PCL: Polycaprolactone

PCLA-PEG-PCLA: Poly(caprolactone-con-lactide)-poly(ethylene glycol)-poly(caprolactone-con-lactide)

PDMS: Polydimethylsiloxane

PEA: Polyester amide

PEG: Poly(ethylene glycol)

PEG-4MAL: Four-arm Poly(ethylene glycol)-maleimide

PLGA: Poly(lactic-co-glycolic) acid

PVA: Poly-vinyl-alcohol

RGD: Integrin-binding pepdide (GRGDSPC)

RDG: Integrin-binding scrambled pepdide (GRDGSPC)

ROS: Reactive oxygen species

scFv: Single-chain antibody variable fragment

SD: Standard deviation

SEM: Standard error of the mean

sCy7: Sulfo-cyanine 7

SW982: Human synovial sarcoma cell line

TGF-β1: Transforming growth factor beta 1

TNFα: Tumor necrosis factor-alpha

VEGF: Vascular endothelial growth factor

WOMAC: Western Ontario and McMaster Universities Osteoarthritis Index

WYR: Collagen type II α1 chain-binding peptide (WYRGRL)

WYR: Collagen type II α1 chain-binding scrambled peptide (YRLGRWC)

SUMMARY

Osteoarthritis (OA) is a joint degenerative disease that affects over 30.8 million adults in the U.S. OA progression is a complex process involving different pathological mechanisms in the articular cartilage, the synovial membrane and the subchondral bone. Treatment at early stages is limited to systemic pain management using analgesics and non-steroidal anti-inflammatory drugs (NSAID). Later, when the symptoms are more severe, OA is treated with intra-articular injections of corticosteroids and visco-supplements such as hyaluronic acid (HA). However, these therapies only offer short term pain relief because they act as anti-inflammatory and lubricating agents respectively and do not mitigate OA progression. Additionally, these compounds are subjected to rapid clearance from the joint space. Finally, at late stages of OA patients often require total joint replacement.

Currently, there are no FDA-approved drugs able to mitigate or halt OA progression. Recent research has led to the discovery of multiple disease modifying drugs that have shown promising results in pre-clinical models of OA. Despite these efforts, the translation of these molecules to the clinic has been challenging in part because of the scarcity of appropriate drug delivery vehicles and the lack of understanding of drug effects on different intra-articular tissues involved on the progression of the disease.

Therefore, the objective of this project was to design an improved intra-articular (IA) drug delivery vehicle using peptide-functionalized poly(ethylene glycol) (PEG) microgels targeting different tissues within the joint to address problems related to intra-articular retention and tissue-specific drug delivery. In studies presented in Chapter 3, I used a microfluidic device to synthesize PEG microgels containing

poly(lactic-co-glycolic) acid (PLGA) nanoparticles (NPs) loaded with a model drug such as Rhodamine B. This delivery vehicle with nano-composite design allowed for loading and sustained release of small molecules. In Chapter 4 it is demonstrated that functionalization of PEG microgels with targeting peptides led to specific binding of these delivery devices to bovine articular cartilage sections and synoviocytes *in vitro*. Finally, in Chapter 5 the IA retention of the engineered drug delivery system and their effect on the joint health in a rat model of OA was evaluated. PEG microgels did not negatively impact joint health and OA progression and were retained in the intra-articular space for at least 3 weeks. Also, synoviocyte-targeting PEG microgels were shown to be retained within the synovial membrane.

Overall, this work provides an intra-articular drug delivery vehicle that in addition to controlling the release of small molecule drugs, allows for improved intra-articular retention and specific binding to tissues involved in OA progression such as articular cartilage and synovium. Also, considering that PEG microgels are tunable systems that could also be used for the encapsulation of biologics and cells, this work may provide a better tool to study the effects of a combination of therapeutic strategies (small molecules, proteins, nucleic acids and cells) on specific joint tissues. This work is expected to contribute to the screening of therapy strategies and the development of tissue-specific treatments to prevent OA progression.

CHAPTER 1
INTRODUCTION

Osteoarthritis (OA) affects 30.8 million adults in the U.S and is the leading cause of disability in the country [1]. OA pathophysiology is not fully understood and was originally described as a progressive degradation of the articular cartilage. However, more recent evidence demonstrates that OA is a multi-tissue disease and its progression is determined by the interaction of different pathological processes occurring in the articular cartilage, the subchondral bone and the synovium [2, 3, 4]. OA treatment is currently limited to systemic pain management using NSAIDs and week opioids, whose long-term use has been associated with adverse effects on the gastrointestinal, renal and circulatory system [5, 6]. Intra-articular injection offers a localized route of administration, which could reduce systemic exposure to therapeutic molecules and therefore, minimize their off-target effects on other organs [7]. However, after intra-articular injection, small molecule drugs ($<$900 Da) are subjected to rapid clearance via lymphatics and capillaries drainage. Consequently, the time that these drugs are retained in the joint space is not sufficient for them to elicit a therapeutic effect [8]. Hence, a drug delivery vehicle that provides sustained release and prolonged intra-articular retention time is needed.

Currently there are no FDA-approved disease modifying drugs able to slow OA progression. However, recent research has proposed multiple molecular targets related to OA progression including IL-1β, TNFα, β-NGF, MMP and their receptors [9, 3]. However, these molecular targets may be involved in different biological

roles depending on their location in the joint. Therefore, a drug could have two different therapeutic effects on two distinct articular tissues [3]. For example, non-steroidal anti-inflammatory drugs (NSAIDs), which are often administered for pain management, have been related to reduced proteoglycan secretion which exacerbates cartilage degradation [10]. Furthermore, intra-articular injection of TGF-β1 has been shown to be beneficial for cartilage repair, but it increases synovium hyperplasia and induces the formation of cartilage-like tissues in ligaments and synovium [11]. Also, corticosteroids such as dexamethasone act as anti-inflammatory drugs on the synovial membrane, but have protective anti-catabolic effects on the articular cartilage [12, 13].

Thus, in order to develop a successful disease modifying strategy to treat OA it is important to design drug delivery systems able to prolong the intra-articular drug retention time and target specific tissues within the joint. This strategy would not only provide drugs sufficient time to exert their therapeutic effect, but would also mitigate the secondary effects that drugs may have on different intra-articular tissues.

Therefore, the **primary objective** of this project was to engineer synoviocyte and articular cartilage-binding small molecule drug delivery vehicles for prolonged intra-articular treatment of OA. The **central hypothesis** is that peptide-functionalized polyethylene glycol (PEG) microgels containing drug-loaded poly(lactic-co-glycolic) acid (PLGA) nanoparticles will support small molecule drug sustained release, will be able to specifically bind to the synovial membrane and the articular cartilage and will be retained in the intra-articular space for a prolonged period compared to free small molecules. The central hypothesis will be tested with the following specific aims:

1.1 Specific Aim 1

Design nano-composite PEG microgles containing PLGA nanoparticles to achieve small molecule drug loading and sustained release.

The *working hypothesis* is that small molecule drugs directly loaded into PEG microgels will rapidly diffuse through the gel's mesh leading to burst release, while PEG microgels containing drug-loaded PLGA particles will exhibit a sustained drug release. PLGA nanoparticles loaded with a model small molecule fluorophore were synthesized and encapsulated into PEG microgels. Nanoparticles encapsulation into microgels was characterized, as well as the small molecule release profile. PEG microgels loaded with PLGA NPs showed to be a promising vehicle able to control the release of model small molecules such as Rhodamine B over 2 weeks.

1.2 Specific Aim 2

Design synoviocytes- and articular cartilage- binding PEG microgels through functionalization with targeting peptides.

The *working hypothesis* for this aim is that PEG microgels tissue-specific binding can be achieved using synoviocyte- and collagen type II-binding peptides covalently linked to the hydrogel network. Targeting assays of fluorescently labeled peptide-functionalized microgels were performed using rabbit (HIG-82) and human (SW-982) synoviocyte cell cultures and bovine articular cartilage sections to assess for their ability to bind to tissues of interest in a specificity manner. PEG microgels functionalized with synoviocyte- (HAP-1) and collagen type II-targeting peptides (WYR) were shown to bind specifically to synoviocytes and articular cartilage, respectively.

1.3 Specific Aim 3

Assess the IA retention of PLGA-loaded peptide-functionalized PEG microgels and their effect on knee joint health in a rat model of OA.

The *working hypothesis* is that peptide-functionalized PEG microgels containing small molecule drug-loaded PLGA nanoparticles will increase the retention time of the encapsulated small molecules and will specifically bind to articular cartilage and synovium without inducing any joint degenerative changes after intra-articular injection. For this purpose, the unilateral rat medial meniscus transection (MMT) model was used. To determine the microgels intra-articular retention time and their effect on joint health and OA progression, PLGA nanoparticles-loaded PEG microgels, presenting binding peptides that were labeled with cyanine 7 (Cy7), were injected bilaterally in the rat knee joints 3 weeks post-surgery. PEG microgels were tracked using an *in vivo* imaging system (IVIS) during the following 3 weeks and then euthanized to evaluate the joint health via histology and equilibrium partitioning of an ionic contrast (EPIC) agent via μCT. Results demonstrated that PEG microgels were retained in the knee joints for at least 3 weeks and did not affect the cartilage morphology or the synovial membrane thickness of healthy or diseased joints. Also synoviocyte-binding microgels were found trapped in the synovial membrane, while cartilage-binding microgels were not found within the synovium. A cargo tracking study was also conducted to evaluate the retention time of a model small molecule (Cy7) encapsulated into PLGA NPs. Some peptide-functionalized PEG microgels formulations significantly increased the retention time of cyanine 7 compared to the free small molecule.

This project presents an innovative approach to achieve prolonged, tissue-specific small molecule administration for osteoarthritis treatment. The design

of the composite drug delivery vehicle addresses multiple shortcomings in current OA therapies such as poor intra-articular drug retention and adverse side-effects on non-targeted tissues. The ability of PLGA nanoparticles-loaded peptide-functionalized PEG microgels to control the delivery of small molecule drugs, enhance the intra-articular retention in a rat model of OA and bind to cartilage and synoviocytes *in vitro* demonstrate the potential of this delivery system to improve the IA administration of disease modifying OA drugs. We expect the results presented in this dissertation to establish a promising platform for the screening and the development of multi-target tissue-specific therapies for OA treatment.

CHAPTER 2
BACKGROUND

2.1 Osteoarthritis (OA)

2.1.1 Prevalence

Osteoarthritis (OA) is a joint degenerative disease characterized by cartilage loss, which leads to joint pain, swelling and stiffness. OA affected 303 million people in the world by 2017 [14] and 30.8 million adults in the U.S. by 2011 [15]. It is calculated that by 2020 OA will affect 50 million people in the U.S. [16]. In 2008 it was estimated that around 14 million people over 25 years old were affected by knee OA alone and around 50% of those cases would require a total knee replacement [17]. Annual medical care expenses associated with OA are approximately $185.5 billion dollars annually in the U.S. [18]. In a country with rapidly aging population and high incidence of obesity, the prevalence of OA is expected to increase. In fact, projections show that by 2032, around 30% of adults over 45 are expected to have consulted a physician for OA and around half of those cases would be related to knee OA [19].

2.1.2 Disease progression

According to its cause, osteoarthritis can be classified in primary or idiopathic and secondary OA. The former has its origin on non-traumatic conditions, where factors such as age and gender have been identified to play a role [20]. The latter, is developed after a traumatic event or a mechanical misalignment [21]. In both

cases, the etiology of OA is not fully understood, but it has been recently recognized that it is a multifactorial disease. Joint injury, abnormal joint development, metabolic disorders, obesity, age, biochemical reactions and inflammation have all been reported as possible OA causes [21, 20]. Some research groups have suggested that these factors could elicit changes in joint biology, mechanics and structure leading to impaired joint remodeling and the associated progressive degenerative changes characteristic of OA [22].

Originally, OA was thought to consist exclusively of articular cartilage degradation. However, recent findings indicate that OA affects the joint as a whole and generates changes in other tissues such as the synovial membrane, subchondral bone, ligaments and peri-articular muscles [21] (Figure 2.1). These changes lead to bone remodeling and osteophyte formation, ligament laxity, weakening of peri-articular muscles and joint swelling [21]. The exact mechanisms involved in OA progression and the interplay between articular tissues remain under investigation [4]. However, recent research has described biological mechanisms and measured biomarker levels that have been used to partly recreate OA progression [7].

As OA advances, the articular cartilage experiences a continuous degeneration process characterized by partial surface lamina loss, chondrocyte hypertrophy and the appearance of cartilage fibrillations, calcified erosions and lesions [7]. These morphological damage is accompanied by cartilage matrix compositional changes such as proteoglycan depletion and collagen type II cleavage [23]. The increase in catabolic activity during OA has been related to the activation of the nuclear factor NF-κB in hypertrophic chondrocytes, synovium macrophages and fibroblasts, leading to the up-regulation of catabolic proteins including matrix metalloproteinases (MMPs), aggrecanases, cathepsins and A disintegrin and metalloproteinase with

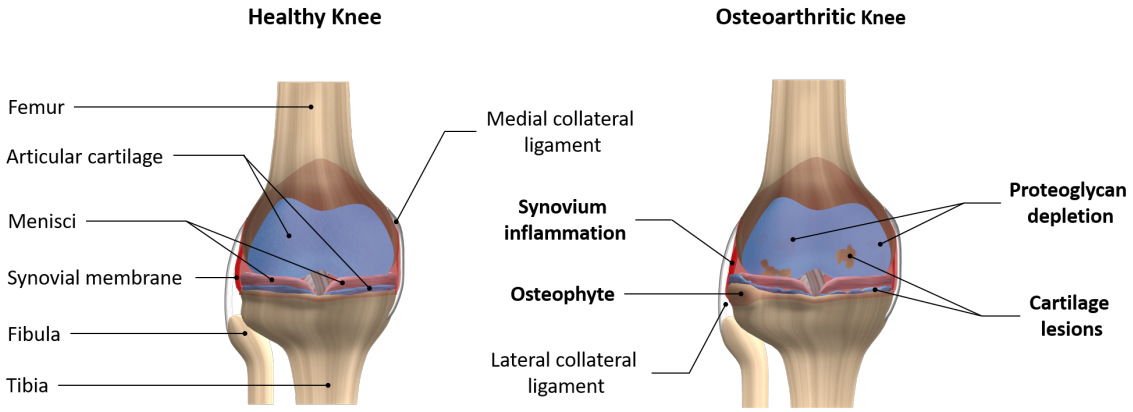

Figure 2.1: Signs of knee OA. Osteoarthritis is characterized by synovial membrane inflammation, osteophyte formation and articular cartilage degradation, which leads to a decrease in proteoglycans and the formation of full thickness lesions.

thrombospondin motifs (ADAMTS) [7, 23, 16]. Moreover, the expression of transforming growth factor beta (TGFβ) and vascular endothelial growth factor (VEGF) in chondrocytes, promotes angiogenesis and results on blood vessel penetration into the hypertrophic cartilage and calcification [23]. This unbalanced bone remodeling induces subchondral bone sclerosis, cysts and osteophyte formation, which results in severe pain [23, 16]. Furthermore, the synovial membrane is affected by the infiltration of T lymphocytes, neutrophils and macrophages [23]. These immune cells secrete pro-inflammatory mediators, cytokines and chemokines such as IL-1, IL-6, IL-15, TNFα, nictric oxide and prostaglandins, which further exacerbate joint inflammation and cartilage degeneration [24]. Additionally, synoviocytes secretion of synovial fluid components is impaired, leading to poor viscous lubrication and shock absorption capacity [7]. Despite the advances on elucidating the mechanisms involved in OA progression, there is still much investigation needed to develop appropriate disease-modifying OA drugs (DMOADs) [23, 7, 16].

2.2 Current clinical treatments for osteoarthritis

2.2.1 Non-pharmacological management

Non-pharmacological approaches constitute the first line of treatment at early stages of OA progression. These strategies aim to reduce the pain and improve the joint functionality. It has been demonstrated that the absence of mechanic loading increases cartilage degeneration [25]. Similarly, excessive mechanic stimuli are also deleterious for joint health [21]. Therefore, weight management and physical therapy are key components of non-pharmacological OA treatment. Exercises types recommended for OA patients at this stage include proprioception, stretching and resistance [21]. However, giving the progressive character of this disease, patients often require pharmacological treatment.

2.2.2 Pharmacological management

Currently there are no approved disease modifying drugs able to reduce OA progression. Therefore, treatment is limited to pain management and the regime depends on the severity of the disease. Commonly used medications include systemic administration of opioids and cyclooxygenase inhibitors such as acetaminophen and non-steroidal anti-inflammatory drugs (NSAIDs). However, their prolonged use is limited due to their secondary effects on the gastrointestinal, renal and cardiac systems, especially in the elder population that often presents a wide range of comorbidities [26, 27, 7, 21]. Therefore, the use of topical NSAIDs is a safer alternative, but their use has only been shown to be effective during the first two weeks of use [28]. Moreover, recent clinical studies have shown that acetaminophen is inferior to NSAIDs and not-superior than placebo for pain management in moderate and severe OA patients [25]. In the case of opioids, increasing awareness regarding their chronic use has limited their administration for long-term pain man-

agement. Also, some studies have shown that opioids do not improve pain scores in OA patients compared to NSAIDs [29, 30].

Other alternative to alleviate the pain is the use of dietary supplements, which present fewer systemic side effects and account for US$25 billion annual sales [31]. Around 69% of OA patients take oral supplements for pain management, with glucosamine and chondroitin sulfate being the most consumed compounds, accounting for a third of the oral supplements market value (US$872 million annual sales) [31]. Liu *et al.* in a meta-analysis study reviewed 69 randomized placebo-controlled clinical trials that evaluated the effect of 20 individual oral supplements for the treatment of hand, hip or knee OA. The results demonstrated that at long term ($>$6 months), no supplements exhibited a clinically important effect on pain or physical function and only green-lipped mussel extract and undenatured type II collagen showed a significant clinical effect on pain reduction between 4 and 6 months [31]. According to this meta-analysis study, despite glucosamine and chondroitin being the most investigated and consumed supplements, they only statistically improve pain scores at short term ($<$3 months), but their clinical effect is debatable [31]. Additionally, clinical trials and meta-analysis studies have shown that the use of glucosamine and chondroitin sulfate in combination does not induce a relevant reduction in pain compared to placebo [32, 33, 34]. Only one of these clinical studies suggested that the combination of glucosamine and chondroitin may be beneficial only in patients with moderate to severe joint pain [33].

To overcome many of the limitations related to systemic drug administration, intra-articular (IA) injections raise an alternative that offers a more localized treatment. IA injection of corticoids has been shown to reduce pain scores and increase joint functionality due to their anti-inflammatory and immunosuppressive

effects. Corticoids reduce pain and inflammation by decreasing IL-1 production, prostaglandins, leukotrienes and metalloproteinases [21, 35, 36]. However, their long term efficacy is questionable primarily due to the short retention time. For example, the intra-articular half-life time of cortisone and dexamethasone are 1.46 h and 3.6 h respectively [37, 38].

Hyaluronic acid (HA) is one of the principal components of the synovial fluid, produced by synoviocytes, chondrocytes and fibroblasts [39]. In healthy joints, it provides viscous lubrication, impact absorption and is thought to have anti-inflammatory and chondroprotective properties [39]. However, these protective characteristics are diminished in OA due to a reduction in HA concentration and molecular weight [36]. Therefore, IA injection of HA has been used as a visco-supplement with the intention of restoring healthy synovial fluid properties [21]. Although clinical trials, systematic reviews and meta-analysis studies on the effect of HA injection on joint pain present confounding results, primarily due to a high variability in HA formulations and small sample size, most evidence suggest that visco-supplementation may be a safe alternative to achieve clinically relevant pain reduction [39]. Meta-analysis studies have shown that HA induces a statistically significant improvement in pain relief, but fails to demonstrate a minimal clinically important difference compared to placebo [40, 41]. However, some evidence suggest that high molecular weight or cross-liked HA formulations are able to induce a clinically relevant reduction in knee pain [40, 42].

Overall, the OA treatment alternatives described in this section, only intend to reduce OA symptoms, but do not prevent or slow down the disease progression. Additionally, most of the currently available treatment options have shown to be ineffective or induce severe systemic adverse effects, which emphasize on the

need of discovering novel disease modifying therapeutics for OA treatment.

2.3 Novel targets for OA treatment and drug candidates

Considering that OA is a complex disease that affects the whole joint, in addition to pain, pathways related to inflammation, cartilage catabolism and subchondral bone remodeling have become targets of interest to develop disease modifying drugs. Regarding inflammation, inhibition of the nuclear factor NF-κB or individual downstream proteins (IL-1β, TNF-α, β-NGF, MMPs) has been investigated [43, 44]. A phase I and II clinical study for a small molecule NF-κB inhibitor, SAR113945, demonstrated drug tolerability but failed to show effectiveness 56 days after intra-articular administration [45].

Compounds such as recombinant human fibroblast growth factor 18 (Sprifermin) that intended to inhibit cartilage catabolic activity have been evaluated. A phase I clinical trial demonstrated that Sprifermin-treated patients presented a reduction in lateral femorotibial cartilage thickness and volume loss compared to placebo control. However, patients in all experimental groups, including placebo, exhibited improved symptoms as determined by the Western Ontario and McMaster Universities Osteoarthritis Index (WOMAC) [46]. Other promising molecule, Kartogenin, has been shown to promote chondrogenic differentiation and reduction of OA progression in pre-clinical animal models [47, 48, 49]. Finally, DMOADs that affect subchondral bone such as the bone resorption inhibitor, salmon calcitonin and the anti-osteoporotic agent strontium ranelate have been suggested to have promising effect on OA progression [7].

Although OA pathogenesis is not fully understood and does not seem to have an inflammatory origin, some researchers believe that synovial inflammation plays

a key role on disease progression and have suggested the use of anti-rheumatic drugs as possible OA treatments [50, 51]. In fact, anti-rheumatic drugs have shown promising results on *in vitro* models and animal studies, but their efficiency in clinical trials is still questionable [52]. Persson *et al.* in a systematic review and meta-analysis study evaluated placebo-controlled clinical trials that investigated the efficacy of FDA-approved anti-rheumatic drugs as possible OA treatments [51]. In the study, small molecule drugs and biologics were investigated, including hydroxychloroquine, methotrexate, anakinra, adalimumab and etanercept. Results demonstrated that although these treatments induce a significant reduction in pain metrics, this effect is not clinically relevant [51].

2.4 Intra-articular (IA) drug delivery strategies in OA

Despite the encouraging advances in the discovery of DMOADs, the translation of these drugs into the clinic is limited given the hostile pharmacokinetics of the joints. Free small molecule drugs and even proteins injected in the joint space are rapidly cleared via lymphatics and capillaries and their retention time does not exceed few hours (Table 2.1). Also, most of them have poor water solubility and require a delivery system in order to be administered via IA injections [7, 53, 3]. Multiple intra-articular drug delivery vehicles including hydrogels, liposomes, nanoparticles and microparticles have been formulated and will be discussed in the following section.

2.4.1 Hydrogels

Hyaluronic acid (HA) is the only formulation currently approved for OA treatment as a lubricating agent [26, 27, 7, 3]. Various products use HA formulations as a lightly cross-linked hydrogel (Synvisc-ONE®, EUFLEXXA®, Gel-One® and MonoVisc®) [39]. Therefore, it is an attractive alternative to use as drug delivery vehicle. Mul-

Table 2.1: Half-life of different molecules after intra-articular delivery.

Molecule	**Half-Life (h)**	**Molecular Weight (Da)**
Paracetamol [54]	1.10	151
Ibuprofen [55]	2.20	206
Naproxen [56]	1.6	230
Ketoprofen [56]	1.90	254
Diclofenac [54]	5.20	296
Cortisone [38]	1.46	360
Dexamethasone [37]	3.60	392
Methotrexate [57]	2.90	454
Hyaluronic Acid [8]	13.20	6,000
IL-1Ra [58]	23.04	65,400
Bovine Serum Albumin (BSA) [59]	15.12	66,000

tiple research groups have shown that drug-loaded HA hydrogel formulations can be used to reduce the frequency of intra-articular injections compared to free drug [60, 61]. However, the retention of HA cross-linked formulations is still a concern. Yoshioka *et al.* demonstrated that the commercially available cross-linked HA formulation Gel-One®, can not be detected in the synovial fluid of rabbit knee joints after day 7, only 30% is retained in the synovial membrane at day 7 and 3.3% at day 28 [62].

In an attempt to improve hydrogel intra-articular retention time, the use of synthetic hydrogels has been explored. For example, poly(caprolactone-co-lactide)-poly(ethylene glycol)-poly(caprolactone-co-lactide) (PCLA-PEG-PCLA) hydrogel, used to deliver celecoxib to horse knees, showed that the drug could be detected at day 28 in the synovial fluid, but more than 90% of it was cleared by day 7 [63]. Despite these advances, hydrogels serve as drug depots but are unable to control small molecule drug release rate because their mesh size is usually orders of magnitude larger than the loaded drugs [64, 65].

2.4.2 Liposomes

Liposomes are an attractive option for intra-articular drug delivery because they can provide controlled release rates of both lipophilic and water-soluble drugs. Also, compared to crystalline drug suspensions formed by hydrophobic drugs upon IA injection, liposomes are less inflammatory [66]. Studies have shown that liposomes loaded with a model small molecule such as the contrast agent iohexol increased the retention time of the free drug from 3h to 124h [67]. However, liposomes have limited long term stability and are not mechanically strong enough to withstand the pressure present in the intra-articular space [64, 7, 68].

2.4.3 Nanoparticles and microparticles

An alternative to overcome the mechanical instability of liposomes is the use of lipid or polymeric nanoparticles as IA drug delivery systems. These vehicles have been shown to be susceptible to microvascular and synovial macrophage-mediated drainage and can be retained in the joint space only for few weeks, depending on their size, charge and composition [7, 69, 70, 71].

The use of larger particles that could better avoid vascular drainage is a potential strategy to achieve IA drug sustained release over longer periods of time. In fact, polycaprolactone (PCL) microparticles with an average size of 16 μm were found to remain in the joint space of rats for up to a month [72]. Janssen et al. synthesized celecoxib-loaded polyester amide (PEA) microspheres with a mean particle size of 25 μm and were able to detect around 20% of the injected PEA 12 weeks after IA injection in Lewis rats [73]. Additionally, the company Flexion Therapeutics recently received FDA approval to commercialize ZILRETTA®, an IA formulation of 45 μm triamcinolone acetonide-loaded PLGA microparticles for pain management in OA patients. The associated clinical trials revealed persistent pain relief until 3 months post-treatment [74, 75]. All together, these studies show the potential of microparticles to provide a sufficient IA retention time able to ensure drug bioactivity during a relevant therapeutic window [7].

2.5 The importance of targeting for IA drug delivery

A wide variety of small molecule drugs are being studied for the treatment of OA. These drugs can be classified according to their function as analgesic, anti-inflammatory, cartilage-protective or bone resorption inhibitors [7]. Depending on their function, these drugs act on specific biologic targets present in different tis-

sues within the joint [3]. Studies have shown that non-tissue specific delivery of these drugs may result in unwanted effects on other tissues in the joint. For example, the use of NSAIDs have been related to reduced proteoglycan secretion, thereby increasing cartilage degradation [10]. Other groups have shown that nerve growth factor (NGF) blockade for pain relief had serious adverse effects including OA progression and osteonecrosis in a phase III clinical trial [76]. Therefore, drugs that act on inflammatory and pain pathways should primarily target the synovium, where these processes occur [3]. Likewise, drugs that induce chondrogenesis should be preferentially delivered to the articular cartilage in order to prevent adverse effects on the surrounding tissues. Intra-articular injection of TGF-β1, although beneficial for cartilage repair, increases synovium hyperplasia and induces the formation of cartilage-like tissues in ligaments and synovium [11]. Similarly, kartogenin (KGN), found to promote chondrogenesis of primary mesenchymal stem cells, has been studied for its ability to repair cartilage lesions and promote cartilage formation in OA pre-clinical models as well as in animal studies of tendon-to-bone injury repair [47, 77, 78, 79, 80, 48]. However, Zhang et al. showed that free KGN injection into a rat model of tendon-to-bone injury resulted in excessive cartilage-like tissue formation in unintended areas and overgrowth of surrounding tissues [77].

All together, these studies show the need to engineer tissue-specific drug delivery vehicles for the treatment of OA. Active tissue targeting can be achieved by drug delivery vehicle functionalization with affinity ligands including antibodies, antibody fragments, peptides, aptamers and small molecule ligands [68]. In the context of OA very limited research has been conducted in this regard.

2.5.1 Cartilage targeting

Targeting cartilage ECM components such as collagen type II and aggrecan has gained attention as a promising strategy to target damaged areas of the articular cartilage where these components get exposed. In fact, monoclonal anti-type II collagen antibodies (MabCII) have been used in multiple drug delivery and diagnostics applications[81, 82, 83]. For example, Cho *et al.* demonstrated that nanosomes functionalized with a collagen type II monoclonal antibody are able to bind cartilage tissue proportionally to the severity of the disease in a mice model of OA after systemic administration [83]. Also, single-chain antibody variable fragment (scFv) specific to reactive oxygen species (ROS)-modified collagen II have been reported [81].

More recently, the use of phage display technology has resulted in the discovery of tissue-specific peptides, which compared to larger proteins such as monoclonal antibodies, offer the advantages of being easier to manufacture, less immunogenic, smaller in size and more stable. Nevertheless, compared to antibodies, peptides can present lower binding affinity for their targets, which can be overcome by incorporating multiple peptide repeats in the drug delivery system [68]. Using this technology, Yanbin *et al.* discovered a cartilage affinity peptide (CAP: DWRVIIPPRPSA) able to specifically bind to rabbit and human chondrocytes isolated from a patient with OA. Compared to the scrambled peptide, conjugation of the CAP peptide to 50 nm polyethylenimine nanoparticles demonstrated to be an effective method to induce particles binding and internalization into chondrocytes *in vitro* and 48 h after intra-articular injection into rabbit knee joints [84]. Later, Cheung *et al.* discovered two peptide sequences (RLDPTSYLRTFW and HDSQLEALIKFM) via phage display able to preferentially bind to aggrecan *in vitro*. However, no scrambled control peptides were used and the ability of these sequences to bind

cartilage *in vivo* was not assessed [85]. Despite the efforts for developing novel cartilage targeting moieties, these aggrecan-biding and CAP peptides have not yet been used by other laboratories for intra-articular drug delivery or diagnostics applications.

Rothenfluh et al. reported the ligand WYRGRL as a collagen type II α1-targeting peptide. Functionalization of poly(propylene sulphide) nanoparticles and subsequent IA injection in mice knees resulted in a 72-fold increase in cartilage-targeting ability compared to nanoparticles functionalized with the scrambled control [86]. In contrast to other reported peptides, this sequence has been successfully used in pre-clinical models for diagnostics and drug delivery applications [86, 87, 88, 89, 5, 90]. In fact, the conjugation of WYR peptide to magnetic resonance imaging (MRI) contrast agents has allowed the *in vivo* localization of cartilage hypertrophic changes in a rat model of OA [88]. Other researchers have coupled this peptide to near infra-red probes (NIR) for *in vivo* imaging and demonstrated that this system is able to detect age-related decrease in collagen type II in mice [90]. Furthermore, conjugation of WYR peptide to dexamethasone has proven to increase its retention into bovine articular cartilage explants and decreased the glycosaminoglycan depletion in an *in vitro* model of OA [5].

2.5.2 Synovial membrane targeting

Although drug delivery into the articular cartilage has been recognized as a key and very challenging aspect in the field, targeted delivery into the synovial membrane has gained interest as well. Originally, synovium targeting emerged as a strategy to minimize the secondary effects of systemic administration of NSAIDs and other anti-inflammatory therapeutics. Two peptides able to bind to inflamed syn-

ovial vasculature [91, 92], have been discovered via phage display and have shown promising targeting results after systemic administration in small animal models of rheumatoid arthritis [93, 94]. The first peptide was discovered by screening the ability of peptides administered intra-venously (IV) to specifically bind to the vasculature of human synovium grafted into immunodeficient mice [91]. The resulting peptide (CKSTHDRLC) was later used by Wythe *et al.* to formulate a fusion protein formed by the anti-inflammatory cytokine IL-4 and the synovium-targeting peptide, and demonstrated that this construct elicited a biological response specifically into human synovium grafts implanted into immunodeficient mice compared to the scrambled control [93]. Up to date, this peptide has not been used in pre-clinical models of OA. Later, another research group reported the discovery of a peptide (ADK: CRNADKFPC) able to bind to inflamed synovial vasculature and showed that intravenous administration of ADK peptide in a rat model of adjuvant arthritis resulted in reduced inflammation scores, decreased T-cell trafficking and angiogenesis inhibition [92]. Additionally systemic administration of ADK-functionalized liposomes loaded with the immunomodulatory cytokine IL-27 resulted in *in vivo* targeting of arthritic joints and significant reduction in rat paws inflammation compared to non-targeting liposomes or free IL-27, in a rat model of rheumatoid arthritis [94]. Despite these results, the ADK peptide is also able to bind to inflamed skin [92] and the control scrambled sequence has not been characterized.

A different approach for synovium targeting was proposed by Mi *et al.* who discovered a peptide (HAP-1: SFHQFARATLAS) that directly binds to synoviocytes and not the tissue vasculature [95]. HAP-1-functionalized liposomes loaded with prednisone [96] or the anti-inflammatory NF-κB-blocking peptide [97] showed promising results in terms of liposomes localization into the arthritic joints and the reduction of rat paws inflammation after IV injection in a rat model of rheumatoid

arthritis. Considering that synovium endothelium is not directly exposed to synovial fluid but synoviocytes are, the most promising strategy to target the synovial lining after IA injection could be HAP-1 peptide.

2.6 Poly(ethylene glycol) (PEG) microgels

Four-arm PEG-maleimide (PEG-4MAL) hydrogels offer a platform that could help overcome some of the main limitations related to intra-articular drug delivery. This hydrogel has been previously used for various tissue engineering applications due to its low toxicity, facile incorporation and presentation of bioligands and high cross-linking efficiency [98, 99]. In fact, PEG-4MAL macromer chemistry allows for easy stoichiometric conjugation of thiolated compounds, via Michael-type addition reaction, which could be used for the formulation of tissue-specific drug delivery vehicles by incorporating targeting bio-ligands (Figure 2.2) [100]. Additionally, given the fast cross-linking kinetics, this polymer can be used to synthesize micron-scale gels (microgels) using a flow focusing microfluidic device, as previously done by the García Lab [101, 102, 103]. This device is able to form polymer droplets that are subsequently cross-linked with the small molecule dithiothreitol (DTT) (Figure 2.3).

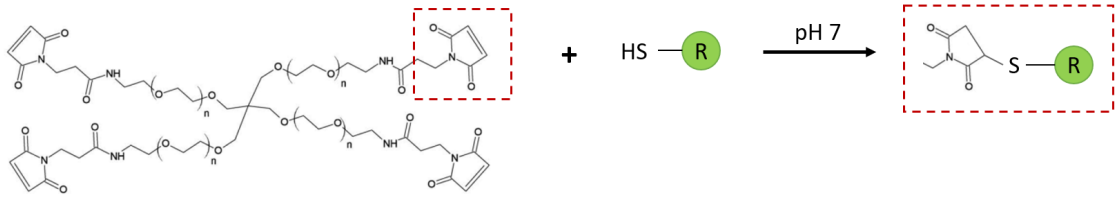

Figure 2.2: PEG-4MAL Chemistry. Michael-type addition reaction between PEG-4MAL macromer maleimide groups and free thiol-containing molecules. This reaction can be used to either functionalize the gel or to crosslink the network. Modified from Headen et al. 2014 [101]

The device has three independent inlets for the flow of 1) Mineral Oil containing 2% SPAN 80 as a surfactant, 2) a cross-linker emulsion of aqueous DTT and

mineral oil with SPAN 80 and 3) an aqueous solution of the desired concentration of PEG-4MAL macromer. For ligand presentation, the PEG-4MAL macromer is functionalized with the desired bioligand via Michael-type addition reaction prior to its infusion into the microfludic device. Likewise, for cell encapsulation applications, PEG-4MAL solution can be mixed with cells before microgels formation [101, 102]. Droplet size can be controlled by changing the flow rates of the three flowing solutions, however it is mainly determined by the device nozzle size [101]. This technology has been shown to be very versatile and has been successfully used to produce adequate vehicles for cell encapsulation and protein sustained release [101, 102, 103], however its application for targeted small molecule drug delivery is still unexplored. PEG-4MAL microgels could serve as promising drug delivery depots for intra-articular administration of therapeutic molecules, which due to their micron-size could escape vascular drainage and improve the poor drug intra-articular retention time often seen in arthritic joints.

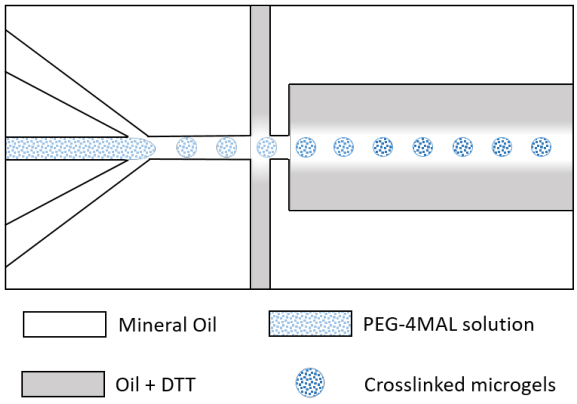

Figure 2.3: Flow-focusing Microfluidic Device Design. PEG microgels synthesis using a microfluidic device with flow focusing geometry. A PEG-4MAL macromer aqueous solution containing cells, proteins and/or nanoparticles is infused in the device. Macromer flow stream is then cut by a mineral oil + 2% SPAN 80 phase to form droplets which are then crosslinked by an emulsion of DTT in mineral oil and SPAN 80.

2.7 Medial meniscus transection (MMT) rat OA model

Animal studies are necessary for the evaluation of new therapeutics and delivery vehicles for the treatment of osteoarthritis. Multiple animal models of spontaneous or surgically induced OA have been developed and characterized. Generally, spontaneous models of OA, although may recapitulate many aspects of idiopathic OA progression in humans, develop very slowly [104], which makes the investigation of new therapeutics highly time-consuming and expensive. In contrast, surgically induced OA models mimic many aspects of post-traumatic OA, and the disease progresses rapidly allowing for faster therapeutics or drug delivery vehicles screening [104].

A well-characterized small animal model of post-traumatic OA, widely used for the evaluation of new drug candidates is the rat medial meniscus transection (MMT) model. In this surgery-induced model, the joint space is exposed after the medial collateral ligament (MCL) is cut, then the medial meniscus is transected at its narrowest point. This results in joint instability which leads to many of the changes seen in OA patients such as articular cartilage fibrillations and lesions, proteoglycan loss and osteophyte formation at 3 weeks post-surgery [104, 105]. Local increased expression of inflammatory genes, joint swelling and macrophage recruitment has been observed in this model [106, 107]. In order to characterize OA progression in this model, the Guldberg Lab has developed a contrast-enhanced microcomputed tomography (μCT) technique named equilibrium partitioning of an ionic contrast agent via μCT (EPIC-μCT), which allows to obtain quantitative 3D metrics related to changes in the joint such as articular cartilage roughness, volume, thickness, lesion volume, proteoglycan loss, subchondral bone thickening and osteophyte volume (Figure 2.4) [108].

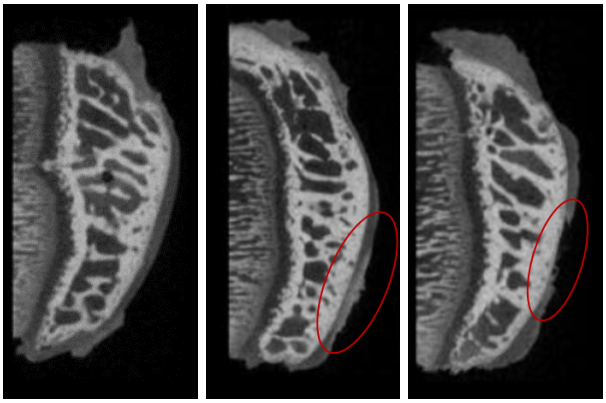

(a) (b) (c)

Figure 2.4: OA Progression in the Rat MMT Model. Representative images obtained from EPIC-μCT. (a) Sham control shows smooth cartilage surface. Cartilage fibrillations, increase attenuation corresponding to proteoglycan loss (b) and lesions (c) are evident in MMT samples

CHAPTER 3
DESIGNING A STRATEGY TO ACHIEVE SMALL MOLECULE DRUG LOADING AND SUSTAINED RELEASE FROM PEG MICROGELS

3.1 Introduction

Micron-scale hydrogels or microgels could be an attractive drug delivery system for the treatment of OA due to their prolonged retention time in the joint space [109]. A good polymer candidate to fabricate such systems is four-arm PEG-maleimide (PEG-4MAL). The García Lab has extensive experience utilizing this material for a variety of tissue engineering applications due to its low toxicity, efficient incorporation and presentation of bioligands and fast cross-linking kinetics [98, 99]. This last characteristic allows the synthesis of microgels using a flow focusing microfluidic device, as previously done at the García Lab for cell encapsulation and protein delivery applications [101, 102, 103]. However, their large mesh size (30-40 nm) represents a limitation to achieve sustained and controlled small molecule drug release [64, 65].

Therefore, the objective of this aim was to engineer a strategy to effectively load and achieve sustained delivery of small molecules ($<$900 Da) from PEG microgels. The working hypothesis was that small molecule drugs directly loaded into PEG microgels will rapidly diffuse through the gel's mesh, while PEG microgels containing a secondary drug-loaded delivery systems such as polymeric nanoparticles, will exhibit a sustained drug release. The rationale is that small molecule drugs, defined in the pharmacology field as compounds with molecular weighs lower than

900 Da and a size around 1 nm [110] are too small compared to the hydrogel mesh size and will rapidly diffuse out of the microgels. Therefore, to achieve small-molecule sustained release, a drug delivery system needs to be incorporated into the microgels. For this purpose, poly(lactic-co-glycolic) acid (PLGA) nanoparticles encapsulated within the microgels network will be used to control the delivery of small molecule drugs. PLGA nanoparticles have been extensively used in the drug delivery field and are know to be a simple, yet effective strategy to achieve encapsulation and sustained release of hydrophobic small molecule drugs [111].

Nano-composite microgels such as those proposed in this aim have not been reported as intra-articular drug delivery systems. This vehicles could serve as drug-loaded nanoparticles depot for improved intra-articular retention. Additionally, the development of PEG microgels able to deliver small-molecule drugs in a sustained manner could expand the applications of these systems to simultaneously deliver a combination of therapeutics such as cells, synthetic small-molecules and biologics.

3.2 Materials and Methods

3.2.1 Materials

All chemicals were used as received. Poly(lactic-co-glycolic) acid (50:50, Mw: 24,000 - 38,000 Da), poly-vinyl-alcohol (Mw: 31,000 - 50,000 Da, 87-89% hydrolyzed), dichloromethane (anhydrous, $\geq$99.8%), mineral oil, SPAN80, bovine serum albumin (BSA, $\geq$98%), Rhodamine B ($\geq$95%) and methanol (anhydrous, 99.8%) were purchased from Sigma. Four-arm poly(ethylene-glycol)-maleimide (20 kDa) was acquired from Laysan Bio, phosphate buffered saline (PBS) from Corning, HEPES buffer (1M) from Life Technologies and ultra-pure dithiothreitol (DTT) from Thermo Fisher Scientific.

3.2.2 Synthesis of PLGA nanoparticles

PLGA particles containing model small molecules such as Rhodamine B and Cyanine 7, were synthesized by oil-in-water emulsion method. Briefly, 210 mg of PLGA were dissolved in 6 mL of dichloromethane (DCM). To obtain PLGA nanoparticles loaded with model small molecules, 1 mL of the desired compound solution in DCM was added to the PLGA. Then, the mix was added to 50 mL of 1% polyvinyl-alcohol (PVA) in distilled water and sonicated using the VibraCell™ Ultrasonic Processor (VCX 130 PB) at a 100% amplitude for 3 min. The obtained emulsion was added to 50 mL 1% PVA solution and magnetically stirred for 4h to promote DCM evaporation and particles formation. The resultant PLGA nanoparticles were washed with distilled water three times via centrifugation at 16,000g for 10 min. Finally, the particles were lyophilized and stored at -20℃. Nanoparticles size was determined using dynamic light scattering (DLS).

3.2.3 Synthesis of PLGA-loaded PEG microgels

PEG microgels were synthesized using microfluidics technology. PDMS flow-focusing devices with a nozzle size of 46.5$\pm$0.5 μm were fabricated using a soft lithography from silicon and SU8 masters. Devices were plasma treated and bonded directly to glass slides. Prior to use, devices were primed with an oil phase solution (2% SPAN80 in light mineral oil). Then a 6% w/v 20 kDa PEG-4MAL solution in an aqueous phase (PBS with Ca^{++} and Mg^{++} ($PBS^{+/+}$): Optiprep (2:1) containing 20 mM HEPES) was infused into the microfluidic device to form polymer droplets, which were cross-linked using an emulsion formed with one part of aqueous DTT (30 mg/mL in $PBS^{+/+}$ with 20 mM HEPES) and 14 parts of 2% SPAN80 in mineral oil. The resultant cross-liked hydrogels were collected in a 15 mL conical tube containing 1% bovine serum albumin (BSA) which acts as a surfactant to prevent microgels aggregation. After formation, microgels were washed in 1% BSA solu-

tion five times by centrifugation at 1000g for 5 min to remove mineral oil and DTT.

In order to obtain PLGA-loaded microgels, PLGA nanoparticles were mixed with the 6% w/v PEG-4MAL solution prior to infusion into the microfluidic device at different concentrations (0.25%, 0.50% and 1.00% w/v). Size distribution of empty and PLGA-loaded microgels was evaluated using microscopy image analysis in ImageJ. Also, PLGA nanoparticles distribution inside the microgels was evaluated using a Matlab image processing algorithm. For every microgel present in the confocal images, the fluorescent area that represents the encapsulated Rhodamine B-loaded PLGA particles was measured as a percentage of the total microgel area. Then, a distribution of the percentage fluorescent area per microgel was generated (Appendix A.2).

3.2.4 Small molecule release profile characterization

Rhodamine B-loaded PLGA nanoparticles were prepared by oil-in-water emulsion as described before. Rhodamine B was then extracted in methanol for 24 h and the loading efficiency was measured using spectrophotometry at λ_{ex} 553, λ_{em} 627. Then, PEG microgels containing three different PLGA nanoparticles concentrations (0.25%, 0.50% and 1.00% w/v) were prepared as described before. Their Rhodamine-B release profile was compared to PLGA nanoparticles alone at a concentration comparable to the 1% PLGA microgels group. Four microgels batches at the three different PLGA concentration were prepared using 27 μL of PEG precursor solution. Empty microgels were also synthesized and loaded with a Rhodamine B solution (5 μg/mL) by physical entrapment. PLGA particles, empty and PLGA-loaded microgels were then incubated at 4℃ with constant stirring in a total volume of 200 μL of 1% BSA solution. At each time point microgels samples were centrifuged at 1000g for 5 min and 150 μL of supernatant were taken for

Rhodamine B release measurements. The taken volume was then replaced with fresh 1% BSA solution. For PLGA nanoparticles alone a centrifugation speed of 16,000g was used instead. The relative cumulative release profiles were analyzed using a zero- and first- order curve fit, which were compared for their goodness of fit using the Akaike's Information Criterion (AIC).

3.3 Results

3.3.1 PLGA nanoparticles and PEG microgels

PLGA nanoparticles exhibited a mean size of 337.5 $\pm$ 91.2 nm (Figure 3.1a). The loading capacity was 3 μg of Rhodamine B per milligram of PLGA. Results show that microfluidic technology can be used to obtain PLGA nanoparticles-loaded PEG microgels with tight size distributions. All microgels formulations presented a mean size between 50.43 and 51.44 μm with coefficients of variation (CV) bellow 6.5% (See Table 3.1). Also, PLGA encapsulation did not significantly affect the microgel mean size, p-value$>$0.99 (Figure 3.1b).

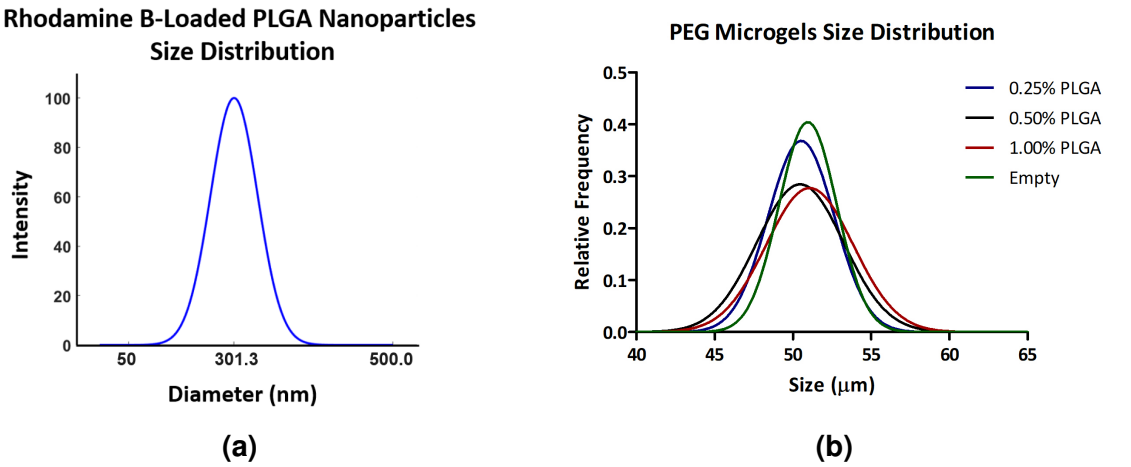

Figure 3.1: PLGA nanoparticles and PEG microgels size distribution. (a) PLGA nanoparticles size distribution (b) Microgels size distribution is not affected by PLGA particles encapsulation at any of the evaluated PLGA concentrations.

Table 3.1: PLGA NPs-loaded microgels mean size and coefficient of variance (CV%).

PLGA NPs (% w/v)	Mean diameter $\pm$ SD (μm)	CV (%)
0.00	50.97 $\pm$ 2.65	5.20
0.25	50.43 $\pm$ 2.21	4.38
0.50	50.94 $\pm$ 3.28	6.44
0.10	51.44 $\pm$ 3.33	6.48

Figure 3.2a shows bright field and fluorescence images of PEG microgels containing PLGA nanoparticles at different concentrations. Microgels loaded with 0.25% w/v PLGA nanoparticles exhibit an unimodal distribution, with microgels containing on average 28% of their area filled with PLGA nanoparticles (Figure 3.2b). However, as the PLGA nanoparticles concentration increases, a bimodal distribution is observed, with higher number of microgels presenting PLGA nanoparticles in 10% and 90% of their area. This phenomenon is more pronounced in the 1.00% w/v PLGA group and can be attributed to the PLGA hydrophobic nature, which leads to nanoparticle aggregation as its concentration increases in the precursor 6% PEG-4MAL solution. (Figure 3.2b).

3.3.2 Small molecule release profile

Figure 3.3 shows the obtained cumulative release profiles in both, absolute and relative scales. Empty PEG microgels released over 90% of their initial Rhodamine B content in the first 2 h. However, the microgels containing Rhodamine B-loaded PLGA nanoparticles presented a sustained release. Figure 3.3a shows that the total released Rhodamine B can be controlled by simply changing the amount of PLGA nanoparticles encapsulated inside the PEG microgels. To determine if the

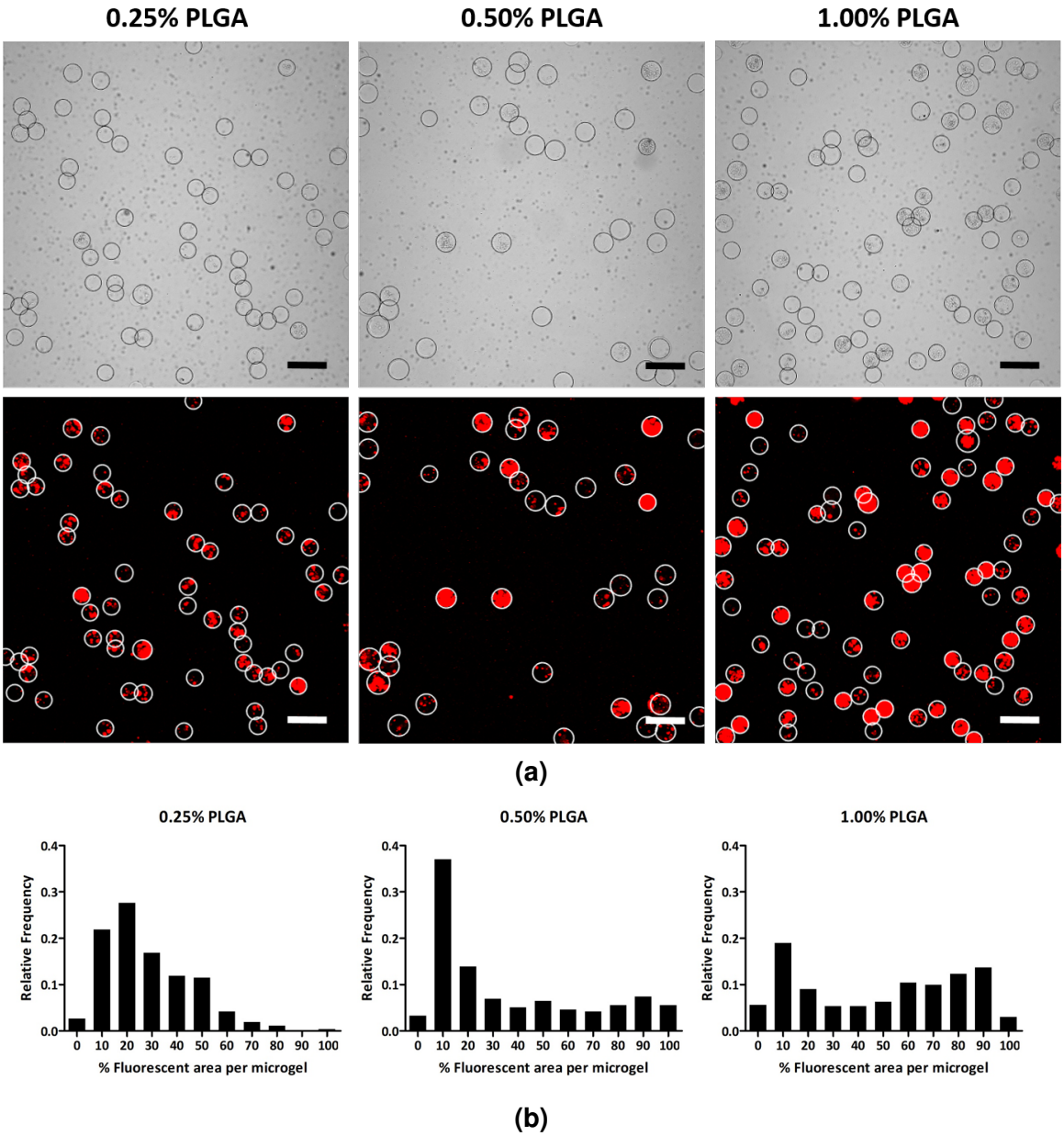

Figure 3.2: PLGA nanoparticles distribution inside PEG microgels. (a) Microgels representative confocal images. Scale bar: 100 μm (b) Poisson distribution of the percentage area filled with PLGA nanoparticles per microgel at 0.25% PLGA, 0.50% PLGA and 1.00% w/v PLGA.

obtained release profiles were better described by a zero- or first-order model, the Akaike's Information Criterion (AIC), which reports a probability that each model is correct, was used. Results suggested that the obtained profiles could be modeled using a zero-order release kinetics equation with a probability higher than 99% compared to a first-order model. As expected, the release rate of Rhodamine B from PLGA nanoparticles alone is comparable to the one observed for microgels containing 1% w/v PLGA (Figure 3.3c). Figure 3.3b show that microgels containing PLGA nanoparticles exhibit a release profile comparable to PLGA nanoparticles alone, achieving around 50% drug release in 16 days. This results suggest that the release rate is mainly controlled by the polymeric nanoparticles and not by the hydrogel. Overall, these results support the hypothesis that small molecule drugs are rapidly released from PEG microgels and need a secondary vehicle able to control the release rate in order to achieve a sustained delivery.

The release rate will depend on the drug properties and the polymer characteristics. In this case, PLGA nanoparticles either alone or encapsulated in PEG microgels exhibited zero-order release kinetics. Typically PLGA nanoparticles containing hydrophobic molecules exhibit a bi-phasic release profile [112, 113]. The initial phase corresponds to the rapid burst release of drug molecules present at the surface of the particles. Then, a diffusion-controlled slow release phase occurs, which usually follows a near-zero order release kinetics [113]. Consistent with research evaluating the release of different molecules from PLGA nanoparticles [114, 115], the rhodamine B release profiles obtained in this study demonstrated a zero-order profile. It is possible to observe that the free PLGA nanoparticles group presented an initial burst release (10.02 $\pm$ 2.76% by day 1) followed by a zero-order profile, while microgels formulations did not exhibit an initial fast release. This can be evident at day 1 when the amount of rhodamine B released from PLGA

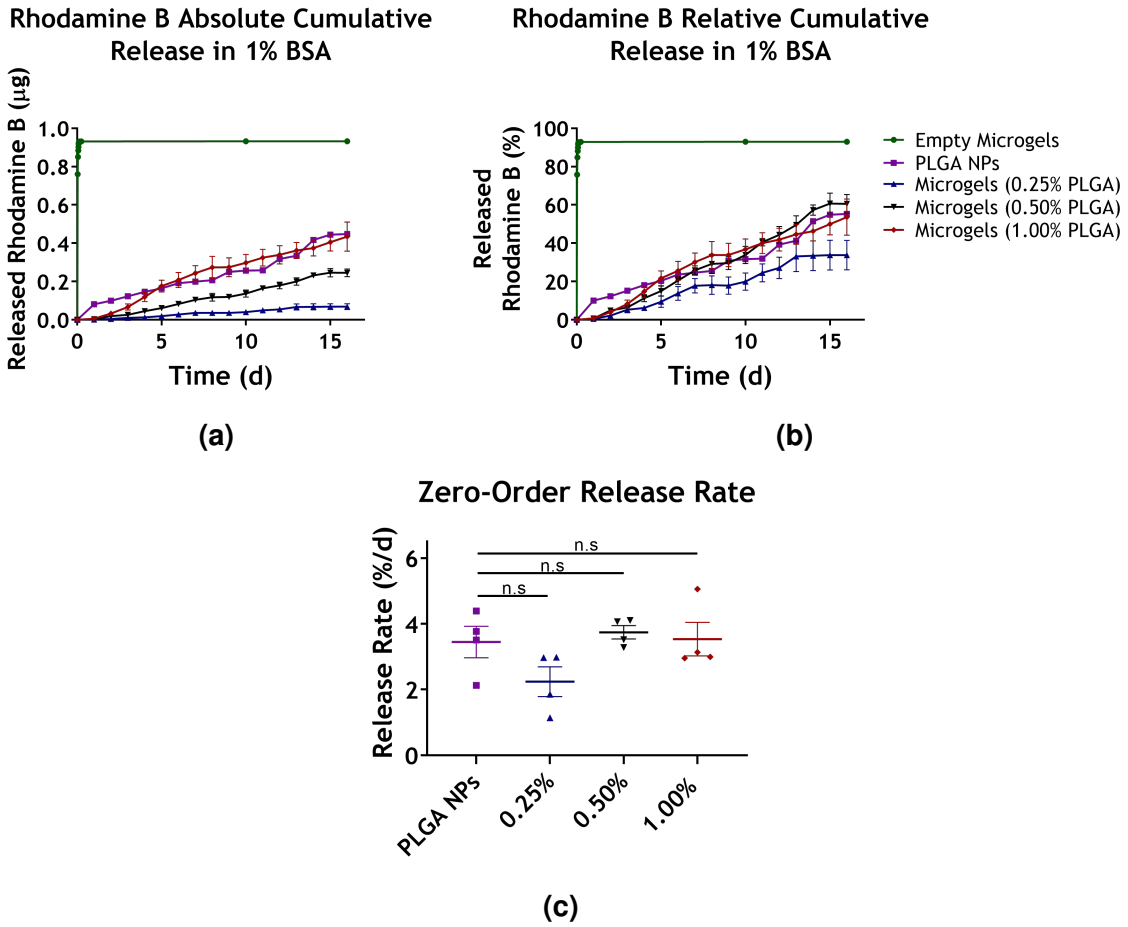

Figure 3.3: Small molecule release profile from PLGA NPs-loaded PEG microgels. Rhodamine B release profile from PLGA nanoparticles-loaded PEG microgels (Mean ± SEM) (a) Absolute cumulative release. (b) Relative cumulative release. n=4. (c) Release rate obtained from a zero-order model fit. Mean ± SEM, ANOVA demonstrated no significant differences among groups, p-value: 0.1071.

nanoparticles alone was significantly higher than that of PEG microgels groups (p-value$<$0.0001). The lack of an initial burst release phase from PLGA nanoparticles contained in PEG microgels could be attributed to the extensive washing steps involved during their synthesis, which can easily remove the rhodamine B molecules present at the PLGA nanoparticles surface.

3.4 Discussion

In this study, the possibility of using PEG microgels as small molecule drug delivery systems was investigated. The use of PEG-4MAL and microfluidics technology allowed for microgels synthesis under physiological conditions. Compared to other materials typically used for the fabrication of microgels as drug delivery systems [116, 117, 118, 119, 120, 121, 122, 123], microfluidics synthesis of PEG-4MAL microgels does not require organic solvents, high temperatures or extreme pH, which makes this technology compatible with other potential therapeutic agents such as biologics, proteins and cells [101, 102, 100].

In this chapter, the use of a secondary drug delivery vehicle such as PLGA nanoparticles was shown to be a simple, yet effective strategy to achieve small molecule loading and sustained release from PEG microgels. Direct encapsulation of small molecule drugs into hydrogels usually results on burst release due to their rapid diffusion through the polymer mesh [101]. Therefore, other studies have proposed the optimization of hydrogel chemical and physical properties to achieve controlled release of drugs from a wide variety of systems. Control over the hydrogel mesh size, swelling ratio, the interactions between the drug and the polymer network and hydrogel degradation rate, have all been used to achieve drug loading and sustained release from hydrogel systems [124]. However, these techniques do not allow independent control of hydrogel properties and drug release rate. Cova-

lent conjugation of small molecule drugs to the hydrogel network has also been reported as an alternative to achieve sustained small molecule release [124], but this approach could interfere with the drug activity.

Hydrogels containing nano-stuctures, known as nano-composite hydrogels, originated as a strategy to improve hydrogel mechanical properties, confer specific optical or magnetic characteristics and develop stimuli-responsive and catalytic systems, particularly in macro-sized gels [125, 126, 127]. More recently, the incorporation of nano-scale drug delivery systems into macro-, micro- and nano-sized hydrogels has open the possibility of independently controlling hydrogel properties and drug release rate [116]. The proposed PLGA nanopoarticles-loaded PEG microgels take advantage of this hybrid design to achieve small molecule drug loading and sustained release as demonstrated in this chapter, while independently controlling PEG hydrogel properties to achieve specific tissue binding and prolonged intra-articular retention as reported throughout this thesis dissertation.

Gelatin, chitosan, PEG, agarose and poly-(N-isopropylacrylamide) have been used for the synthesis of multiple nano-composite micro- and nano-gels loaded with metallic or polymeric nanoparticles, carbon nano-tubes and liposomes [116, 128, 117, 118, 119, 120, 121, 122, 123]. These formulations have been studied for the passive or stimuli-responsive (i.e. temperature, pH, magnetic field) release of small molecule drugs for applications in cancer and infection treatment, ocular drug delivery, spinal chord injury and inflammatory bowel disease [116]. Although nano-composite microgels have been extensively studied for a variety of biomedical applications, to the best of our knowledge this is the first time that a nanoparticle-microgel hybrid system is reported as an intra-articular drug delivery vehicle.

Considering the complexity and multi-target nature of OA, the ideal intra-articular drug delivery system for the treatment of osteoarthritis should allow drug sustained release, be retained in the intra-articular space without inducing further joint degenerative changes or significant synovial inflammation and support tissue-specific drug delivery. The reported nano-composite PEG microgel system offers a highly customizable platform that permits the control of drug delivery rate independently of PEG hydrogel properties, which could be optimize to comply with all the aforementioned design criteria. The results presented in this chapter demonstrated that for 6% w/v 20 kDa PEG microgels, small molecule drug delivery is only controlled by polymeric nanoparticles contained within the hydrogels. In this case, rhodamine B was delivered from PLGA nanoparticles with zero-order release kinetics during 16 days. It is important to note that the exact formulation used for the studies reported in this chapter may not be ideal for every small molecule. Depending on the drug hydrophobicity, size and nature (synthetic or biologic), the nano-sized delivery vehicle incorporated into PEG microgels will need to be optimized. In this regard, polymeric nanoparticles such as PLGA are not always ideal and the use of other types of delivery vehicles such as liposomes, micelles or solid lipid nanoparticles may be required.

Although the encapsulation of gold nanoparticles and DNA aptamer-loaded solid lipid nanoparticles into PEG microgels using microfluidic technology was explored, thorough characterization of small molecule controlled release from PEG microgels was only conducted using one type of delivery system and rhodamine B as model drug. To demonstrate the versatility of microfluidics technology, systematic evaluation of the encapsulation of multiple drug-loaded nano-sized structures into PEG-based hydrogels would be needed. These future investigations could

open the possibility of loading PEG microgels with a combination of nano-sized delivery vehicles for the evaluation of combinatorial therapeutic strategies for OA treatment. Thus, microfluidic technology could allow high throughput synthesis of PEG microgels containing multiple drug-loaded nano-sized delivery systems with different properties and independent release kinetics.

3.5 Conclusions

The results presented in this chapter support the hypothesis that PEG-4MAL microgels alone are not able to control the release rate of small molecule drugs, thus an additional drug delivery system such as PLGA nanoparticles should be incorporated into the microgels in order to achieve a sustained release. In particular, rhodamine B loaded into PLGA nanoparticles, was used as a model small molecule drug, which was released following zero-order kinetics. However, microfluidics technology could allow the synthesis of versatile PEG microgels, which could be used to encapsulate other drug-loaded nanoparticles vehicles in order to achieve the desired release rate for a particular drug. The use of nano-composite PEG-4MAL microgels could expand on the possibility of using complex delivery vehicles for the release of a combination of therapeutics including synthetic small molecules, biologics and cells for the treatment of OA.

CHAPTER 4
ENGINEERING SYNOVIUM- AND CARTILAGE-BINDING PEG MICROGELS THROUGH ACTIVE TARGETING STRATEGIES

4.1 Introduction

A variety of molecular targets and small molecule drugs for the treatment of OA have been identified and are being evaluated for their ability to either reduce pain and inflammation or to decrease OA progression in pre-clinical models[7]. However, off-target effects on surrounding tissues have hindered their translation into the clinic [10, 76, 11, 77]. Molecules intended to reduce pain an inflammation, processes that occur primarily in the synovial membrane, can negatively affect the articular cartilage. Examples include NSAIDs and nerve growth factor (NGF) blockers, which reduce proteoglycan secretion and worsen OA progression [10, 76]. On the other hand, drug candidates that have promising effects on articular cartilage regeneration, have shown off-target effects. For example, intra-articular injection of TGF-β1 increases synovium hyperplasia and induces the formation of cartilage-like tissues in ligaments and synovium [11]. Moreover, the use of a chondrogenic molecule, Kartogenin (KGN), in a rat model of tendon-to-bone injury resulted in excessive cartilage-like tissue formation in unintended areas and overgrowth of surrounding tissues [77].

Thus, the objective of this aim was to design cartilage- and synoviocyte-binding PEG microgels using targeting peptides. The working hypothesis was that peptide-functionalized PEG microgels will be able to specifically bind to synoviocytes or ar-

ticular cartilage. The rationale for this hypothesis is that active targeting strategies such as conjugation of targeting peptides to PEG microgels can be used to achieve tissue-specific binding of these delivery vehicles. For this purpose, a cell targeting peptide (HAP-1) able to bind to synoviocytes [95], and an ECM-targeting peptide (WYR) shown to bind to collagen type II α1 [86] will be used to target synovium and articular cartilage respectively.

In the future, tissue-specific intra-articular drug delivery vehicles could serve as a platform to better study the off-target effects of drug candidates or facilitate their translation into the clinic. Also, considering that OA is a complex disease involving all intra-articular tissues, the proposed delivery system could offer the possibility of engineering fine multi-target treatments for OA.

4.2 Materials and Methods

4.2.1 Materials

Articular cartilage- and synoviocytes-binding peptides were purchased from GenScript. The amino acid sequences of the used peptides is shown in Table 4.1. Cartilage-binding peptide (WYRGRLC) will be abbreviated as WYR, synoviocytes-binding peptide (CSFHQFARATLAS) as HAP-1 and integrin-binding peptide (GRGDSPC) as RGD. Their scrambled sequences, YRLGRWC, CALSQAFRHAFTS and GRDGSPC, will be referred as WYRsc, HAP-1sc and RDG, respectively. Gibco™ Ham's F12 nutrient mix and CellTracker Green™ were purchased from Thermo Fisher Scientific. Human synovial sarcoma cell line (SW982), rabbit fibroblast-like synoviocytes (HIG-82) and mouse myoblasts (C2C12) were purchased from ATCC, mouse preosteoblasts (MC3T3-E1) were acquired from RIKEN.

4.2.2 Synthesis of peptide-functionalized PEG microgels

Peptide-functionalized PEG microgels were synthesized using microfluidics technology as described in Chapter 3 with minor modifications. PEG-4MAL macromer solution (6% w/v) was reacted at room temperature and pH 7 with 1 mM of cartilage-targeting peptide (WYR), synoviocyte-targeting sequence (HAP-1), integrin-binding peptide (RGD) or their respective scrambled controls, resulting in a maleimide (MAL) to peptide ratio of 12:1. Then, the functionalized 6% w/v macromer solution was infused into the microfluidic device to form microgels as described before. Studies conducted in the Garía laboratory using RGD demonstrate that for MAL:peptide ratios of 1:1 and higher, this is a very efficient reaction that presents near 100% of peptide incorporation [100]. Therefore, a final 1mM peptide concentration will be assumed for all the peptides used in this study.

Table 4.1: Synoviocytes, cartilage and integrin-binding peptide sequences.

Peptide	**Sequence**
HAP-1	CSFHQFARATLAS
HAP-1sc	CALSQAFRHAFTS
WYR	WYRGRLC
WYRsc	YRLGRWC
RGD	GRGDSPC
RDG	GRDGSPC

4.2.3 Peptide-functionalized PEG microgels binding assays

The selected peptides HAP-1 and WYR are expected to target synoviocytes and articular cartilage respectively. However, their targeting mechanism is different. HAP-1 peptide has been shown to bind to rabbit synoviocytes, but the exact mechanism and targeted receptor is still unknown [95]. In contrast, WYR sequence has been proven to bind specifically to collagen type II α1 [86] and not directly to chondrocytes. Therefore, to conduct binding assays for these peptides, two platforms were used. First, synoviocytes were cultured in monolayer to asses HAP-1-functionalized PEG microgels binding ability. On the other hand, a collagen type II-rich tissue such as fresh bovine cartilage was used to evaluate WYR-functionalized microgels. These two experimental platforms are described below.

Cell monolayer platform: synoviocytes targeting peptide (HAP-1) binding and specificity assays

To evaluate the ability of HAP-1 peptide to bind specifically to synoviocytes, rabbit and human synoviocytes (HIG-82 and SW982), mouse myoblasts (C2C12) and mouse preosteoblasts (MC3T3-E1) were cultured in a 24-well plate at an initial seeding density of 100,000 cells/well for one day to achieve over 95% confluency. C2C12 and MC3T3-E1 cell lines were used as negative controls to assess microgels binding specificity. Cells were then stained using CellTracker Green^{TM} according to the manufacturer's instructions.

PEG microgels containing Rhodamine B-loaded PLGA particles and functionalized with either 1 mM HAP-1, HAP-1sc, RGD or RDG (n = 4 wells per group) were suspended in growth media (Ham's F12 media supplemented with 10% fetal bovine serum (FBS)) and incubated with the different cell lines for 30 min (500 μL of microgels solution per well). For this experiment, the peptide RGD was used as positive control because it is recognized by 12 out of 20 known integrins [129],

thus it was expected to bind any of the used cell types. Then, unbound microgels were washed three times using growth media. Ten images per well were taken at random positions using confocal microscopy and bound microgels were manually quantified. Data was subjected to a natural logarithm transformation to correct for its non-normality and heteroscedasticity and then analyzed via a one-way nested ANOVA [130].

Bovine cartilage platform: cartilage targeting peptide (WYR) binding and specificity assay

The binding assays to evaluate the cartilage targeting peptide WYR and its scrambled control (WYRsc) were conducted on 10 μm thick fresh bovine cartilage frozen sections. This system was chosen because WYR peptide has been shown to bind to collagen type II α1 [86], therefore a collagen II-rich surface, such as bovine cartilage was desired. Sections of approximately 1 cm^2 were stained with DAPI and incubated for 30 min with 100 μL of WYR or WYRsc-functionalized PEG microgels at a concentration of 170,000 microgels/mL in growth media (10% FBS supplemented Ham's F12 media). Three cartilage sections were analyzed. Then, samples were washed twice using growth media to remove unbound microgels. A minimum of 7 randomly located images per sample were taken using confocal microscopy and bound microgels were then manually quantified.

To assess for the specificity of the cartilage-targeting peptide and confirm that it does not bind to synoviocytes, a microgels binding assay was conducted using the HIG-82 cells monolayer platform as described in section 4.2.3.

4.3 Results

4.3.1 Synoviocytes targeting peptide (HAP-1) binding and specificity assays

Microgels functionalized with synoviocyte-targeting peptide (HAP-1) were evaluated for their ability to specifically bind to synovial cells. As expected, Figure 4.1 shows that positive control microgels, functionalized with RGD peptide, bind to all evaluated cell types to a greater extent compared to its scrambled control RDG.

Moreover, HAP-1-functionalized PEG microgels bind to rabbit synoviocytes to the same level as RGD microgels but in a specific manner as evidenced by their lower binding capacity to C2C12 and MC3T3-E1 cells. Also, HAP-1sc presented a binding level comparable to RDG negative control microgels in all cell types. These results demonstrate that HAP-1 is able to bind specifically to rabbit synoviocytes allowing for active binding of functionalized PEG-4MAL microgels.

HAP-1 peptide, was discovered via phage display using HIG-82 rabbit synoviocyte cells [95]. Therefore, to evaluate if PEG microgels functionalized with HAP-1 are able to bind to human synoviocytes as well, binding assays using a cell monolayer system were conducted with synovial human sarcoma cell line SW982. In this case, rabbit synoviocytes (HIG-82) were used as a positive control cell line and RGD-functionalized PEG microgels were utilized as a positive control formulation. Figure 4.2 shows representative confocal images and quantitative data confirming the feasibility of using HAP-1 peptide to target human synoviocytes via PEG microgels as well. As expected and consistent with previous experiments, RGD-conjugated PEG microgels bind synovial human sarcoma cells at a higher level compared to RDG control. Also, HAP-1-functionalized microgels bind to SW982 cells to level comparable to RGD and present higher binding capacity compared to its scrambled control peptide HAP-1sc.

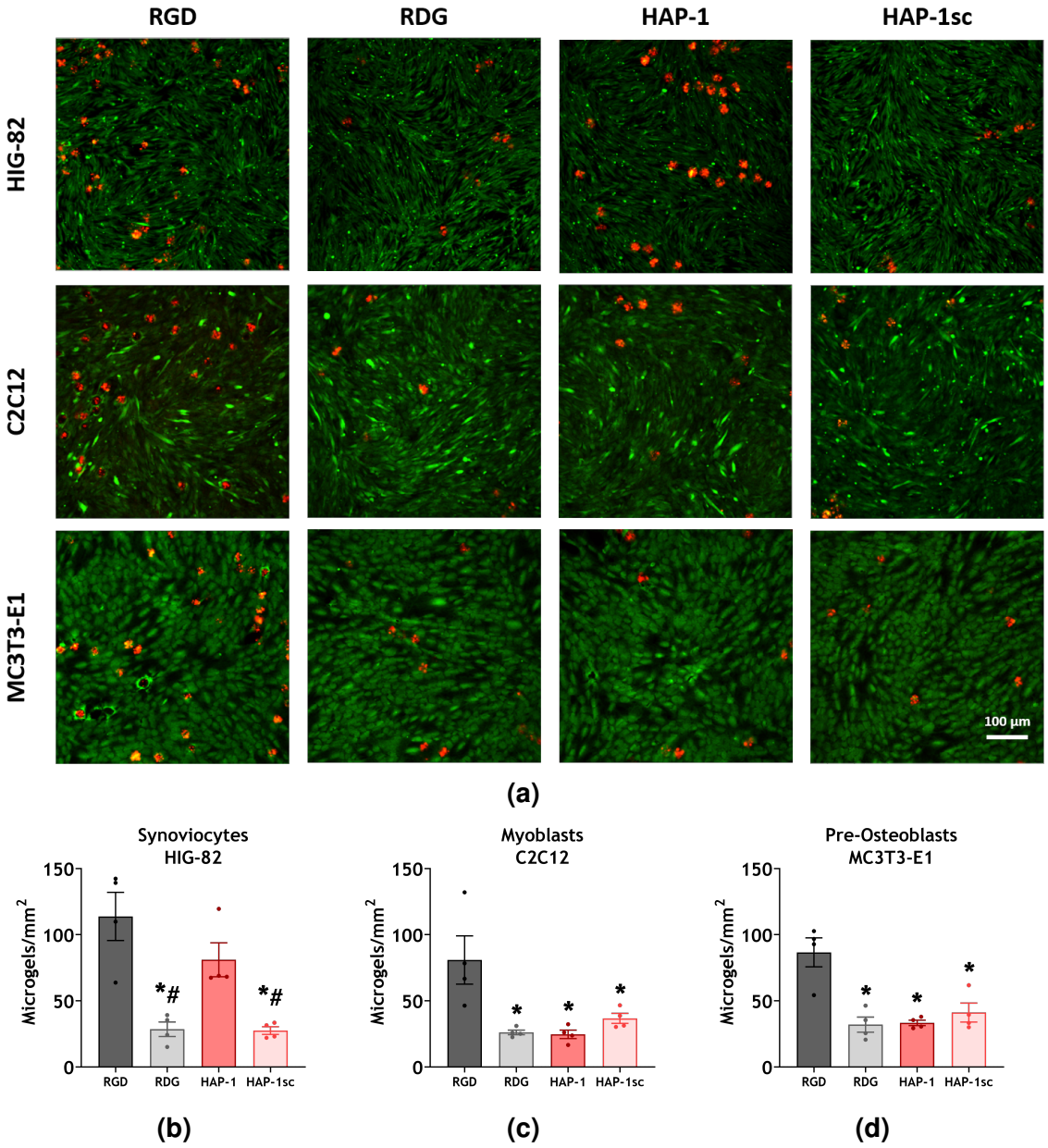

Figure 4.1: HAP-1 peptide-functionalized PEG microgels binding to rabbit synoviocytes. (a) Representative confocal images of PEG microgels (red) bound to cells stained with Cell Tracker Green^{TM}. Scale bar: 200 μm. (b-d) Bound microgels quantification. RGD-functionalized microgels bind to rabbit synoviocytes (HIG-82), mouse myoblasts (C2C12) and mouse pre-osteoblasts (MC3T3-E1). HAP-1 peptide-functionalized PEG microgels bind to synoviocytes (HIG-82) to the same extent as RGD-functionalized microgels and is specific for HIG-82 cells. Mean $\pm$ SEM, *p$<$0.05 compared to RGD, #p$<$0.05 compared to HAP-1, n = 4 wells, 10 images per well. Nested-ANOVA

4.3.2 Cartilage targeting peptide (WYR) binding and specificity assays

WYR-functionalized PEG microgels were evaluated for their ability to specifically target collagen type II present in bovine articular cartilage fresh frozen sections. Figure 4.3 show that WYR-functionalized PEG microgels bind to bovine cartilage to a greater extent than the scrambled control (WYRsc). This results demonstrate that WYR conjugation of PEG microgels can be used to achieve binding to articular cartilage.

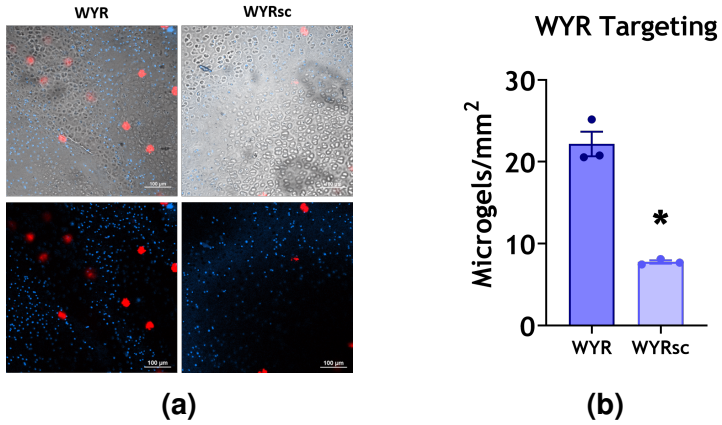

Figure 4.3: WYR peptide-functionalized PEG microgels binding assays. (a) Representative confocal images of PEG microgels (red) bound to bovine articular cartilage sections stained with DAPI (blue). Scale bar: 100 μm. (b) WYR-functionalized microgels bind to bovine cartilage sections to a higher level than the scrambled control WYRsc. Mean $\pm$ SEM, n=3, *p$<$0.05.

Then, to evaluate if the WYR-functionalized PEG microgels specifically bind to articular cartilage, a binding assay was conducted using a synoviocyte monolayer platform. Consistent with previous experiments, RGD- and HAP-1-functionalized

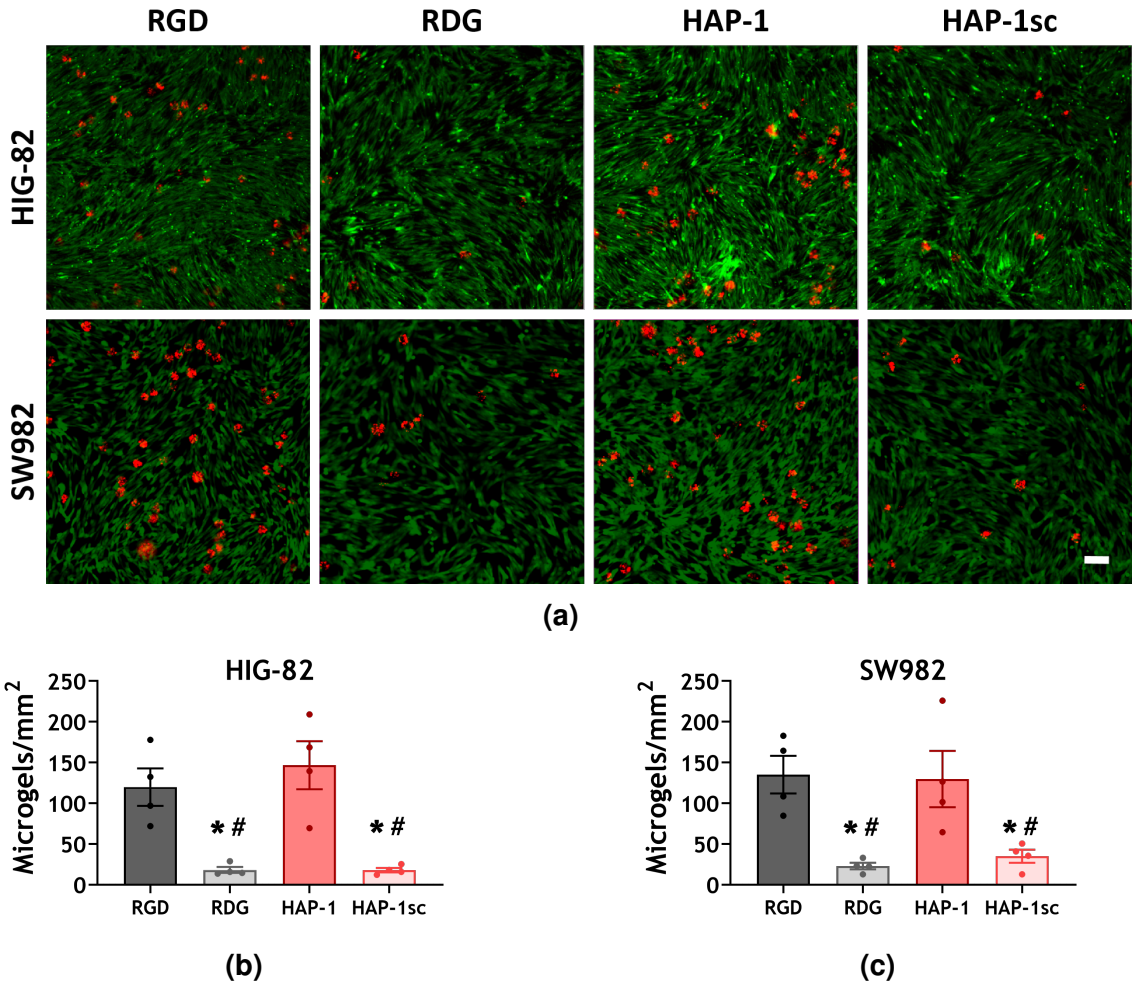

Figure 4.2: HAP-1-functionalized PEG microgels binding to human synoviocytes. (a) Representative confocal images of PEG microgels (red) bound to cells stained with Cell Tracker Green^{TM}. Scale bar: 100 μm. Bound microgels quantification. RGD- and HAP-1-functionalized microgels bind to (b) rabbit synoviocytes (HIG-82) and (c) synovial human sarcoma cells at a higher level than negative control microgels (RDG and HAP-1sc). Mean $\pm$ SEM, *p$<$0.05 compared to RGD, #p $<$ 0.05 compared to HAP-1, n = 4 wells, 10 images per well.

PEG microgels bound to synoviocytes to a greater extent compared to negative control microgels (RDG and HAP-1sc), while WYR-microgels exhibited binding levels comparable to those of the negative controls RDG, HAP-1sc and WRYsc (Figure 4.4). These results confirm that WYR-functionalized microgels do not preferentially bind to synoviocytes and could be a promising strategy to achieve specific binding to articular cartilage.

4.4 Discussion

In this chapter, the possibility of using tissue targeting peptides to achieve PEG microgels specific binding to articular cartilage and synoviocytes was investigated *in vitro*. PEG-4MAL microgels were functionalized with previously discovered targeting peptides [86, 95] and their binding ability to tissues of interest and specificity was demonstrated. In particular microgels functionalized with HAP-1 peptide exhibited higher binding levels when incubated with rabbit and human synoviocytes than other cell types such as myoblasts and pre-osteoblasts, demonstrating its binding specificity for fibroblast-like synovial cell lines. On the other hand, microgels functionalized with the collagen type II targeting peptide (WYR) bound to bovine articular cartilage and presented low binding when incubated with rabbit synoviocytes.

Osteoarthritis treatment has evolved towards a more localized therapy in recent years. In this regard, intra-articular injection emerged as a possibility to deliver therapeutics into the joint space both, to prevent the possible secondary effects related to systemic drug delivery and to achieve a sufficiently high intra-articular drug concentration to elicit a desired response. However, research on the detrimental effects of commonly used NSAIDs on articular cartilage and a better understanding

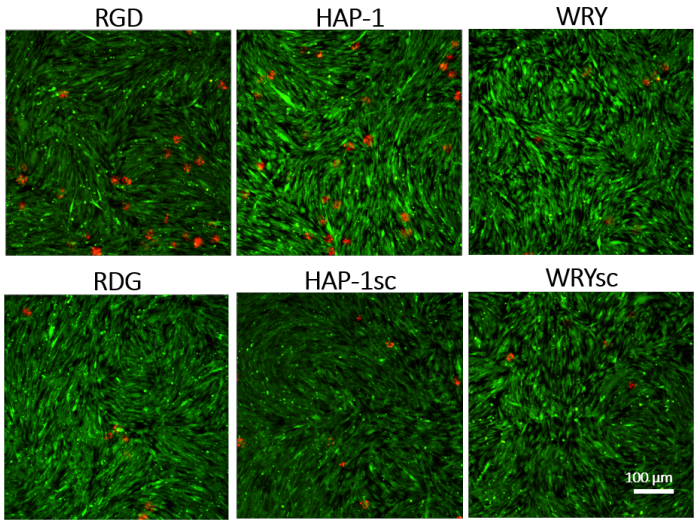

(a)

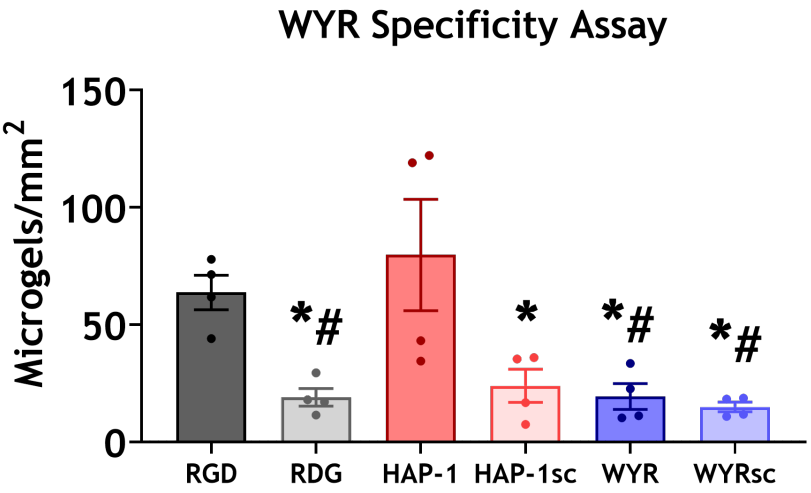

(b)

Figure 4.4: WYR peptide-functionalized PEG microgels specificity assay. (a) Representative confocal images of PEG microgels (red) bound to rabbit synoviocytes stained with Cell Tracker Green^{TM}. Scale bar: 100 μm. (b) Binding level of WYR peptide-functionalized PEG microgels to synoviocytes is significantly lower than RGD- and HAP-1-functionalized microgels. Mean $\pm$ SEM, n=4, 8 images per group, *p$<$0.05 compared to HAP-1, # p$<$0.05 compared to RGD

of the off-target effects of some promising drug candidates have shown the necessity of engineering specific tissue-binding drug delivery methods for OA treatment like those proposed in this dissertation [3, 53, 7].

Traditionally, OA has been understood as a disease affecting primarily the articular cartilage. Therefore, research regarding targeted therapy for OA treatment has mainly focused on cartilage passive and active targeting approaches. The physicochemical properties of the articular cartilage pose a challenge to the delivery of therapeutic molecules into this tissue [131]. First, direct drug transport via vascular structures is not possible due to its avascular, aneural and alymphatic nature. Also, cartilage extracellular matrix, primarily composed of collagen type II and sulfated glycosaminoglycans, presents a small pore size (60-200 nm) and high negative charge, which difficult the penetration of molecules into this tissue [87, 131].

Delivery vehicles in the micron scale, like those described in this dissertation, are unable to penetrate the articular cartilage and administer the therapeutic molecules directly into the tissue. However, Ambika *et al.* used pharmacokinetics modeling to explain that although micron-scale delivery systems may not be ideal for direct intra-cartilage drug release, non-penetrating particles able to bind to the surface of the articular cartilage may enable higher intra-cartilage drug concentrations compared to non-penetrating particles that do not present any cartilage-binding mechanism after intra-articular injection [131]. However, these computational modeling results have not been experimentally evaluated. In this chapter WYR-functionalized PEG microgels were shown to bind to bovine articular cartilage sections *in vitro* and are expected to bind to the cartilage surface, particularly to damaged areas where collagen type II fibers are exposed *in vivo*. However, the ability of cartilage-binding PEG microgels to deliver small molecule drugs into the

tissue was not investigated. To the best of our knowledge, this is the first time that active cartilage targeting peptide is utilized for the conjugation of micron-size drug delivery systems, thus the proposed microgels could be used to expand the field knowledge regarding the effect of cartilage targeting on drug pharmacokinetics. For example, WYR-functionalized PEG microgels could be a promising platform to study whether or not non-penetrating cartilage-binding drug delivery systems present an advantage over conventional non-targeting vehicles in terms of drug penetration and retention into the cartilage, as pharmacokinetics modeling suggests [131].

Furthermore, the type of cartilage targeting moieties (active or passive) could have important consequences on the effectiveness of the delivery vehicle's binding ability to cartilage. Both, active and passive targeting strategies have been extensively studied for cartilage penetrating nanoparticles [132, 81, 82, 83, 84, 85, 86]. In fact, Vedadghavami *et al.* recently demonstrated that the depth of penetration into the articular cartilage for cationic peptide carriers of 7 nm in diameter, depends on their charge and the cartilage glycosaminoglycan content. The researchers demonstrated that for healthy bovine cartilage explants the uptake of cationic nano-carriers increased proportionally with net charge up to +14 mV. However, the authors reported that positively charged nano-carriers uptake and retention in articular cartilage explants with lower glycosaminoglycan content were reduced due to a decrease in the cartilage negative charge [132]. Therefore, passive targeting via electrostatic interactions may not be as effective on later stages of OA progression.

Active targeting strategies offer an alternative for achieving cartilage binding independently on glycosaminoglycan content. For that reason, the PEG-based drug delivery vehicles described in this dissertation used a collagen type-II targeting

peptide (WYR) to confer cartilage binding ability to microgels. As demonstrated in this chapter, WYR-functionalized PEG microgels were able to bind bovine articular cartilage sections and presented low binding levels compared to other microgels (HAP-1 and RGD) when incubated with synoviocytes. However, one of the limitations of this dissertation is that direct comparison of the binding levels of WYR microgels between articular cartilage and synoviocytes is not possible due to the use of two different experimental platforms. To better investigate if WYR-functionalized PEG microgels preferentially bind to articular cartilage over synoviocytes, the development and standardization of binding assays using co-culture models would be necessary. These types of experiments could allow direct comparison of both WYR- and HAP-1-functionalized microgels binding levels to multiple intra-articular tissues, including the articular cartilage, synovial membrane, meniscus and ligaments.

In terms of synoviocytes targeting, our results demonstrate that HAP-1-functionalized PEG microgels are able to specifically bind to rabbit and human synovial cell lines. One limitation of these studies is that the specificity of HAP-1 microgels was assessed using myoblast and pre-osteoblasts, which are not normally exposed to the synovial fluid where these particles would be injected. To better predict whether HAP-1-functionalized PEG microgels would preferentially bind to the synovial membrane *in vivo*, binding assays using relevant cell lines such as ligament fibroblasts and chondrocytes would be necessary. Although HAP-1 peptide ability to target synoviocytes has been reported [95, 97, 96], the specificity of this interaction has never been evaluated using cell lines present in tissues exposed to the intra-articular space.

Moreover, HAP-1 peptide has been shown to induce internalization of peptide

complexes upon synoviocytes binding *in vitro* and in the synovial lining in a rabbit model [95]. Even though, the proposed 50 μ PEG microgels are considerable big to be internalized, the biological effect of the HAP-1 peptide in this delivery system is yet to be investigated. Bédouet *et al.* demonstrated that non-degradable PEG-dimathacrylate microgels get trapped in the synovial membrane and induce a foreign body response characterized by the presence of giant cells around the hydrogels [109]. Although the PEG chemistry used in this dissertation is different than the one reported by Bédouet *et al.*, it would be important to study if the conjugation of PEG-4MAL microgels with HAP-1 peptide would induce a more aggressive inflammatory response compared to HAP-1sc resulting from the activation of HAP-1-mediated particles internalization processes [95]. In fact, this dissertation could benefit from future investigation on the cellular response to long-term PEG microgels exposure in terms of inflammation and cytotoxicity. Additionally, synovium and articular cartilage *in vitro* co-culture models would be necessary to elucidate if tissue-binding of drug-loaded PEG microgels can in fact promote preferential drug delivery and penetration into the tissues of interest.

Overall, the results presented in this chapter demonstrate that peptide-functionalized PEG microgels bind to articular cartilage and synoviocytes *in vitro*. Further characterization would be required to assess the ability of these drug delivery vehicles to promote tissue-localized drug release. In the future, the use of the system proposed in this dissertation could facilitate the characterization and clinical translation of current drug candidates, that due to concerning off-target effects have not proven to be successful for the treatment of OA.

4.5 Conclusions

The results of this study demonstrate that PEG-4MAL microgels can be functionalized with cartilage- or synociocyte-binding peptides to achieve specific tissue binding. *In vitro* studies showed that HAP-1 functionalized microgels can bind to rabbit and human synoviocyte monolayer cultures and exhibited low binding levels to other cell types. Similarly, microgels conjugated with the collagen type II-binding peptide (WYR), effectively bound to bovine articular cartilage sections and presented a low binding levels when incubated with rabbit synoviocytes. Therefore, peptide-functionalized PEG microgels offer a promising injectable platform that could allow intra-articular tissue-specific binding and may be used for localized delivery of therapeutics for the treatment of OA.

CHAPTER 5
EVALUATING THE *IN VIVO* EFFICACY OF PLGA-LOADED PEPTIDE-FUNCTIONALIZED PEG MICROGELS AS SMALL MOLECULE DRUG DELIVERY SYSTEMS IN A RAT MODEL OF OA

5.1 Introduction

One of the main challenges in the development of a successful OA therapeutic is the design of a drug delivery system able to withstand the rapid clearance mechanisms of an arthritic joint. It has been shown that free small molecule drugs and proteins only remain in the intra-articular space for couple of hours (Table 2.1), whereas drug-loaded microparticles can extend this time up to few weeks [7]. Particles ranging from 1 to 180 μm have been evaluated in the field, however it has been shown that vehicles smaller than 3 μm are subjected to lymphatic clearance from arthritic joints [69] and larger particles have been associated with synovial inflammation [7]. The only FDA-approved microparticle-based technology for IA drug delivery is a 45 μm triamcinolone acetonide-loaded PLGA microparticle formulation for pain management in OA patients [74, 75]. Therefore, there is a need for micron-scale drug delivery systems able to withstand the joint clearance mechanisms without causing any joint damage. Moreover, although intra-articular injection enables localized drug delivery, tissue-specific drug release inside the joint space still remains a challenge [10, 76, 11, 77].

Therefore, the objective of this aim was to evaluate the behavior of the previously designed tissue-binding PEG microgels *in vivo* in terms of their effect on

joint health and retention time in a rat model of OA. The working hypothesis was that peptide-functionalized PEG microgels containing small molecule drug-loaded PLGA nanoparticles will increase the retention time of the encapsulated small molecules and will be retained in the joint space without inducing any degenerative changes after intra-articular injection. The rationale for this aim is that the designed PEG microgels are large enough (50 μm) to avoid rapid clearance from the joint space, enabling a prolonged small molecule drug residence time. Also, considering that PEG microgels are not hard structures and are primarily composed of water (94%), they are not expected to induce mechanical wear of the articular cartilage or significant inflammation in the synovial membrane.

5.2 Materials and Methods

5.2.1 Materials

Male Lewis rats (250g-300g) were acquired from Charles River Laboratories after Georgia Tech's Institutional Animal Care and Use Committee (IACUC) approval. Near-infrared (NIR) dyes cyanine 7 (Cy7), sulfo-cyanine 7 (sCy7) and cyanine 7-NHS ester were purchased from Lumiprobe Life Science Solutions and Alexa Fluor™488-NHS ester from Thermo Fisher Scientific. Thiol-PEG-Biotin (1 kDa) was acquired from Nanocs Inc, Conray (60%) from Henry Schein®and the RNeasy Plus Mini Kit's lysis buffer from Qiagen was used.

5.2.2 Unilateral medial meniscus transection (MMT) procedure

All *in vivo* procedures were approved by the Georgia Tech's Institutional Animal Care and Use Committee (IACUC). Male Lewis rats (250g-300g) were subjected to unilateral medial meniscus transection (MMT). Briefly, rats were anesthetized using 5% isoflurane in an induction chamber and maintained at 1.5-3% delivered by face mask. Sustained release buprenorphine (1 mg/kg) was administered sub-

cutaneously after initial induction of anesthesia. A skin incision was made on the medial side of the left knee and the medial collateral ligament (MCL) was exposed by blunt dissection. The MCL was then transected to reflect the meniscus, which was cut through the full thickness to simulate a complete tear. Finally the blunt-dissected muscles were sutured using a 4.0 vycryl absorbable suture and the skin was closed using staples.

5.2.3 Microgels intra-articular mechanical stability

Considering that the designed PEG microgels are soft structures containing around 94% water, we investigated in a pilot study if these systems could withstand the mechanical loads generated in the intra-articular space as the animal walks. To do so, fluorescently labeled microgels were synthesized by conjugating WYR peptide to AlexaFluor 488-NHS ester, prior to microgels formation. Then, 50 μL of PEG microgels suspended in sterile saline at a concentration of 530,000 microgels/mL were injected bilaterally in healthy knee joints of male Lewis rats. Only one rat was used at each time-point (n=2 knees). A knee lavage using 100μL of sterile saline was performed on days 4, 8, 14 and 21, then withdrawn microgels were imaged using confocal microscopy and the area of at least 80 microgels per group was calculated using a customized MATLAB script. Before imaging, 100 μL of each sample were incubated with 50μL of lysis buffer for 5 minutes to promote cell rupture and obtain clean images that could be analyzed using the automated MATLAB script.

5.2.4 Microgels intra-articular retention and their effect on knee joint health and OA progression

To assess the microgels intra-articular retention time, a tracking experiment was conducted using the near-infrared Cyanine 7 dye (Cy7). In this case, to incorpo-

rate the Cy7 dye into the microgels, HAP-1 and WYR peptides were conjugated with Cy7-NHS ester prior to PEG microgels formation. Three weeks after MMT procedure, rats received bilateral injections of the following formulations in 50μL saline: (1) Free sulfo-Cy7 dye (negative control, represents free small molecule), (2) Cy7-WYR-functionalized microgels or (3) Cy7-HAP-1-functionalized microgels (n=9). All microgels formulations contained 0.5% w/v PLGA nanoparticles and were injected at a concentration of 530,000 microgels/mL. Rats were scanned before and immediately after injection in the Perkin Elmer IVIS Spectrum CT *in vivo* imaging system to measure the initial fluorescence signal emitted by the injected formulation. Animals were then scanned on days 1, 3, 5, 7, 10, 13, 16, 19 and 26 post-injection and euthanized at day 26. Data was fitted to a one-phase exponential decay function and the resulting half-life time was compared across formulations for healthy and MMT joints. Half-life times were transformed using a logarithmic function and subjected to outliers removal using a maximum false discovery rate of 1%. This allowed for normal data distributions with different variances among groups. Therefore, Welch's ANOVA was used to determine statistical differences between formulations. Also, a t-test was performed to compare HAP-1 or WYR formulations between healthy and OA joints.

Rat legs were collected to evaluate the microgels effect on knee joint health and OA progression. Harvested tissues were fixed in 10% neutral buffered formalin for 3 days and then stored in PBS without Ca^{++} and Mg^{++}. For each experimental group, 3 legs were processed for histology analysis and 6 were used to assess cartilage degradation and osteophyte formation via equilibrium partitioning of ionic contrasting agent micro-computed tomography (EPIC μ-CT). For histology processing, samples were decalcified for 10 days using a formic/citric acid solution, which was changed every other day. Then, knee joints were dissected leaving

the knee cap intact with some muscle around, embedded in paraffin and sectioned through the coronal plane (5 μm sections). Samples were then stained using Toluidine Blue and synovial membrane thickness measured using ImageJ.

To quantify markers of degenerative joint changes, the tibias from the remaining samples (n=6) were incubated in 37.5% Conray contrast agent for 40 min at room temperature. Then, the tibial plateaus were scanned in the Scanco μCT 40 (45 kVp, 177 μA, 8 W, 16 μm resolution). After scanning, samples were incubated in 10 mL of PBS without Ca^{++} and Mg^{++} to remove the contrast agent. Finally, images were contoured and analyzed for cartilage attenuation, lesion volume, roughness and calcified osteophyte volume.

5.2.5 Intra-articular drug retention time

To assess for the *in vivo* drug retention time, Cy7 was used as a model small molecule drug. Cy7 was first loaded into PLGA nanoparticles by oil-in-water emulsion method as reported in Chapter 3. Microgels functionalized with WYR, WYRsc, HAP-1 and HAP-1sc peptides, containing 0.5% w/v Cy7-loaded PLGA nanoparticles were injected into the knee joints of male Lewis rats (50μL, 530,000 microgels/mL), three weeks after surgical induction of OA (n=7). Also, sulfo-Cy7 free dye and Cy7-loaded PLGA nanoparticles were used as controls. Rats were scanned before and immediately after injection in the Perkin Elmer IVIS Spectrum CT *in vivo* imaging system to measure the initial fluorescence signal emitted by the injected formulation. Animals were then scanned on days 1, 3, 5, 7, 10, 13, 16, 19 and 26 post-injection and euthanized at day 26. Data was fitted using a one-phase decay model and the half-life time and plateau values were analyzed. The data corresponding to the curve-fitting parameters was transformed using a logarithmic function and outliers analysis was performed to comply with normality and

homoscedasticity assumptions. Then, data was analyzed via a one-way ANOVA.

5.2.6 *In vivo* localization of nano-composite microgels

The *in vivo* localization of peptide-functionalized microgels was analyzed via histology. OA was induced in male Lewis rats and 2 weeks after surgery received intra-articular injections of WYR, WYRsc, HAP-1 and HAP-1sc-functionalized PEG microgels (n=8, 50μL injection containing 530,000 microgels/mL suspended in saline). This time point was chosen because as early as 1 week after OA induction, cartilage fibrillations appear in this model, which exposes collagen type II fibers that are probably able to bind the WYR peptide-functionalized microgels. Then, animals were sacrificed at 4 and 6 weeks post-surgery (n=4 per time point) and their left knees harvested and processed for cryosectioning. Briefly, tissue samples were fixed for 3 days in 10% neutral buffered formalin and then decalcified for 10 days in a formic/citric acid solution that was changed every other day. Then, samples were embedded in optimal cutting temperature compound (OCT) following the protocol reported in the appendix section A.1 and sectioned through the mid-coronal plane. For each sample, 3 sections (15 μm thick), separated around 100 μm from each other were collected and stained with hematoxylin and eosin. The area occupied by microgels trapped within the synovial membrane was quantified in ImageJ and normalized to the total synovial membrane area in each section. Right knee samples served as non-treated controls.

5.3 Results

5.3.1 Microgels intra-articular mechanical Stability

To determine if PEG microgels containing PLGA nanoparticles were able to withstand the mechanical loads that occur in the intra-articular space, WYR-functionalized PEG microgels were injected in healthy Lewis rat knee joints and analyzed for

their size and morphology at different time points. Results presented in Figure 5.1 show that microgels are stable up to 8 days and then start breaking into smaller pieces as demonstrated by the presence of a bimodal area distribution at days 14 and 21. The percentage of microgels that remained intact at day 14 and 21 are approximately 60% and 40%, respectively.

A limitation of this study is that only WYR-functionalized microgels were used and the mechanical degradation of HAP-1-conjugated microgels or the scrambled controls were not evaluated. Although all PEG microgels formulations are expected to have very similar mechanical properties, their location in the knee joint could induce different mechanical degradation patterns. It has been demonstrated that compression and shear stresses in the knee joint are not equally distributed, instead some areas of the femoral and tibial plateaus withstand higher stresses in healthy and knees with meniscal tears [133]. Therefore, if the tissue-targeting peptides linked to PEG microgels actually promote tissue-preferential localization of these systems within the joint, it is highly possible that WYR- and HAP-1-functionalized microgels would present different modes of mechanical degradation. Although this study gives some insight on how non-chemically degradable PEG microgels may be degrading *in vivo*, differences in how this degradation occurs for distinct microgels formulations still remains a question for future investigation.

5.3.2 Microgels intra-articular retention

The previous pilot study showed that peptide-functionalized PEG microgels containing PLGA nanoparticles could be found in the intra-articular space for at least 3 weeks, but does not give information regarding the microgels clearance over time. Therefore, a microgels tracking experiment was conducted. Figure 5.2 shows IVIS

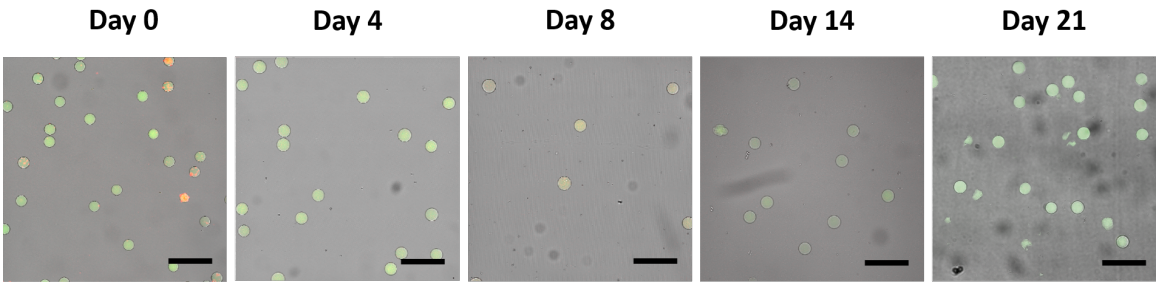

(a)

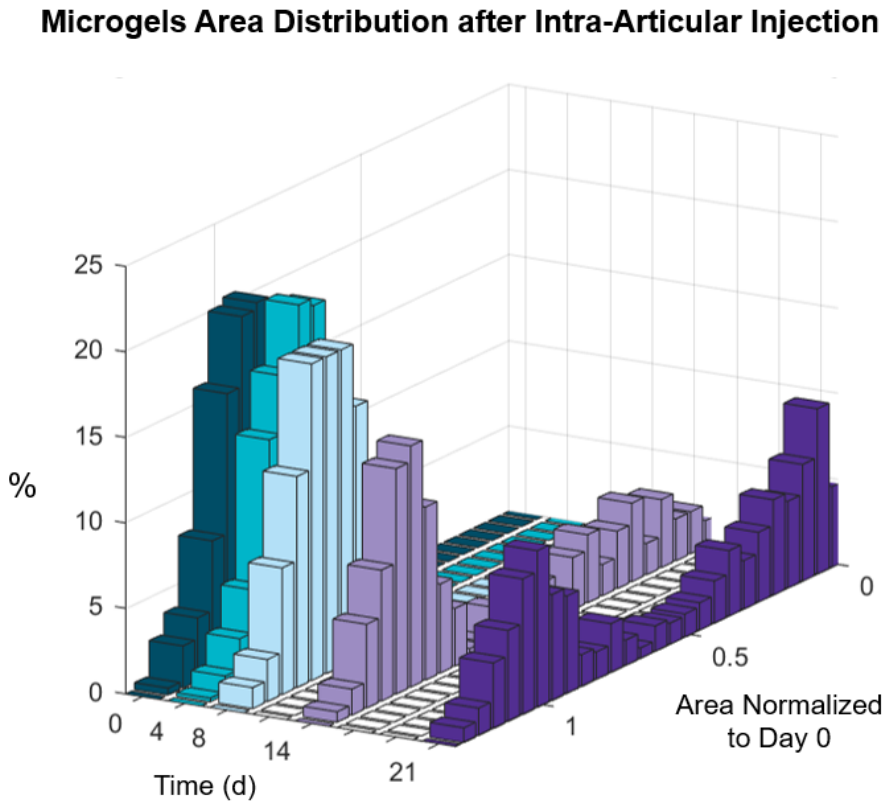

(b)

Figure 5.1: WYR peptide-functionalized PEG microgels *in vivo* mechanical stability. (a) Representative confocal images of PEG microgels (green) after being recovered via intra-articular lavage. Scale bar: 200 μm. (b) Microgels area histogram at different time points after intra-articular injection. Lavage from 2 knees at every time point.

representative images and the microgels retention profiles that were fitted to a one-phase exponential decay (Figure 5.2b) to obtain the half-life times (Figure 5.2c).

It is important to note that WYR-functionalized microgels injected in OA and healthy joints exhibited an increase in the radiance efficiency from day 0 (immediately after injection) to day 1. This phenomena could be attributed to the self-quenching effect characteristic of cyanine dyes, which is explained in more detail in appendix B.1. Therefore, the retention profiles for all experimental groups were fitted to a one-phase exponential decay, but for both WYR-containing experimental groups, the data taken on day 0 was not included. The resulting half-life time data was subjected to outliers analysis and the clean data was evaluated using non-parametric test to determine differences between formulations in the OA and naïve joints, independently.

Results show that for both, disease and naïve joints, free Cy7 dye is rapidly cleared, presenting a half-life time of 0.21 $\pm$ 0.06 and 0.14 $\pm$ 0.04 days, respectively. In contrast, HAP-1- and WYR-functionalized microgels presented a significant increase in the intra-articular half-life time compared to the free dye control in MMT knees (HAP-1: 6.03 $\pm$ 4.76 days, p-value: 0.0005; WYR: 2.48 $\pm$ 0.70 days, p-value: 0.006). Similarly, in naïve joints, microgels also increased the intra-articular retention compared to the free dye control (HAP-1: 3.37 $\pm$ 2.82 days, p-value: 0.0056; WYR: 4.70 $\pm$ 1.78 days, p-value: 0.0003). These findings demonstrate that peptide-functionalized PEG microgels can be retained in the knee space for a significantly longer period of time compared to free small molecules such as Cy7.

Moreover, these results suggest that WYR-functionalized microgels are cleared faster in OA joints compared to healthy ones. Research in the field have revealed

that inflamed joints present higher vascular permeability, which has been correlated with faster clearance of molecules and nanoparticles from OA joints compared to healthy ones [69]. It is possible that as WYR-functionalized microgels start degrading mechanically, small hydrogel fragments get cleared from the joint at a higher rate in OA joints than naïve ones. Interestingly, the half-life time of HAP-1-functionalized microgels was not altered by the state of the disease. As is going to be discussed bellow, synoviocyte-targeting PEG microgels get trapped in the synovial membrane of healthy and MMT rats (Figure 5.5), which can explain why the retention of this formulation resulted similar in both cases.

5.3.3 Effect of microgels on knee joint health and OA progression

To evaluate whether peptide-functionalized PEG microgels affect knee joint health, samples from the microgel tracking study were taken for cartilage and synovial membrane morphological analysis via EPIC-μCT and histology. Figure 5.3 show that articular cartilage of animals that received MMT surgery present significant degenerative changes compared to healthy joints for all formulations. In this experiment, the dye group was considered negative control, given that free Cy7 dye is cleared from the joint in less than 5 h and to the best of our knowledge, does not negatively affect the knee joint. As expected, OA animals presented higher attenuation values, which demonstrates an increase in proteoglycan depletion as a result of OA induction. Also, cartilage surface roughness, lesion and calcified osteophyte volume were significantly increased compared to naïve joints. Interestingly, microgels functionalized with either WYR or HAP-1 peptide did not affect any of the joint parameters in healthy joints. In the case of osteoarthritic knees, microgels did not worsen OA progression as measured by cartilage attenuation, surface roughness and osteophyte volume. Interestingly, although animals that were ad-

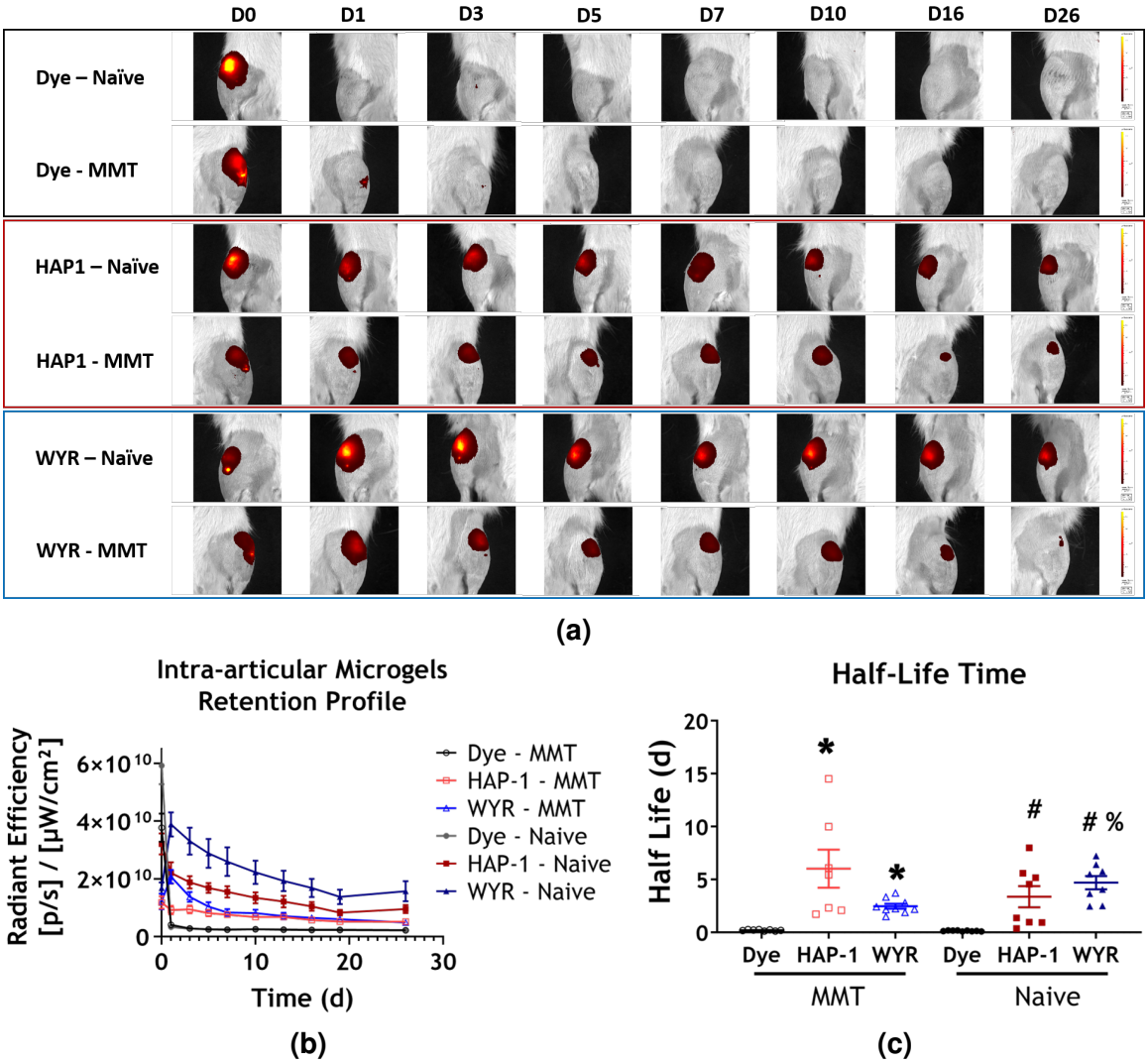

Figure 5.2: Peptide-functionalized PEG microgels *in vivo* retention. (a) Representative IVIS images of fluorescently labeled PEG microgels after intra-articular injection. (b) Retention profile raw data (n=9) and (c) half-life times for different microgels formulations. Mean $\pm$ SEM, n=9. Data subjected to outlier analysis and Welch's ANOVA: *p-value$<$0.05 compared to dye in MMT joints, #p-value$<$0.05 compared to dye in naïve joints. t-test %p-value$<$0.05 compared to WYR-functionalized microgels in MMT joints.)

ministered WYR-functionalized PEG microgels presented a significant difference in lesion volume compared to healthy knees, one of the animals did not exhibit any cartilage lesions and three of them presented smaller lesions than HAP-1 and free dye treated rats. This is an interesting result because in the rat MMT model at 6 weeks post-surgery animals usually develop considerable big full-thickness cartilage lesions [134]. This observation establishes basis for future evaluation of WYR-functionalized PEG microgels and their effect on OA progression.

Histological evaluation of synovial membrane thickness as a marker of inflammation resulted in no significant differences between the treatments in naïve and MMT rats (Figure 5.4). Most importantly, in both naïve and MMT joints, synovial thickness of microgels-treated joints was not different from the free dye control-treated knees. This suggest that the intra-articular presence of microgels does not induce a strong inflammatory response evident as synovial membrane thickening at three weeks post-injection. However, it is important to note that there was no significant difference between MMT and naïve animals. Although this could be explained by the small sample size, it is important to consider that the MMT model induces a mechanical instability within the joint, but is not known for being an inflammatory model of OA.

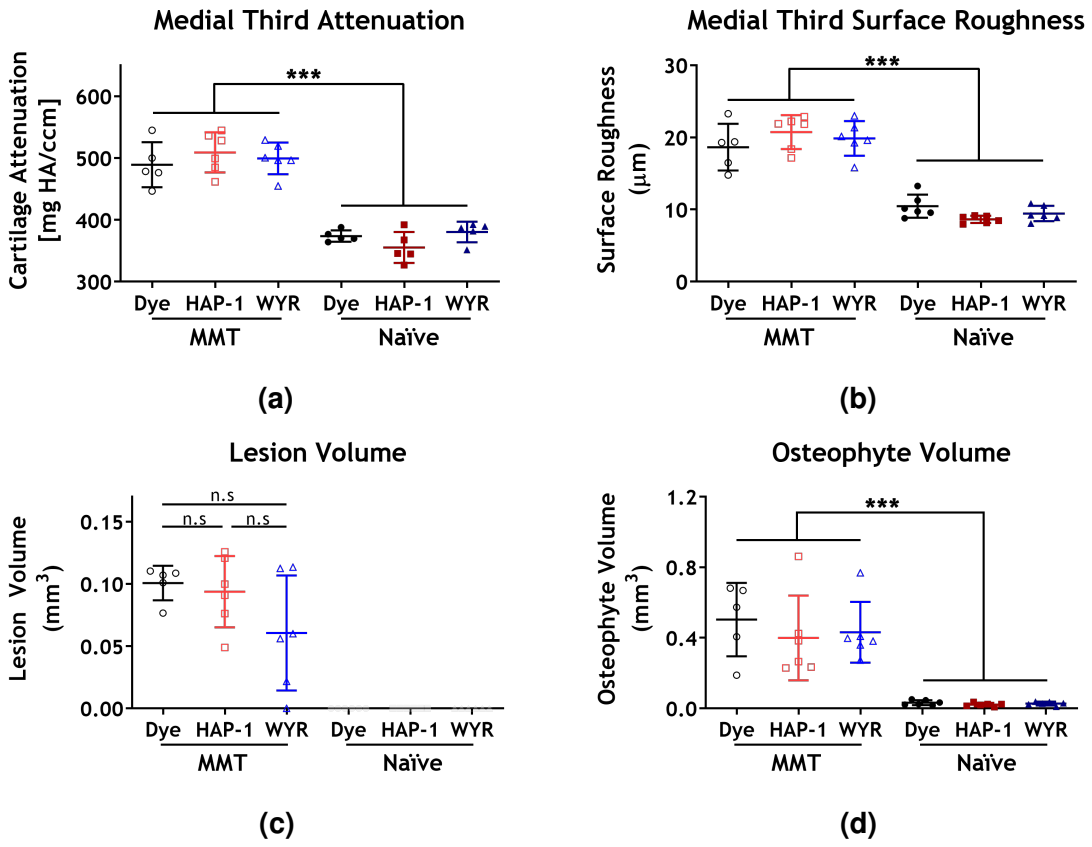

Figure 5.3: Peptide-functionalized PEG microgels effect on cartilage degradation and osteophyte formation. Parameters indicating joint health were measured by EPIC μCT in the medial tibial plateau, including (a) medial third attenuation, which is inversely proportional to proteoglycan content; (b) medial third surface roughness as a measurement of cartilage fibrillation and erosion; (c) total lesion volume and (d) calcified osteophyte volume. (a) and (b) were directly analyzed via a one-way ANOVA, while (c) and (d) required data transformation to correct for heteroscedasticity prior to one-way ANOVA analysis. Mean $\pm$ SEM, n=6, *p-value$<$0.05

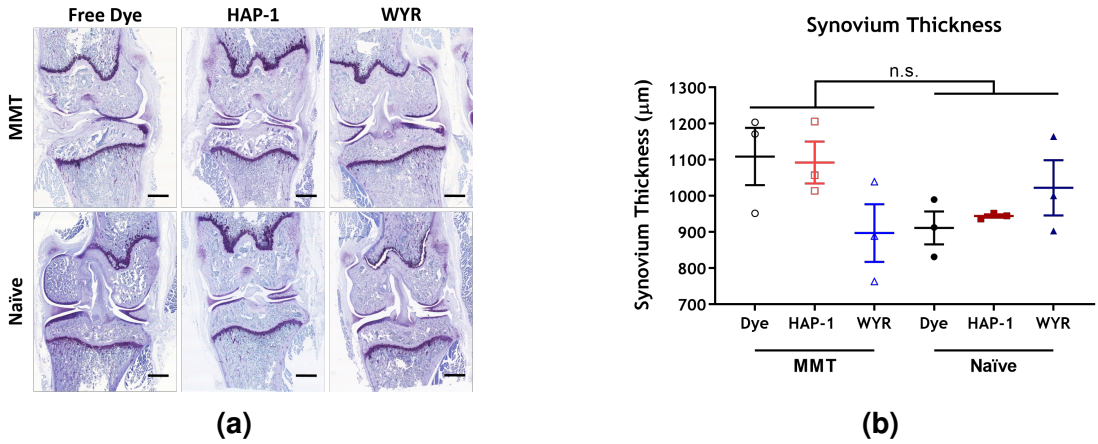

Figure 5.4: Peptide-functionalized PEG microgels effect on synovial membrane thickness. (a) Coronal rat knee sections stained with toluidine blue showing cartilage lesions and changes in proteoglycan content in MMT samples. Scale bar 2000 μm (b) Synovial membrane thickness (Mean $\pm$ SEM). Three images analyzed per sample (n=3). Nested one-way ANOVA demonstrated no significant differences between microgels formulations and free dye.

Histological analysis of toluidine blue stained sections revealed that HAP-1-functionalized microgels were embedded into the synovial lining and promoted the infiltration of cells in the areas that surround the material in both, healthy and MMT joints (Figure 5.5). The HAP-1-functionalized PEG microgels can be seen in Figure 5.5 as white circles surrounded by a dark purple tissue with high cellularity. In contrast, WYR-functionalized microgels were not found in the synovial membrane and the appearance of this tissue resulted comparable to that of free Cy7 dye-treated joints. Generally, microparticles injected intra-articularly get trapped in the synovial membrane [109]. Therefore, it is not surprising that HAP-1-functionalized microgels resulted embedded within the synovium. Interestingly, WYR-functionalized microgels were not trapped in the synovial membrane, possibly due to their ability to bind the articular cartilage. However, based on these histology images, it is impossible to determine where the WYR-microgels were located and further evaluation on microgels intra-articular location is still needed.

5.3.4 Model small-molecule drug-loaded microgels intra-articular retention time

Previous results suggest that intra-articular injection of PEG microgels containing PLGA nanoparticles do not result in articular cartilage damage or synovial membrane inflammation. Additionally, considering that PEG microgels are retained in osteoarthritic rat knee joints for at least 3 weeks, we investigated the intra-articular retention time of a model small molecule drug. In this study, PLGA nanoparticles loaded with Cy7 dye were encapsulated into peptide-functionalized PEG microgels and its retention in the joint was analyzed via *in vivo* imaging system (IVIS). Figure 5.6 shows the retention profile and parameters resulting from a one-phase exponential decay curve fit for the different microgels formulations. Comparable to previous studies, free dye injected into the knee joint resulted in a fast clearance (half-life time: 0.25 ± 0.073 days) which leads to the elimination of most of this small molecule as indicated by the plateau value ($0.48 \pm 0.22\%$). In contrast, all delivery systems presented a 10-fold increase in the radiant efficiency plateau values (Figure 5.6c) compared to free dye (p-value$<$0.0001), suggesting that PLGA nanoparticles alone or loaded into PEG microgels could increase the small molecule retention in the joint. Additionally, only HAP-1-, HAP-1sc- and WYRsc-functionalized PEG microgels exhibited a significant increase in the half-life time compared to free dye, presenting a 6-, 7- and 3-fold increase in half-life time values, respectively. However, none of the microgels formulations increased the half-life time compared to PLGA nanoparticiles.

The intra-articular retention time of a small molecule loaded in a delivery system is controlled by two phenomena: the clearance of the free released molecule and the elimination of the delivery vehicle via cell-mediated or vasculature-mediated

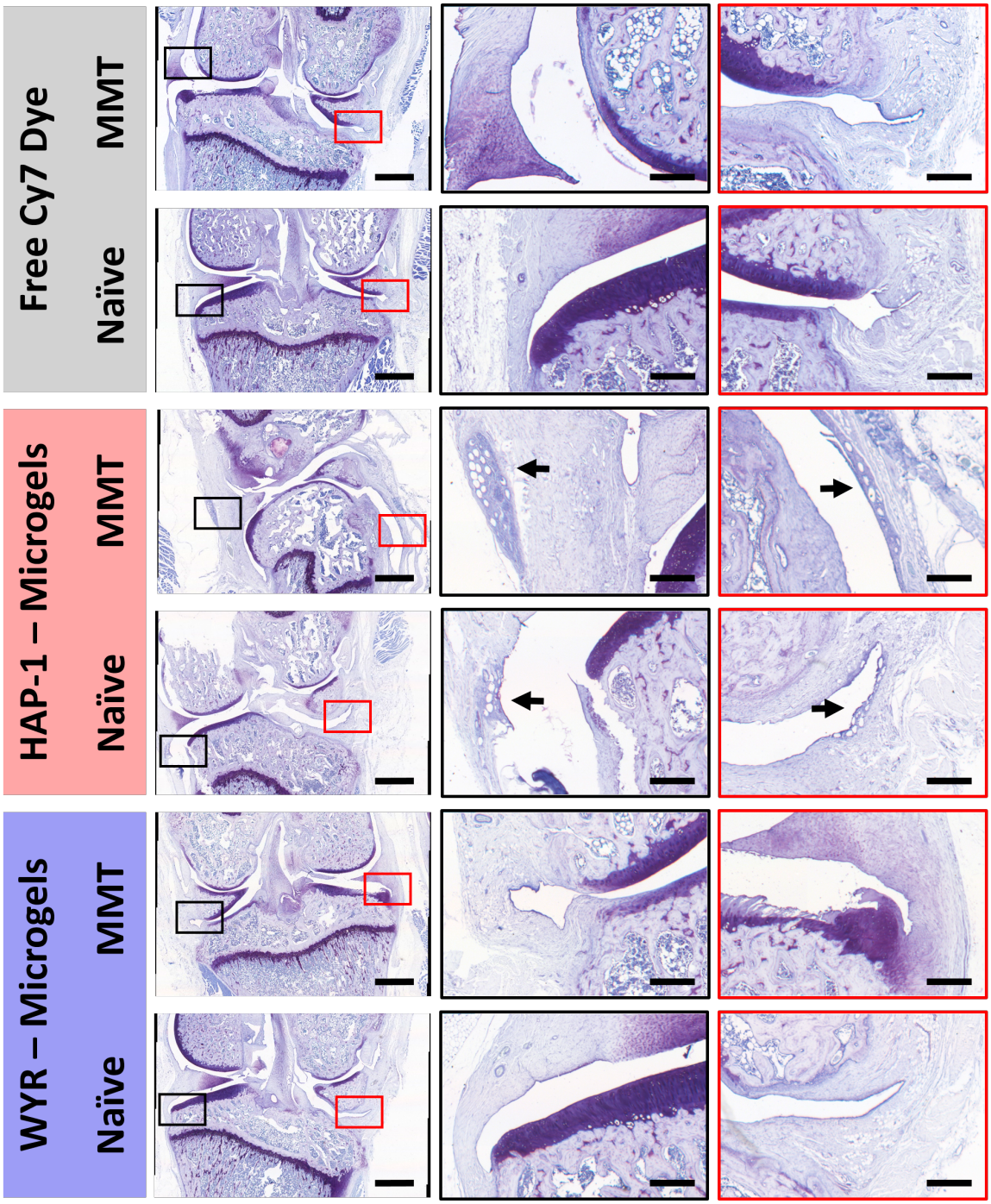

Figure 5.5: *In vivo* localization of peptide-functionalized PEG microgels. First column presents whole joint histology sections stained with toluidine blue. Scale bar 2000 μm. Black and red boxes highlight the zoom areas shown in the second and third column, respectively. Scale bar 500 μm. Black arrows point at microgels trapped in the synovial membrane.

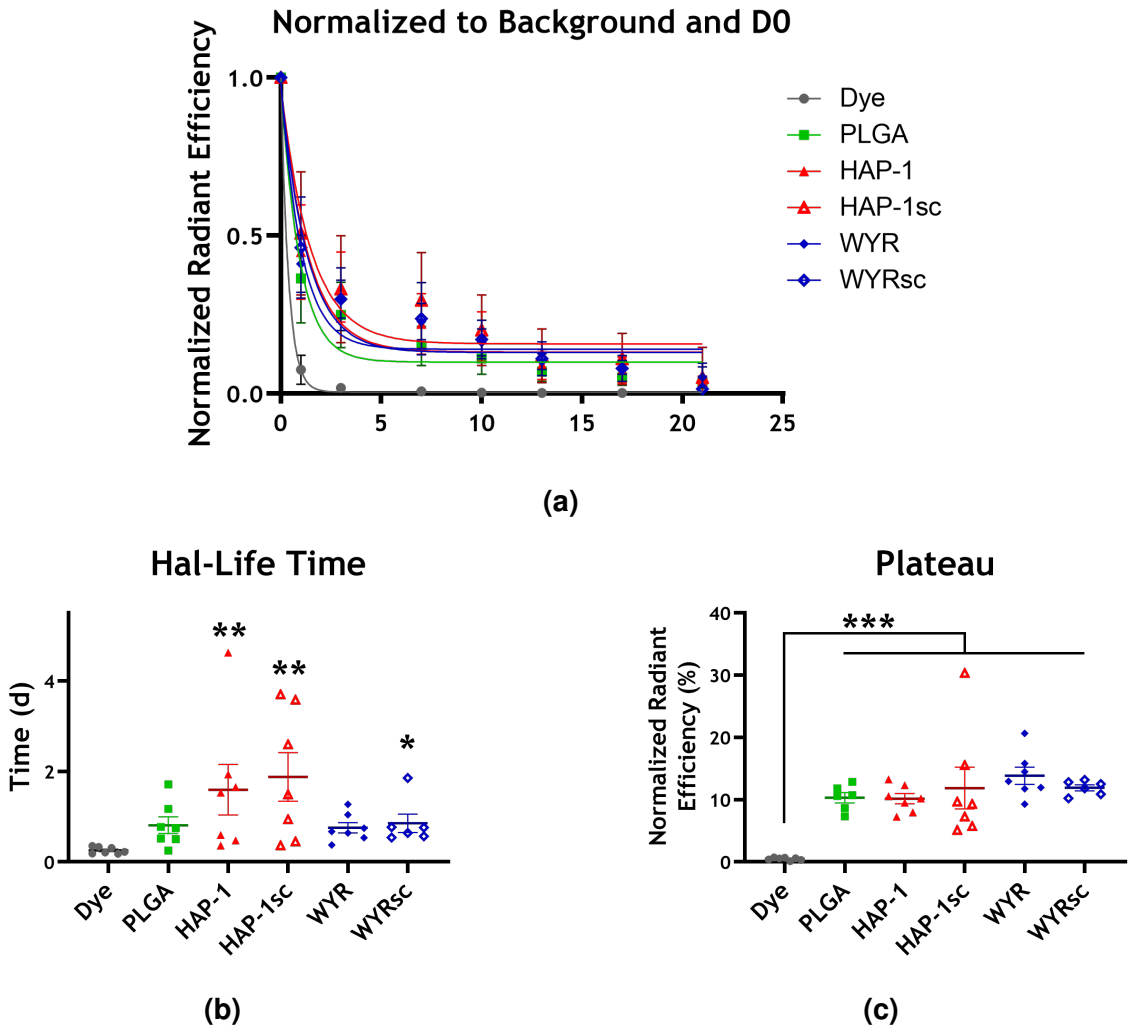

Figure 5.6: Intra-articular cargo retention time of Cy-7-loaded peptide-functionalized PEG microgels. (a) PEG microgels intra-articular retention profile. Data normalized to day 0 (b) Intra-articular half-life time of cyanine 7 dye encapsulated into free PLGA nanoparticles or PEG microgels containing PLGA nanoparticles. One-way ANOVA test, n=7, *p-value$<$0.05, **p-value$<$0.002 compared to free dye. (c) Plateau radiant efficiency values after intra-articular injection of PEG microgels containing Cy7-loaded PLGA nanoparticles. One-way ANOVA, ***p-value$<$0.0001.

mechanisms. Assuming that the PLGA nanoparticles or the PEG microgels can not get cleared from the synovial membrane, the small molecule retention time would be controlled only by the release rate. As shown in the appendix B.2, Cy7 release profile from nano-composite PEG microgels is controlled by the PLGA nanoparticles. Therefore, PLGA nanoparticles alone and PLGA-loaded PEG microgels presented similar release profiles. In *in vivo*, the small molecule released from these delivery systems is rapidly cleared from the joint as demonstrated by the free dye control. This observation could explain why the intra-articular half-life time of microgels formulations were not significantly different than PLGA nanoparticles alone. Additionally, the fast release kinetics of Cy7 from the system (over 80% during the first 5 to 7 days) could explain why the IA half-life time of this molecule did not exceed 2 days after injection of PLGA NPs alone or microgel formulations.

However in reality, the clearance of the free small molecule and the delivery systems occur simultaneously. Considering that the release rate of a small molecule from PLGA and PLGA-loaded microgels is similar, as shown in Chapter 3, the differences observed in this study in terms of the intra-articular half-life time could be attributed to the clearance of the delivery systems. As shown in Figure 5.6b, PLGA nanoparticles alone and WYR microgels did not significantly increase Cy7 half-life time compared to the free dye, but HAP-1, HAP-1sc and WYRsc microgels did. These results suggest that PLGA nanoparticles may be getting cleared from the joint faster than PEG microgels containing PLGA nanoparticles, which is consistent with other studies that demonstrate that bigger particles can better avoid cell-mediated and lymphatics clearance mechanisms compared to nanoparticles. [7, 69, 70, 71, 72, 73]. As shown in Figure 5.1, WYR-functionalized PEG microgels are subjected to mechanical degradation, and around 2 weeks post-injection microgel pieces can be observed in the synovial fluid. As microgels break, PLGA

nanoparticles contained inside the hydrogel, can be released into the synovial fluid and then get cleared. This could potentially explain why this microgel formulation did not increase Cy7 half-life time compared to free dye. In contrast, HAP-1, HAP-1sc and WYRsc microgels did significantly improved Cy7 half-life time compared to free dry. According to our results, HAP-1-functionalized microgels get trapped in the synovial membrane (Figure 5.5), which could help protect these microgels from the joint compression and shear stresses, having a positive impact on mechanical stability and intra-articular retention compared to WYR-conjugated microgels. Entrapment intro the synovial membrane could also be the case for non-targeting delivery systems such as WYRsc and HAP-1sc microgels, as suggested by Bédouet *et al.*, who demonstrated this effect using non-functionalized PEG-dimethacrylate microgels [109].

Deeper understanding of the mechanical degradation of the different microgels formulations and rigorous research to determine the fate of free PLGA nanoparticles and PEG microgels, could give insights on the mechanisms involved in intra-articular small molecule clearance and provide valuable information to optimize the PLGA-loaded PEG microgel delivery system presented in this dissertation in order to achieve prolonged retention and sustained release of therapeutic molecules in the joint.

5.3.5 *In vivo* localization of nano-composite microgels

All microgel formulations were found trapped within the synovial membrane, but no microgels bound to the articular cartilage or floating in the synovial fluid could be detected using this technique. Figure 5.7a shows representative histology images of the synovial membrane, demonstrating that all microgel formulations get trapped in this tissue and appear as empty pockets within the synovial membrane. Con-

sistent with the results presented in Figure 5.5, all microgel formulations induced localized cellular infiltration at both time points. These structures were not found in healthy joints that did not receive IA microgels injection.

No significant differences in microgels entrapment within the synovial membrane were observed between formulations at any time point (figure 5.7b). Other studies have demonstrated that micron-size materials injected in the IA space get trapped in the synovial membrane [109, 135]. However, in our studies the use of a synoviocyte-binding peptide did not result in improved microgels localization within the synovium compared to other formulations. In contrast to the study presented in section 5.5.3 (Figure 5.5) where no WYR-microgels were observed in the synovial membrane, in this study cartilage-binding microgels were also trapped within this tissue at both time points. Given that histology did not allow for microgels localization in other areas of the joint, this study resulted inconclusive regarding the WYR microgels ability to bind to the articular cartilage. It is possible that, even though some of these microgels are trapped within the synovial membrane, a portion of them may be able to bind damaged areas of the cartilage. However, more appropriate techniques and further investigation would be necessary to determine if this is the case.

Unfortunately, histologic evaluation presents several limitations to determine the location of microgels within the joint. Even though our results demonstrate that microgels can be retrieved via synovial fluid collection up to 3 weeks post-injection (Figure 5.1), sample processing for both paraffin (section 5.5.3) and cryo-histology demonstrated to be damaging for microgels preventing their direct visualization. Instead, only microgels trapped in the synovial membrane were evident as empty pockets within this tissue. Therefore, although histology analysis could be used to

detect microgels trapped within the synovial membrane, this technique does not allow to determine if microgels remain floating in the synovial fluid or can bind the articular cartilage.

On the other hand, histology only allows for two-dimensional analysis. In particular, in this experiment only sections around the mid-coronal plane were evaluated. To better determine whether targeting microgels present a preferential localization within the joint, a full joint analysis should be performed. In this regard, tools that allow for 3D imaging such as μCT or magnetic resonance imaging (MIR) could be a better alternative compared to histological analysis. In fact, Hu, *et al.* developed cartilage-targeting probes by conjugating the MRI contrast agent DOTAM to the peptide WYR. These probes were administered via IA injection in the knees of rats after surgical induction of OA, which allowed for the *in vivo* localization of focal cartilage lesions and osteophytes via MIR [88]. This type of technology could be adopted to conjugate PEG microgels with MRI contrast agents, potentially allowing for longitudinal and three-dimensional localization of microgels within the joint space.

5.4 Discussion

In this chapter, the possibility of using peptide-functionalized PEG microgels containing PLGA nanoparticles for localized intra-articular drug delivery was investigated in a rat model of OA. First, microgels were analyzed for their ability to be retained in the intra-articular space. Our findings demonstrate that PEG microgels get mechanically degraded after intra-articular injection (Figure 5.1), but are retained for at least 3 weeks, exhibiting a half-life time significantly higher than free model small molecule (Figure 5.2). Additionally, microgels did not induce degenerative changes in the articular cartilage as measured via EPIC μCT and the synovial

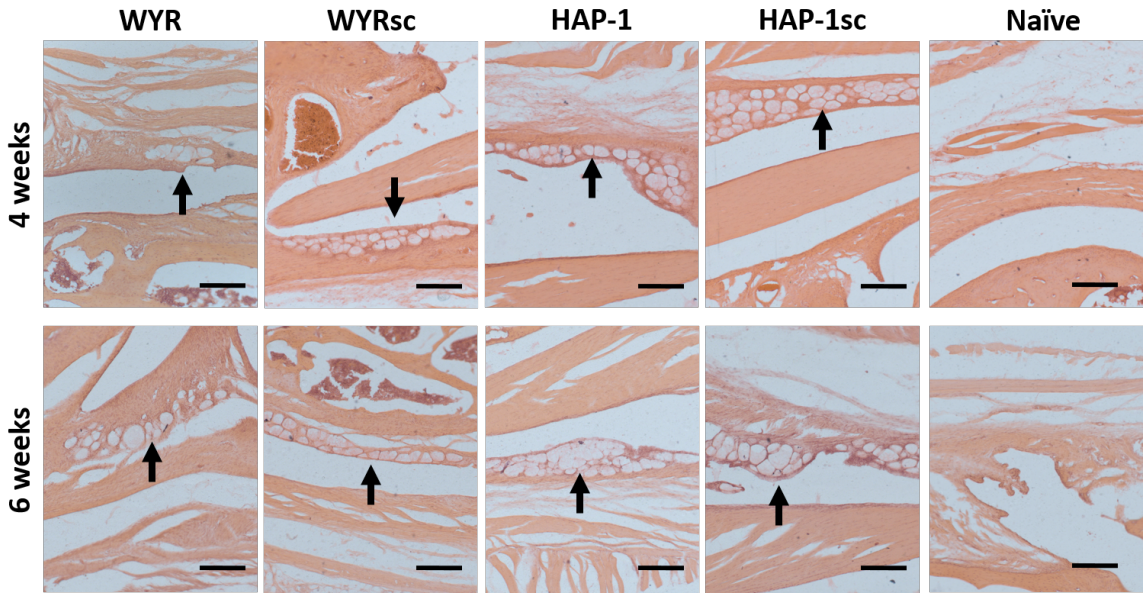

(a)

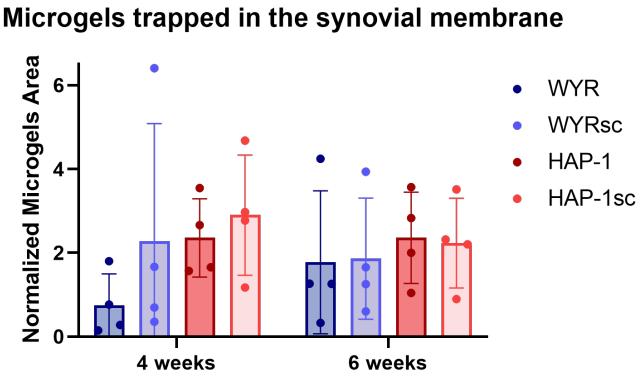

(b)

Figure 5.7: Microgel formulations get trapped within the synovial membrane. (a) Representative histology images show microgels localized within the synovial membrane at 4 and 6 weeks after OA induction. Scale bar: 200 μm. Arrows indicate microgels trapped in the synovium. (b) Quantification of microgels trapped within the synovial membrane. Microgels area was normalized to the synovial membrane area in each histology section. Three images per replicate were analyzed. Data was transformed using a logarithmic function and evaluated via a one-way nested ANOVA (n=4).

membrane did not show significant signs of inflammation in both, healthy and OA knee joints.

Microparticles as intra-articular drug delivery systems have been extensively studied for their retention time and their ability to induce inflammation in the joint. Characteristics such as particle size, shape and material have been shown to have a direct impact on retention and inflammation, but despite the advances on the field, there is still no consensus on the optimal microparticles characteristics. In general, particles in the nanometer scale and up to few microns in diameter are easily phagocytosed, tend to be more inflammatory and get cleared by lymphatics drainage or cell-mediated elimination faster than bigger particles [7]. In contrast, microparticles are retained in the intra-articular space for longer periods of time compared to nanoparticles, they usually get trapped in the synovial membrane and induce a multinuclear giant cell response [7, 136, 53]. This phenomena was studied by Horisawa, *et al.*, who injected PLGA particles of 265 nm or 26μm in diameter into the knee joint in a rat model. Results showed that nanoparticles (265 nm) were phagocytosed by synovial macrophages and therefore, infiltrated into the tissue, whereas microparticles (25μm) were surrounded by multinucleated giant cells [137]. Other studies demonstrate that PLGA microspheres injected in rabbit knee joints with diameters between 1-20μm elicit a greater inflammatory response than particles ranging between 35-105μm [138].

In general, microparticles perform better as intra-articular drug delivery vehicles in terms of prolonged retention and inflammation compared to nanoparticles. However, Park *et al.* demonstrated that irregular polyethylene microparticles like those produced by prosthesis wear in partial joint arthroplasties, lead to up-regulation of pro-inflammatory cytokines and apoptosis of chondrocytes, meniscal fibrochon-

drocytes and synoviocytes *in vitro* and promoted cartilage and meniscus degeneration as well as synovitis in a rat MMT model [139]. These findings raise some concerns in the field regarding the use of hard polymeric microparticles for intra-articular drug delivery. Nano-composite microgels, as those presented in this dissertation, could help overcome this limitation while still providing sustained drug release and prolonged intra-articular retention time. The engineered hybrid PEG microgels combine the advantages of polymeric nanoparticles for sustained drug delivery (see Chapter 3) with the ability of micron-scale particles to be retained in the intra-articular space for at least 3 weeks. Additionally, the use of a soft material such as a hydrogel, instead of solid polymeric microparticles allowed for prolonged retention without inducing any detectable degenerative changes in the articular cartilage or promoting synovium thickening as demonstrated in this chapter. Moreover, PEG microgels formulations could serve as a nanoparticle depot that could help reduce their clearance, offering an advantage over free nanoparticle administration. One limitation of the presented PLGA nanoparticles-loaded PEG microgels is that this system may not be ideal for intra-cellular or intra-cartilage drug delivery, which most likely require nano-sized particles that could be internalized or penetrate into the articular cartilage [7, 87, 131]. However, this platform could allow the loading of nanoparticles, small enough to be able to get out of the PEG microgels and then release their contents to the tissues of interest in a localized manner.

To the best of our knowledge, only one study utilized a similar hydrogel-based microsphere system composed of linear PEG cross-linked with either, degradable short PLGA regions or non-degradable PEG-dimethacrylate. Bédouet *et al.* demonstrated that degradable and non-degradable PEG microgels were found trapped in the synovial membrane 4 weeks after injection in the intra-articular space of the shoulder sheep joint, with non-degradable microgels inducing a for-

eign body response characterized by the presence of giant cells surrounding the microgels [109]. In our studies, HAP-1 functionalized microgels, designed with the intention of targeting the synovial membrane were found embedded in this tissue 3 weeks after injection and induced localized infiltration of cells (Figure 5.5). Although these microgels did not induce a significant synovial thickening (Figure 5.4) or cartilage damage over 3 weeks (Figure 5.3), detailed characterization of the immune response could provide insight on the long-term effect of these microgels on the inflammatory processes involved in OA progression. Even though the MMT model is not typically considered an inflammatory model of OA and animals do not necessarily present a thickened synovial membrane as observed in the presented results, recent research on the topic demonstrates that metrics such as synovium cellularity, cell alignment and cell aspect ratio, could be used to detect disease progression- or material-induced changes in the synovial membrane [140]. Such metrics could be used to better understand the effect of PEG microgels on synovial membrane, even if they do not get trapped within the tissue.

Interestingly, even though micron-scale particles usually get trapped in the synovial membrane [109], cartilage-targeting microgels were not found in this tissue (Figure 5.5). These findings suggest that WYR functionalization may be promoting binding to the articular cartilage and therefore, could be preventing microgels to get trapped in the synovium. However, the histology protocols used in this dissertation did not allow direct visualization of PEG microgels, most likely due to the destructive solvents and high temperatures used in traditional paraffin histology processing, which may cause hydrogels degradation and shrinkage [109]. Therefore, the development of techniques that permit the visualization of these microgels *in vivo* could provide better understanding on whether these particles effectively bind the articular cartilage. Magnetic resonance imaging (MRI) could offer a promising tool,

in fact Hu *et al.* conjugated free WYR peptide to an MRI contrast agent for *in vivo* evaluation of hyperthrophic cartilage lesions in a rat model of OA [88]. These type of techniques could allow better determination of PEG microgels location *in vivo* compared to histology.

WYR-functionalized microgels were shown to get mechanically degraded (Figure 5.1) and were the only microgel formulation that did not significantly increase the half-life time of Cy7 compared to free dye (Figure 5.6b). One possible explanation is that since WYR-functionalized PEG microgels avoid getting trapped in the synovial membrane, they may be more susceptible to mechanical degradation than HAP-1 microgels, which at the same time could be correlated to shorter cargo half-life times, either due to microgels fragments clearance or due to the elimination of PLGA nanoparticles that get released as the microgels break. Using a higher PEG concentration to stiffen the hydrogel or establishing covalent conjugation of the nanoparticles to the PEG macromer are some alternatives to improve the performance of WYR-functionalized microgels in terms of mechanical stability and cargo retention. On the other hand, smaller and irregular particles functionalized with WYR peptide that result from mechanical degradation, may be able to get entrapped into the cartilage lesions easier than smooth intact microgels, providing better binding capacity. The results presented in this chapter, establish interesting basis for further characterization of the clearance mechanisms involved in PEG microgels elimination from the joint space and how these relate to cartilage binding.

The results presented throughout this document demonstrate that these delivery vehicles allow for small molecule sustained release (see Chapter 3), can bind to articular cartilage and synoviocytes *in vitro* (see Chapter 4), HAP-1-functionalized microgels get trapped in the synovial membrane of healthy and OA rat knee joints,

microgels are retained in the intra-articular space for at least three weeks and some formulations significantly improve small molecule retention compared to a free model dye (see Chapter 5). Although overall these results suggest that peptide-functionalized PEG microgels could be promising intra-articular drug delivery systems, the main limitation of this dissertation is that the *in vivo* localized delivery of therapeutic molecules or model drugs was not investigated. Future research could optimize these nano-composite PEG microgels for the delivery of cell membrane tracers that could be used to determine if microgels tissue-specific binding actually supports localized drug delivery in the intra-articular space using the MMT rat model.

Nano-composite microgels like those developed in this thesis represent a novel alternative for intra-articular drug delivery, which could overcome the limitations of nanoparticles and microparticles in terms of intra-articular retention time, immunogenicity and their possible negative effects on cartilage degradation. Additionally, the implementation of targeting peptides to achieve tissue-specific binding is an attractive approach to develop multi-target therapies for osteoarthritis treatment. In this regard, microfluidics technology could be optimized for the encapsulation of different types of delivery vehicles into PEG microgels, including polymeric, gold and lipid nanoparticles, liposomes and cells. This could broaden the possibilities for intra-articular localized delivery of multiple therapeutics or their combinations with independent release kinetics. Considering the complexity of OA pathophysiology and the multiple processes that could be targeted to reduce its progression, the proposed peptide-functionalized microgel intra-articular delivery system could be a good strategy to achieve a combinatorial, multi-target treatment for the disease.

5.5 Conclusions

The results shown in this chapter demonstrate that PEG-4MAL microgels could overcome the main limitation related to intra-articular treatment of OA, poor retention time, and could potentially be used for localized tissue-specific drug delivery. In a rat model of OA, microgels injected intra-articularly did not promote any detectable degenerative changes in the articular cartilage of healthy joints, nor did they worsen the progression of the disease. Our results suggest that peptide-functionalized PEG microgels can be retained in the intra-articular space for at least three weeks, showing the possibility of using this system for long-term drug delivery. Moreover, the proposed microgel-based delivery system would need to be optimize for particular drugs in order to obtain the desired release kinetics and intra-articular retention. Finally, synovium-targeting microgels remained trapped in the synovial membrane at 3 weeks post-injection, while cartilage-targeting microgels are not retained into the synovium. All together, these results demonstrate that peptide-functionalized PEG microgels containing polymeric nanoparticles for controlled drug release, may be an attractive intra-articular delivery system for the treatment of OA.

CHAPTER 6
FUTURE CONSIDERATIONS AND CONCLUSIONS

The results presented in this dissertation establish a small molecule drug delivery system that not only exhibits prolonged intra-articular retention, but also allows for articular cartilage and synoviocytes targeting. In Chapter 3, encapsulation of drug-loaded polymeric nanoparticles into a microgel system using microfluidics technology, was shown to be an effective and simple method that enabled small molecule loading and sustained release from PEG microgels. In Chapter 4, the ability of peptide-functionalized PEG microgels to target articular cartilage and synoviocytes was investigated *in vitro*. Characterization of microgels binding ability and specificity was conducted using cell monolayer platforms and bovine articular cartilage sections, demonstrating that WYR-conjugated PEG microgels are able to target fresh bovine cartilage, while HAP-1-functionalized microgels bind specifically to rabbit and human synoviocyte cells lines. In Chapter 5, peptide-functionalized PEG microgels were shown to be retained in the intra-articular space for at least 3 weeks, exhibiting a significantly higher half-life time compared to a free small molecule near infra-red (NIR) dye. Additionally, microgels did not induce cartilage damage in healthy or diseased knee joints as measured by EPIC μCT and did not promote significant synovial membrane thickening at 3 weeks post-injection. After intra-articular injection, HAP-1-functionalized microgels were found entrapped in the synovial membrane of healthy and diseased joints, surrounded by a highly cellularized tissue. Further characterization of the immune response induced by these microgels is still needed. Interestingly, WYR-functionalized microgels were

not seen in the synovial membrane, suggesting that this formulation is escaping from being trapped by the synovial membrane, probably due to their binding to the articular cartilage. Additionally, synoviocyte-targeting PEG microgels loaded with the model small molecule Cy7 significantly increased the small molecule retention time compared to free dye.

6.1 Contributions to the field

One of the main difficulties that has limited the translation of multiple OA drug candidates into the clinic is the lack of appropriate intra-articular delivery vehicles able to prolong drug retention time in the joint [7]. Moreover, recent understanding of the negative off-target effects of a variety of drugs on different joint tissues, has evidenced the need for targeting intra-articular delivery vehicles [3, 53, 7]. In this dissertation nano-composite microgels as intra-articular delivery vehicle is presented for the first time in the field. This platform combines the advantages of particulate delivery systems in the nano- and micro-scale to overcome limitations related to poor intra-articular drug retention time and tissue targeting. Additionally, the presented PEG microgels offer a highly customizable system that could allow the design of more complex combinatorial and multi-target formulations for OA treatment.

6.1.1 Hydrogel microspheres for improved intra-articular retention of small molecule drugs

Traditionally, hydrogel formulations have been used for intra-articular injection acting as drug depots [60, 61]. For example, hyaluronic acid (HA), commonly used as a visco-supplementation treatment in OA patients was used by Palmieri *et al.* to load either sodium clodronate or diclofenac sodium for the treatment of OA in a clinical study. Preliminary results demonstrated that the combination of HA with

these drugs had a synergistic effect at reducing patients pain after 3 and 6 months post-treatment as measured by a visual analog scale (VAS) of pain [60]. However, the real effectiveness of HA hydrogels is questionable given its short intra-articular retention (half-life=13.2 h) [8]. Additionally, injectable hydrogel formulations do not support drug sustained release and do not protect drugs from joint clearing mechanisms. Therefore, the use of hydrogel-based microspheres or microgels emerges as an alternative for prolonged intra-articular sustained release [141, 142, 109]. Srinivasan *et al.* formulated hyaluronan-based microgels for the intra-articular release of bone morphogenetic protein 2 (BMP-2) and demonstrated that these microspheres effectively reduced cartilage degeneration and increased the expression of aggrecan and collagen type II in a mouse model of reversible OA [141]. However, to the best of our knowledge microgel delivery systems have not been formulated for intra-articular administration of small molecule drugs. Therefore, the delivery vehicles presented in this dissertation offer an alternative to address limitations related to intra-articular release and retention of small molecule drugs for the treatment of osteoarthritis.

The PEG microgels containing drug-loaded polymeric nanoparticles presented in this dissertation were shown to be retained in the rat knee joint space for at least 3 weeks after injection. The hybrid nature of this system could offer advantages over the intra-articular delivery of free polymeric nanoparticles. Small molecule retention time in the joint space depends on the drug release rate from the delivery vehicle and on the elimination of the aforementioned system via cell-mediated or lymphatics mechanisms. Nano-scale up to few micron particles, have been shown to be phagocytosed by synovial macrophages which then transport these particles out of the tissue, or are eliminated via lymphatic drainage [7, 136, 53]. Therefore, the proposed PEG microgel system could act as a shield to prevent encapsulated

nanoparticles from getting cleared as fast as free particles formulations. Although this hypothesis was not evaluated in this dissertation, further investigation may offer interesting answers regarding the clearance mechanisms involved in the elimination of these novel non-degradable PLGA-loaded PEG microgels.

Additionally, the microfluidic technology used to synthesize PEG microgels allows for the encapsulation of virtually any type of drug-loaded nanoparticle delivery system. Polymeric nanoparticles, in particular PLGA, were used in this thesis for characterization purposes, but the encapsulation of solid lipid and gold nanoparticles is also possible. Microfluidics methods permit high throughput microgel synthesis and independent control over variables such as drug-loaded nanoparticles type and concentration, releases kinetics, macromer molecular weight, bio-ligand presentation and microgels size. These features could be optimized for the delivery of a wide variety of small molecule drugs and even biologics, which can expand the potential use of this platform for prolonged and sustained intra-articular delivery and screening of therapeutics for OA treatment.

6.1.2 Intra-articular tissue-specific drug delivery

Small molecules traditionally used to manage pain in OA patients, such as NSAIDs, and novel disease modifying drug candidates have been shown to present off-target effects even if administered locally via intra-articular injections. For example, drugs that target processes in the synovial membrane such as NSAIDs and nerve growth factor (NGF) blockers have been related to a reduction in proteoglycan secretion and faster OA progression [10, 76]. Likewise, molecules that target regenerative pathways in the articular cartilage such as TGF-β1 and Kartogenin, a pro-chondrogenic small molecule drug, have been shown to induce synovium hyperplasia and promote the formation of cartilage-like tissues in ligaments and

synovial membrane [11, 77]. These examples highlight the need for tissue-specific drug delivery vehicles that could help minimize the off-target effects of different therapeutics and therefore facilitate their translation into the clinic. By conjugating PEG microgels with tissue-targeting peptides, the reported approach offers an alternative to overcome this limitation.

HAP-1 microgels demonstrated to effectively bind to rabbit and human synoviocytes *in vitro* and were found trapped in the synovial membrane of rat knee joints 3 weeks after intra-articular injection. Also, WYR-functionalized microgels were shown to bind bovine articular cartilage sections *in vitro* and were not localized in the synovial membrane at 3 weeks post-injection in the rat MMT model. All together, these data suggest that the proposed peptide-conjugated microgel system could be used for intra-articular tissue-specific drug delivery, which could impact the translation of multiple drug candidates such as Kartogenin.

Considering that OA is a complex disease involving diverse processes that take place in different intra-articular tissues, it is not surprising to think that its treatment may require the use of a combination of drugs in order to effectively address the multiple pathways related to OA progression. In this regard, the delivery system presented in this thesis could be an excellent platform to administer a combination of molecules to specific tissues inside the joint. It is important to note that customization of this system could allow the tissue-specific delivery of biologics such as proteins and nucleic acids, small molecule drugs, cells [101, 103, 102] and their combinations.

6.2 Future Directions

Overall, the findings presented in this work suggest several potential directions of future investigation ranging from a deeper characterization of the presented nanocomposite microgels, up to translational research applications.

6.2.1 Effect of HAP-1-functionalized PEG microgels on internalization and inflammation

The synovium-targeting peptide HAP-1 was discovered via phage display, but its target on synoviocytes is still unknown. When this peptide was discovered, Mi *et al.* demonstrated that HAP-1 linked to a pro-apoptotic peptide was able to induce conjugate internalization and promote apoptosis in rabbit synoviocytes, but the mechanisms involved in this process remain a question for future investigation [95]. Additionally, the effect of HAP-1 peptide on micron-scale drug delivery systems is also unknown. If HAP-1 is shown to activate cell pathways related to extracellular molecules internalization, it could have a direct impact on synovial inflammation.

To investigate whether HAP-1-functionalized PEG microgels activate pathways related to cellular internalization upon binding, a monolayer platform as the one used in Chapter 4 to asses microgels binding ability, can be used. Synoviocytes could be incubated with HAP-1 microgels and the activation of energy-dependent internalization processes could be evaluated via immuno-staining of protein complexes involved in clathrin-mediated endocytosis, caveolae-mediated endocytosis or macro-pinocytosis [143]. Also, the effect of HAP-1-functionalized PEG microgels on binding-induced synovial inflammation could be characterized. *In vitro* cultures of rabbit and human synoviocytes incubated with peptide-functionalized microgels

could be used to assess their cytokine expression using a multiplex ELISA. Additionally, since HAP-1 microgels were found to remain trapped in the synovial membrane surrounded by a highly cellularized tissue, immunohistochemistry (IHC) offers a good tool to assess for markers of inflammation *ex vivo*. Characterization of the cell types that surround the microgels would be necessary to understand the foreign body response that these delivery vehicles elicit.

6.2.2 *In vivo* localization of WYR-functionalized PEG microgels via magnetic resonance imaging

The localization of cartilage-binding microgels after intra-articular injection via histology demonstrated to be challenging. As evidenced by the images shown in Chapter 5 (Figure 5.5), microgels could not be seen in paraffin sections, instead the spaces that were occupied by trapped hydrogels were observed in the synovial membrane. This could happen due to the use of dehydrating solvents and high temperature during paraffin processing that cause hydrogel damage and shrinkage. WYR-conjugated microgel would remain attached to the articular cartilage in the interface with the synovial fluid, but would not be embedded in a tissue. Therefore, these microgels would be prone to removal and damage throughout histology processing, making it very difficult to determine their original *in vivo* location in the intra-articular space.

To better evaluate whether WYR-functionalized microgels are able to bind the articular cartilage and if they preferentially bind damaged areas, *in vivo* imaging tools may be more adequate techniques. Hu *et al.* conjugated WYR peptide to a magnetic resonance imaging (MRI) contrast agent for *in vivo* evaluation of hyperthrophic cartilage lesions in a rat model of OA [88]. These kind of mechanisms could be used to assess the *in vivo*, longitudinal location of WYR-functionalized

PEG microgels. This delivery vehicles could be engineered to either be conjugated or loaded with a gadolimium-based MRI contrast agent such as the one used by Hu, Et. al. This could allow the localization of WYR microgels, which could be correlated with areas of damaged cartilage recognized using end-point EPIC μCT analysis. This study would offer a more reliable and sensitive technique to determine the *in vivo* location of WYR-functionalized PEG microgels.

6.2.3 Effect of WYR-functionalized PEG microgels on drug delivery, penetration and retention into articular cartilage

Ideally, the delivery of drugs that target processes in the chondrocytes for OA treatment should be released inside the articular cartilage. To do so, the most effective approaches involve the use of cartilage targeting drug-loaded nanoparticles with a diameter of around 10 nm [132]. However, Ambika *et al.* suggest that surface-binding non-penetrating particles could improve intra-cartilage drug delivery compared to non-binding free-floating systems [131].

To better understand how WYR-functionalized PEG microgels could delivery small molecule drugs into the articular cartilage, drug penetration and retention assays could be conducted *in vitro* using bovine articular cartilage explants [132, 87]. A neutrally charged fluorescent probe such Cy3 [144] could be used as model small molecule drug. This fluorophore could be loaded into PEG microgels using a light sensitive liposome system [145]. Then, Cy3-loaded WYR-microgels would be compared to non-binding WYRsc-functionalized microgels for their ability to promote Cy3 penetration into bovine articular cartilage following procedures reported by Brown, Et. al. Briefly, cartilage explants could be incubated with microgel formulations for 30 min to allow WYR-conjugated microspheres to bind to the tissue. Then, burst release of Cy3 from the liposomes could be induced using light and

the small molecule would be allow to penetrate into the cartilage for 1h. Then, explants would be washed and the concentration of retained dye could be analyzed via spectrophotometry after cartilage explants digestion. This study would allow to determine if incorporating targeting moieties into non-penetrating microgels could improve drug bio-availability into the cartilage compared to non-targeting microgels.

6.2.4 Evaluation of the efficacy of peptide-functionalized PEG microgels as intra-articular drug delivery systems for OA treatment

The results presented in this dissertation provided deep characterization of the engineered delivery system. Thus, all the studies were conducted using model small molecules. To evaluate if the proposed system could be a promising strategy for tissue-specific delivery and prolonged intra-articular drug retention for OA treatment, an efficacy study should be conducted using a therapeutic molecule. For instance, the pro-chondrogenic drug Kartogenin (KGN), could be loaded into WYR-functionalized PEG microgels to assess its effect on OA progression in the rat MMT model. As a proof of concept, saline or KGN could be delivered intra-articularly as free drug or encapsulated in WYR or WYRsc-microgels to evaluate if the targeting peptide incorporation has a beneficial effect. Injection can be done 1 day after MMT surgery and the effect on the articular cartilage could be assessed via EPIC μCT 3 weeks after injection. Also, to determine if the targeting strategy prevents KGN from inducing synovium or ligaments chondrogenesis, a known off-target effect of this small molecule drug, these tissues could be harvested and analyze for markers of chondrogenesis via ELISA and IHC. This study could provide solid information regarding the effectiveness of WYR-microgels as tissue-targeting drug delivery vehicles for the treatment of OA.

6.3 Clinical Translation

The ultimate goal of this thesis is to engineer an intra-articular drug delivery system able to overcome some of the limitations that have hindered the clinical translation of several DMOAD candidates. The composite microgels presented in this thesis may help improve the therapeutic efficacy of these drug candidates by increasing their intra-articular retention time and possibly localizing them into the tissues of interest.

It is well known in the field that free drugs administered via intra-articular injection are rapidly cleared from the joint space, which prevents drugs from reaching therapeutically effective concentrations and prolonged times to exert a significant effect [7]. However, according to the clinical trials database run by the United States National Library of Medicine (NLM) at the National Institutes of Health (NIH) [146], most clinical trials evaluating the intra-articular injection of therapeutics use these compounds as free drug formulations (Table 6.1). The only biomaterial-based drug delivery vehicles explored in the clinic are hyaluronic acid (HA) and PLGA microparticles. Additionally, it is worth noticing that although several DMOAD are being evaluated, most clinical studies for this type of molecules fail to progress into Phase 3 clinical studies, with the exception of Samumed LLC. (Lorecivivint) and Bone Therapeutics (JTA-004), which are currently recruiting patients to evaluate their formulations in a phase 3 clinical study. These observations not only evidence the need to develop effective DMOAD, but also highlight the lack of clinical research to evaluate the potential use of drug delivery systems to enhance DMOAD therapeutic effectiveness.

Table 6.1: Clinical trials using intra-articular drug administration.

Phase	Molecule	Drug Type	Delivery Vehicle	Drug Effect	Sponsor	Status	Next Phase Status
1	LNA043	Small molecule	No	DMOAD (Chondrogenic)	Novartis	Completed 2018	Recruiting
	FX201	Gene therapy	Adenovirus	DMOAD (IL-1Ra gene)	Flexion Therapeutics	Recruiting	-
	UBX0101	Small molecule	No	DMOAD (Senolytic)	Unity Biotechnology	Completed 2019	Ongoing
	KA34	Small molecule	No	DMOAD (Chondrogenic)	Calibr and TSRI	Completed 2020	-
	XT-150	Gene therapy	No	DMOAD (IL-10 variant)	Xalud Therapeutics	Completed 2019	Recruiting
	Resiniferatoxin	Small molecule	No	Analgesic	Sorrento Therapeutics	Ongoing	-
	sc-rAAV2.5IL-1R	Gene therapy	Adenovirus	DMOAD (IL-1R)	Mayo Clinic	Recruiting	-
2	SI-613	Small molecule	HA	Anti-inflammatory (Diclofenac)	Seikagaku Corporation	Completed 2018	-
	TPX-100	Peptide	No	DMOAD (Chondrogenic)	OrthoTrophix	Completed 2017	-
	SM04690 (Lorecivivint)	Small molecule	No	DMOAD (WNT inhibitor)	Samumed LLC.	Completed 2018	Recruiting
	Canakinumab	Protein	No	DMOAD (IL-1 monoclonal antibody)	Novartis	Completed 2011	-
	Fasitibant	Small molecule	No	Analgesic	Menarini Group	Completed 2015	-
	BMP-7	Protein	No	DMOAD	Stryker	Completed 2011	-
	Sprifermin	Protein	No	DMOAD	EMD Serono	Completed 2019	-
	JTA-004	Plasma proteins	HA	DMOAD	Bone Therapeutics	Completed 2018	Recruiting
3	CNTX-4975	Small molecule	No	Analgesic (Capsaicin)	Centrexion Therapeutics	Ongoing	-
	Hydros-TA	Small molecule	HA	Anti-inflammatory (Triamcinolone acetonide)	Carbylan Therapeutics	Completed 2016	-
	Traumeel® / Zeel®	Small molecule	No	Homeopathic	Biologische Heilmittel Heel GmbH	Completed 2014	-
	Cingal®	Small molecule	HA	Anti-inflammatory (Triamcinolone hexacetonide)	Anika Therapeutics	Completed 2018	-
Approved	ZILRETTA®	Small molecule	PLGA Microparticle	Anti-inflammatory (Triamcinolone acetonide)	Flexion Therapeutics	FDA-approved 2017	

Similar to the studies presented in this dissertation, most research on IA drug delivery vehicles is limited to the characterization of these systems and their evaluation in pre-clinical animal studies using model drugs or NSAIDs [147, 63, 142, 71, 6, 148, 67]. However, few studies have coupled the use of IA drug delivery systems with DMOADs [149, 58, 75]. Additionally, the discovery of novel therapeutic compounds for OA treatment is mostly done by pharmaceutical companies, which sponsor clinical trials that do not use appropriate IA drug delivery vehicles [146] (Table 6.1).

Therefore, the first step towards the clinical translation of the composite PEG microgels presented in this dissertation is to establish collaborations with research labs or pharmaceutical companies that produce DMOADs. This could allow to investigate whether the sustained release profile and prolonged IA retention offered by drug delivery vehicles could improve DMOADs' therapeutic effect, specially of those drugs that failed to show significant improvements during clinical investigation.

The coupling of drug delivery systems research with investigational DMOADs would also require better characterization techniques to determine the effect of these drugs in small and large animal models of OA. This includes the use and standardization of functional outcome measures such as radiographic or MRI analysis of OA progression, gait analysis, pain assessment and more traditional *ex vivo* evaluation techniques such as OARSI scoring via histology analysis and EPIC-μCT [150, 151, 140]. Moreover, in order to determine whether tissue-binding PEG microgels offer a beneficial tissue-localized drug delivery, a deeper pre-clinical characterization of drug effects on different IA tissues would be required. In this regard, techniques such as localized tissue-specific gene expression analysis have been

used to elucidate the mechanisms of action of DMOAD [152] and could provide strong bases to determine if tissue-binding drug delivery vehicles, like those proposed in this dissertation, can minimize drugs' off-target effects.

Once pre-clinical studies using actual DMOADs show promising results, clinical trials for the combination product (delivery vehicle + drug) could be conducted to determine its safety and efficacy. Overall, the peptide-functionalized nanocomposite PEG microgels presented in this thesis supported model small molecule sustained release and prolonged IA retention in a rat model of OA without inducing degenerative changes in the joint, which evidence their potential use as IA delivery systems. However, their clinical translation would require further pre-clinical characterization using investigational DMOADs to determine if their use can improve drug's therapeutic efficacy and minimize potential off-target effects.

6.4 Conclusions

The results presented in this dissertation provide basis for future investigation of the potential use of peptide-functionalized PEG microgels as intra-articular targeting drug delivery systems for OA treatment. Future studies on the mechanisms involved in targeting and material binding-induced inflammation in the synovial membrane, drug penetration into the tissues of interest and the standardization of better *in vivo* microgels localization techniques, could provide important information for the improvement of peptide-conjugated PEG microgels. Further characterization of this system and its optimization could facilitate the translation of current drug candidates that have failed to show a relevant improvement in clinical studies, primarily due to the lack of appropriate drug delivery vehicles for intra-articular treatment of OA.

Appendices

APPENDIX A
SUPPLEMENTARY METHODS

A.1 Optimal cutting temperature (OCT) embedding of tissue samples containing PEG microgels

After tissue samples were fixed and decalcified, they were embedded in OCT using the following protocol.

1. Place the rat knee joints in 15 mL falcon tubes containing 3 mL of 5% sucrose (dissolved in PBS with calcium and magnesium) and vacuum infiltrate for 1 hour.
2. Add 1.5 mL of 20% sucrose, mix by hand agitation or shaker table for 1 min to obtain a final concentration of 10% sucrose. Vacuum infiltrate for 30 min.
3. Add 1.5 mL of 20% sucrose, mix by hand agitation or shaker table for 1 min to obtain a final concentration of 12.5% sucrose. Vacuum infiltrate for 30 min.
4. Add 3 mL of 20% sucrose, mix by hand agitation or shaker table for 1 min to obtain a final concentration of 15% sucrose. Vacuum infiltrate for 30 min.
5. Place the samples into 3 mL of 20% sucrose:OCT (4:1) solution and vacuum infiltrate for 1 hour.
6. Place the samples into 3 mL of 20% sucrose:OCT (3:1) solution and vacuum infiltrate for 1 hour.
7. Place the samples into 3 mL of 20% sucrose:OCT (2:1) solution and vacuum infiltrate for 1 hour.

8. Place the samples into 3 mL of 20% sucrose:OCT (1:1) solution and vacuum infiltrate for 1 hour.

9. Place the samples into 3 mL of 20% sucrose:OCT (1:2) solution and vacuum infiltrate overnight.

After OCT infiltration, for each sample, 20% sucrose:OCT (1:2) solution was poured into a cryomold to form a layer of approximately 2 mm. The mold was placed in a -20℃ freezer for 3-5 min to allow this OCT layer to harden, but not completely freeze. Then, to prevent bubbles formation around the sample, an additional thin layer of 20% sucrose:OCT (1:2) solution was added into the mold and the sample was placed on top of the unfrozen layer. Holding the rat knee joint in the desired position, the bottom of the cryomold was submerged into liquid nitrogen for 5 seconds to prevent sample from moving or rotating. Finally, the knee joint was covered with 20% sucrose:OCT (1:2) solution and the cryomold submerged into liquid nitrogen again until OCT hardened. Samples were kept in a -80℃ freezer until ready to be sectioned.

A.2 PLGA nanoparticles distribution in PEG microgels

The encapsulation of PLGA nanoparticles into PEG microgels is not homogeneous, primarily due to aggregation of the polymeric nanoparticles. Therefore, to measure the distribution of the encapsulated PLGA particles into the microgels, a Matlab script was used to calculate what percentage of the cross-sectional area of each microgel corresponds to PLGA fluorescent nanoparticles. This was calculated for every microgel present in 6 confocal images per experimental group. The Matlab script used to calculate this parameter first reads the brightfield and fluorescent confocal images and finds the microgels present using the built-in function *imfindcircles* as shown bellow.

```
%% Read confocal BF images
% Bright field channel undergos sharpen function to make
   microgels edges
% more clear
bfImage = imread('Bright_Field_Image_Name.JPG');
grayImage = rgb2gray(bfImage); % Transform image into gray
   scale
bfSharpen = imsharpen(grayImage); % Highlight the features
   borders
bfSharpen1 = imsharpen(bfSharpen);
bfSharpen2 = imsharpen(bfSharpen1);

%% Read fluorescence channel
fluorImage = imread('Fluorescence_Image_Name.JPG');
redChannel= fluorImage(:,:,1);
[xDim,yDim]=size(bfSharpen);  % Image dimensions

%% Find the gels. Use 'Dark' parmeter since gels edges are
   darker than background
% Adjust radius,sensitivity and edge threshold accordingly.
[centers,radii] = imfindcircles(bfSharpen2,[12 17], ...
'ObjectPolarity','Dark','Sensitivity',0.9728,'EdgeThreshold
   ',0.085);

figure
imshow(bfImage) % Show bright field image
title('Bright Field')

figure
imshow(fluorImage) % Show red channel image
title('Red Channel')

figure
imshow(bfSharpen2) % Show processed bright field
title('Processed Image')

figure
imshow(bfSharpen2) % Show processed bright field with found
    circles
hBright = viscircles(centers, radii,'Color','b','LineWidth'
   , 1);
title('Found circles')
```

Figure A.1 shows the imaging processing and intermediate steps used to find the microgels in the confocal images. After the circles have been found, the PLGA

nanoparticles area in each microgel is calculated using the following script, which utilizes the open source function *createCirclesMask.m* [153].

```
%% Create a mask for each microgel and calculate
   fluorescent area
numberCircles = numel(radii); % Number of found microgels
areaFrequency = zeros(numberCircles,1); % Vector containing
    the flourescent area(%) for each microgel

for i = 1:numberCircles
    % Create a binary mask for circle number i: Pixels
       within the circle
    % are white (1) in a black (0) background.
    mask = createCirclesMask([xDim,yDim],centers(i,:),radii
       (i));

    % Calculate total of pixels inside circle number i
    white_pixels_index = find(mask == 1);
    microgel_total_area = numel(white_pixels_index);

    % Binarize red channel image with a threshold of 50 in
       a 0-255 scale
    fluorPixels = find(redChannel > 50);
    bwFluorImage = zeros(xDim,yDim);
    bwFluorImage(fluorPixels) = 1;

    % Find total of fluorescent pixels inside the circle of
        interest
    singleGel = times(bwFluorImage,mask); % Multiply mask
       and binarized fluorescence image
    GelFluorPixels_Index = find(singleGel == 1);
    microgel_fluorescence_area = numel(GelFluorPixels_Index
       );
    percentage_fluorescence_area = 100*(
       microgel_fluorescence_area/microgel_total_area);

    areaFrequency(i) = percentage_fluorescence_area; % Add
       the fluorecence area(%) for earch microgel in the
       vector areaFrequency
end
```

Finally, the script gives a vector (*areaFrequency*) containing the microgel area percentage that corresponds to encapsulated PLGA nanoparticles for each gel present in the confocal image. After analyzing all the images in each experimental

group, the histogram of the fluorescent area distribution was plot using GraphPad Prism.

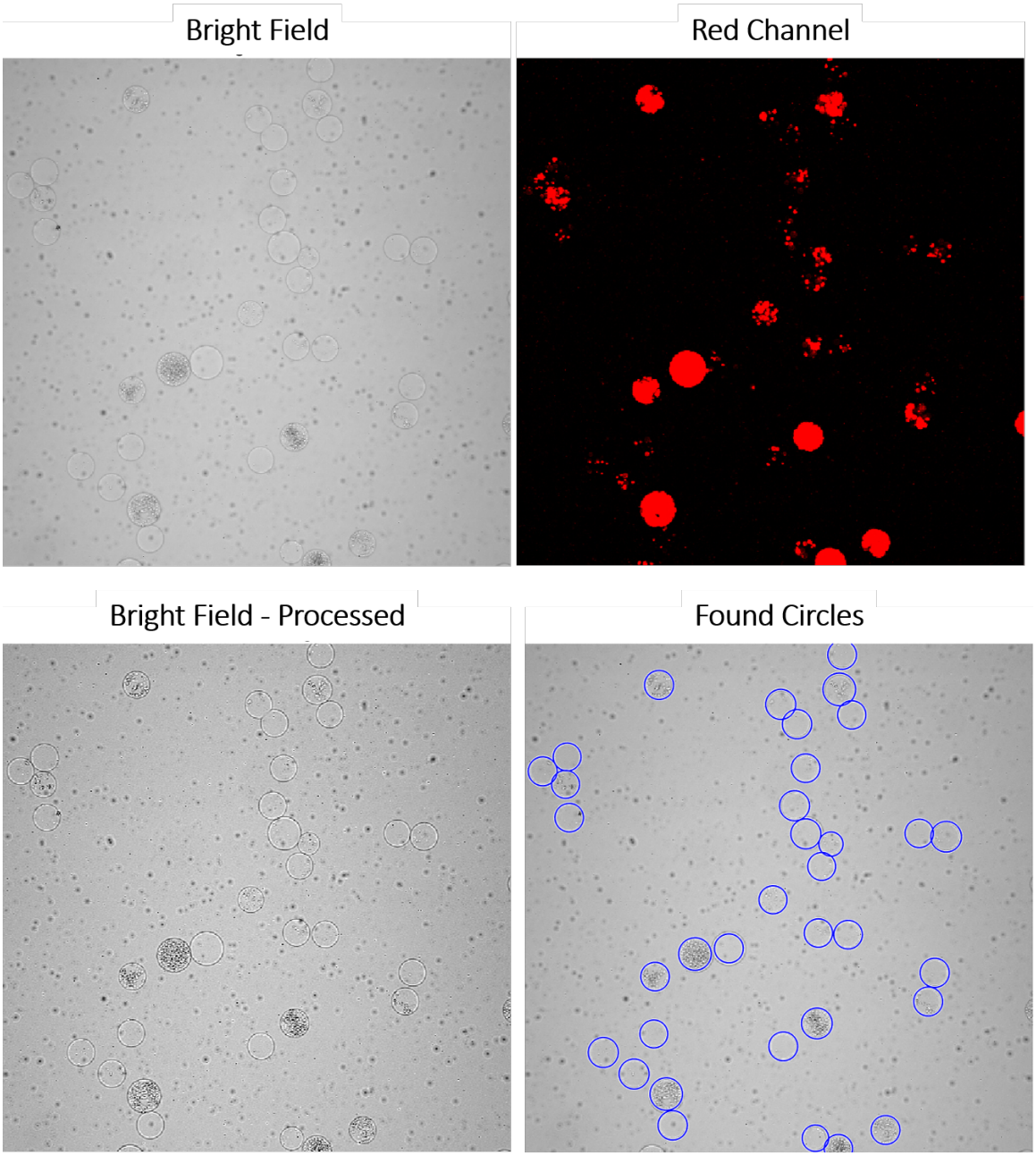

Figure A.1: PLGA nanoparticle distribution in PEG microgels: Image processing. In the first row the bright field and fluorescence confocal images are shown. Then, the bright field image is processed to make the microgels borders more evident. Finally, microgels are found using the Matlab function *imfindcircles*.

APPENDIX B
SUPPLEMENTARY RESULTS

B.1 Self-quenching effect in cyanine dyes

Self-quenching effect refers to a phenomenon when aggregation of fluorescence dye molecules results in up to 90% reduction on their brightness [154]. This represents a concern when preparing probes for *in vivo* imaging through the conjugation of cyanine dyes to molecules with multiple labeling sites, such as proteins and peptides. When the conjugation sites are located close to each other, dye molecules cluster leading to a significant energy transfer between them, resulting in severe quenching [154]. Additionally, when conjugated to a molecular probe, dye aggregation is also controlled by the solvent. Liquids like water have lower solvation power for hydrophobic dyes such as cyanine 7, compared to organic solvents. Therefore, aggregation and consequently self-quenching can be reduced by using a better solvent [154].

This effect could explain why WYR-functionalized microgels presented a significant increase in fluorescence intensity one day after intra-articular injection (Figure5.2). Cyanine 7-NHS ester was conjugated to amine-containing residues in the peptide sequence. Both WYR and HAP-1 peptides have two possible labeling sites, but in WYR peptide these residues are closer to each other than those of HAP-1. Therefore, Cy7 molecules conjugated to WYR would tend to cluster in a greater extent compared to HAP-1. We hypothesized that WYR-functionalized microgels will present a greater self-quenching effect compared to that of HAP-1

conjugated microgels. Also, diluting or placing both peptide-functionalized microgels into a better solvent will result in an increases in fluorescence intensity, which will be more pronounced in WYR-functionalized microgels.

To test this hypothesis and find an better explain the increase in fluorescence intensity seen on the *in vivo* microgel tracking study, we recapitulated the intra-articular injection procedure in an *in vitro* setting. The fluorescence intensity of microgels formulations functionalized with either Cy7-HAP-1 or Cy7-WYR peptides (n=4) was measured using an *in vivo* imaging system (IVIS). These formulations were equivalent to those used on *in vivo* studies (6μL of PEG in 50μL of saline). Then, intra-articular injection was simulated by mixing 50 μL of peptide-functionalized microgels with 50μL of 1% BSA or saline as a control. Fluorescence intensity was measured immediately after microgels dilution in saline or 1% BSA and every 20 min for a period of 100 min.

Figure B.1 shows that HAP-1 functionalized microgels, when diluted in saline, exhibit a fluorescence radiant efficiency similar to the one before mixing. In contrast, WYR-functionalized microgels diluted in saline presented a slight increase in fluorescence intensity after mixing with saline. If self-quenching effect was not present, diluting a fluorescent dye will result in a decrease in radiant efficiency proportional to the dilution factor. However, this was not the case in this experiment, suggesting that both HAP-1 and WYR experimental groups exhibit some Cy7 molecular clustering that leads to self-quenching at higher dye concentrations. When microgels were diluted in 1% BSA, both formulations exhibited an increase in the fluorescence radiant efficiency that stabilizes over time, which was more pronounced in the WYR group. Consistent with our hypothesis, increasing the solvation power by adding BSA into the solvent, resulted in a higher fluores-

cence signal compared to only diluting the samples in saline. The fact that this effect was greater in WYR-functionalized microgels suggests that the dye molecule aggregation is higher in Cy7-WYR compared to Cy7-HAP-1, resulting in higher self-quenching effect.

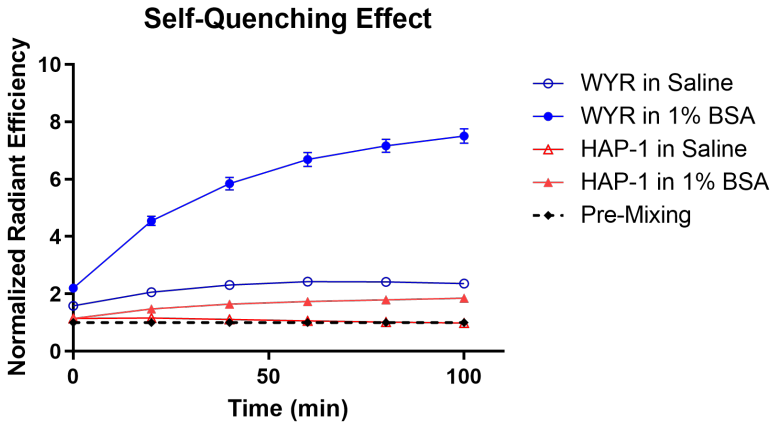

Figure B.1: Cyanine 7 self-quenching effect. An apparent increase in radiant efficiency is observed in peptide-functionalized samples dissolved in BSA compared to saline. This effect is more pronounced in WYR microgels suggesting that Cy7 molecules conjugated to this peptide present a higher degree of self-aggregation and therefore, a higher level of self-quenching than HAP-1 microgels.

The synovial fluid, similar to the 1% BSA condition in this experiment, is a better solvent compared to saline due to its protein and glycosaminoglycan content. Additionally, according to these results, the increase in fluorescence intensity does not occur immediately after microgels dilution in saline or 1% BSA, in contrast, this process takes around 2 h. Considering that in the *in vivo* microgels tracking study, the initial radiant efficiency measurement was taken immediately after injection, we did not capture the increase in the fluorescence signal at day zero. This explains the increase in fluorescence intensity observed one day after intra-articular injection, specially in the WYR-functionalized microgels group.

B.2 Cyanine 7 release profile

Figure B.2 shows the in vitro release profile of Cy7 in 1% BSA. Consistent with the results presented in chapter 3, the small molecule release from nano-composite PEG-4MAL microgels is controlled by PLGA NPs. Therefore, microgels exhibit a release profile comparable to that of PLGA NPs alone, where over 80% of Cy7 is released by day 5.

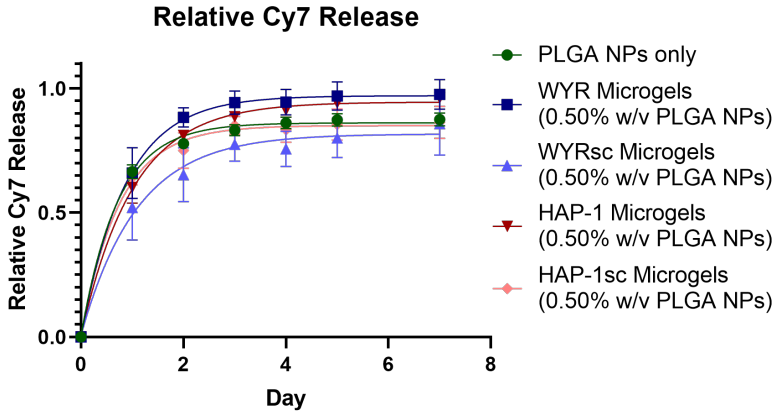

Figure B.2: Cyanine 7 release profile. Nano-composite microgels exhibit a Cy7 release profile similar to that of Cy7-loaded PLGA NPs alone.

REFERENCES

[1] R. C. Lawrence, D. T. Felson, C. G. Helmick, L. M. Arnold, H. Choi, R. a. Deyo, S. Gabriel, R. Hirsch, M. C. Hochberg, G. G. Hunder, J. M. Jordan, J. N. Katz, H. M. Kremers, and F. Wolfe, "Estimates of the prevalence of arthritis and other rheumatic conditions in the United States. Part II.," *Arthritis and rheumatism*, vol. 58, no. 1, pp. 26–35, 2008.

[2] A. Mathiessen and P. G. Conaghan, "Synovitis in osteoarthritis: current understanding with therapeutic implications," *Arthritis research & therapy*, vol. 19, no. 18, pp. 1–9, 2017.

[3] P. T. H. Brett C. Geiger, Alan J. Grodzinsky, "Designing Drug Delivery Systems for Articular Jointst," *Chemical Engineering Progress*, vol. 114, no. 5, pp. 46–51, 2018.

[4] R. F. Loeser, S. R. Goldring, C. R. Scanzello, and M. B. Goldring, "Osteoarthritis: a disease of the joint as an organ.," *Arthritis and rheumatism*, vol. 64, no. 6, pp. 1697–707, 2012.

[5] F. A. Formica, G. Barreto, and M. Zenobi-Wong, "Cartilage-targeting dexamethasone prodrugs increase the efficacy of dexamethasone," *Journal of Controlled Release*, vol. 295, pp. 118–129, 2019.

[6] M. Janssen, U. T. Timur, N. Woike, T. J. Welting, G. Draaisma, M. Gijbels, L. W. van Rhijn, G. Mihov, J. Thies, and P. J. Emans, "Celecoxib-loaded PEA microspheres as an auto regulatory drug-delivery system after intra-articular injection," *Journal of Controlled Release*, vol. 244, pp. 30–40, 2016.

[7] P. Maudens, O. Jordan, and E. Allémann, "Recent advances in intra-articular drug delivery systems for osteoarthritis therapy," *Drug Discovery Today*, vol. 23, no. 10, pp. 1761–1775, 2018.

[8] T. Brown, U. Laurent, and Fraser, "Turnover of hyaluronan in synovial joints: elimination of labelled hyaluronan from the knee joint of the rabbit," *Experimental Physiology*, vol. 76, no. 1, pp. 125–134, 1991.

[9] A. G. Bajpayee and A. J. Grodzinsky, "Cartilage-targeting drug delivery: can electrostatic interactions help?" *Nature Publishing Group*, vol. 13, no. 3, pp. 183–193, 2017.

[10] J.-K. Suh, T. S. Muzzonigro, and F. H. Fu, “Injury and Repair of Articular Cartilage: Related Scientific Issues,” *Operative Techniques in Orthopaedics*, vol. 7, no. 4, pp. 270–278, 1997.

[11] A. C. Bakker, F. A. J. Van De Loo, H. M. Van Beuningen, P Sime, P. L. E. M. Van Lent, P. M. Van Der Kraan, C. D. Richards, and W. B. Van Den Berg, “Overexpression of active TGF-beta-1 in the murine knee joint: evidence for synovial-layer-dependent chondro-osteophyte formation,” *Osteoarthritis and Cartilage*, vol. 9, pp. 128–136, 2001.

[12] K. D. Huebner, N. G. Shrive, and C. B. Frank, “Dexamethasone inhibits inflammation and cartilage damage in a new model of post-traumatic osteoarthritis,” *Journal of Orthopaedic Research*, vol. 32, no. 4, pp. 566–572, 2014.

[13] A. J. Grodzinsky, Y. Wang, S. Kakar, M. S. Vrahas, and C. H. Evans, “Intraarticular Dexamethasone to Inhibi the Development of Post-traumatic Osteoarthritis,” *J Orthop Res*, vol. 35, no. 3, pp. 406–411, 2017.

[14] M Kloppenburg and F Berenbaum, “Osteoarthritis year in review 2019: epidemiology and therapy,” *Osteoarthritis and Cartilage*, vol. 28, pp. 242–248, 2020.

[15] M. G. Cisternas, L. Murphy, J. J. Sacks, D. H. Solomon, D. J. Pasta, and C. G. Helmick, “Alternative Methods for Defining Osteoarthritis and the Impact on Estimating Prevalence in a US Population-Based Survey,” *Arthritis Care Res.*, vol. 68, no. 5, pp. 574–580, 2016.

[16] D. Chen, J. Shen, W. Zhao, T. Wang, L. Han, J. L. Hamilton, and H.-J. Im, “Osteoarthritis: toward a comprehensive understanding of pathological mechanism,” *Bone Research*, vol. 5, no. 16044, 2017.

[17] B. R. Deshpande, J. N. Katz, D. H. Solomon, E. H. Yelin, D. J. Hunter, S. P. Messier, L. G. Suter, E. Losina, and J. Katz, “The number of persons with symptomatic knee osteoarthritis in the United States: Impact of race/ethnicity, age, sex, and obesity HHS Public Access,” *Arthritis Care Res (Hoboken)*, vol. 68, no. 12, pp. 1743–1750, 2016.

[18] H. Kotlarz, C. L. Gunnarsson, H. Fang, and J. a. Rizzo, “Insurer and out-of-pocket costs of osteoarthritis in the US: Evidence from national survey data,” *Arthritis and Rheumatism*, vol. 60, no. 12, pp. 3546–3553, 2009.

[19] A. Turkiewicz, I. F. Petersson, J. Björk, G. Hawker, L. E. Dahlberg, L. S. Lohmander, and M. Englund, “Current and future impact of osteoarthritis

on health care: A population-based study with projections to year 2032," *Osteoarthritis and Cartilage*, vol. 22, no. 11, pp. 1826–1832, 2014.

[20] M Blagojevic, C Jinks, A Jeffery, and K. P. Jordan, "Risk factors for onset of osteoarthritis of the knee in older adults: a systematic review and meta-analysis.," *Osteoarthritis and cartilage / OARS, Osteoarthritis Research Society*, vol. 18, no. 1, pp. 24–33, 2010.

[21] J. C. Mora, R. Przkora, and Y. Cruz-Almeida, "Knee osteoarthritis: Pathophysiology and current treatment modalities," *Journal of Pain Research*, vol. 11, pp. 2189–2196, 2018.

[22] T. P. Andriacchi, J. Favre, J. C. Erhart-Hledik, and C. R. Chu, "A Systems View of Risk Factors for Knee Osteoarthritis Reveals Insights into the Pathogenesis of the Disease.," *Annals of biomedical engineering*, vol. 43, no. 2, pp. 376–387, 2015.

[23] R. F. Loeser, S. R. Goldring, C. R. Scanzello, and M. B. Goldring, "Osteoarthritis: A Disease of the Joint as an Organ," *Arthritis & Rheumatism*, vol. 64, no. 6, pp. 1697–1707, 2012.

[24] M. Kapoor, J. Martel-Pelletier, D. Lajeunesse, J. P. Pelletier, and H. Fahmi, "Role of proinflammatory cytokines in the pathophysiology of osteoarthritis," *Nature Reviews Rheumatology*, vol. 7, no. 1, pp. 33–42, 2011.

[25] S. Esser and A. Bailey, "Effects of Exercise and Physical Activity on Knee Osteoarthritis," *Curr Pain Headache Rep*, vol. 15, pp. 423–430, 2011.

[26] National Institute for Health and Care Excellence, "Osteoarthritis: Care and management in adults," Tech. Rep., 2014, pp. 259–407.

[27] T. E. McAlindon, R. R. Bannuru, M. C. Sullivan, N. K. Arden, F. Berenbaum, S. M. Bierma-Zeinstra, G. a. Hawker, Y. Henrotin, D. J. Hunter, H. Kawaguchi, K. Kwoh, S. Lohmander, F. Rannou, E. M. Roos, and M. Underwood, "OARSI guidelines for the non-surgical management of knee osteoarthritis," *Osteoarthritis and Cartilage*, vol. 22, no. 3, pp. 363–388, 2014.

[28] J. Lin, W. Zhang, A. Jones, and M. Doherty, "Primary care Efficacy of topical non-steroidal anti-inflammatory drugs in the treatment of osteoarthritis: meta-analysis of randomised controlled trials," *British Medical Journal*, vol. 329, no. 324, pp. 1–6, 2004.

[29] S. R. Smith, B. R. Deshpande, J. E. Collins, J. N. Katz, and E. Losina, "Comparative pain reduction of oral non-steroidal anti-inflammatory drugs

and opioids for knee osteoarthritis: systematic analytic review S.R.," *Osteoarthritis and Cartilage*, vol. 24, no. 6, pp. 962–972, 2016.

[30] E. E. Krebs, A. Gravely, S. Nugent, A. C. Jensen, B. DeRonne, E. S. Goldsmith, K. Kroenke, M. J. Bair, and S. Noorbaloochi, "Effect of opioid vs nonopioid medications on pain-related function in patients with chronic back pain or hip or knee osteoarthritis pain the SPACE randomized clinical trial," *Journal of the American Medical Association*, vol. 319, no. 9, pp. 872–882, 2018.

[31] X. Liu, G. C. Machado, J. P. Eyles, V. Ravi, and D. J. Hunter, "Dietary supplements for treating osteoarthritis: a systematic review and meta-analysis," *Br J Sports Med*, vol. 52, pp. 167–175, 2018.

[32] S. Wandel, P. Jüni, B. Tendal, E. Nüesch, P. M. Villiger, N. J. Welton, S. Reichenbach, and S. Trelle, "Effects of glucosamine, chondroitin, or placebo in patients with osteoarthritis of hip or knee: Network meta-analysis," *British Medical Journal*, vol. 341, no. 7775, p. 711, 2010.

[33] D. O. Clegg, D. J. Reda, C. L. Harris, M. A. Klein, J. R. O'dell, M. M. Hooper, J. D. Bradley, C. O. Bingham, M. H. Weisman, C. G. Jackson, N. E. Lane, J. J. Cush, L. W. Moreland, H. R. Schumacher, C. V. Oddis, F. Wolfe, J. A. Molitor, D. E. Yocum, T. J. Schnitzer, D. E. Furst, A. D. Sawitzke, H. Shi, K. D. Brandt, R. W. Moskowitz, H. J. Williams, and H. Veterans, "Glucosamine, Chondroitin Sulfate, and the Two in Combination for Painful Knee Osteoarthritis," *New England Journal of Medicine*, vol. 354, no. 8, pp. 795–808, 2006.

[34] A. D. Sawitzke, H. Shi, M. F. Finco, D. D. Dunlop, C. O. Bingham, C. L. Harris, N. G. Singer, J. D. Bradley, D. Silver, C. G. Jackson, N. E. Lane, C. V. Oddis, F. Wolfe, J. Lisse, D. E. Furst, D. J. Reda, R. W. Moskowitz, H. J. Williams, and D. O. Clegg, "The effect of glucosamine and/or chondroitin sulfate on the progression of knee osteoarthritis: A report from the glucosamine/chondroitin arthritis intervention trial," *Arthritis and Rheumatism*, vol. 58, no. 10, pp. 3183–3191, 2008.

[35] M. M. Richards, J. S. Maxwell, L. Weng, M. G. Angelos, and J. Golzarian, "Intra-articular Treatment of Knee Osteoarthritis: from Anti-inflammatories to Products of Regenerative Medicine," *The Physician and Sports Medicine*, vol. 44, no. 2, pp. 101–108, 2016.

[36] E. Ayhan, H. Kesmezacar, and I. Akgun, "Intraarticular injections (corticosteroid, hyaluronic acid, platelet rich plasma) for the knee osteoarthritis," *World Journal of Orthopedics*, vol. 5, no. 3, pp. 351–361, 2014.

[37] L. R. Soma, C. E. Uboh, Y. Liu, X. Li, M. A. Robinson, R. C. Boston, and P. T. Colahan, "Pharmacokinetics of dexamethasone following intra-articular, intravenous, intramuscular, and oral administration in horses and its effects on endogenous hydrocortisone," *Journal of Veterinary Pharmacology and Therapeutics*, vol. 36, no. 2, pp. 181–191, 2013.

[38] J. J. B. Ralph E. Peterson, Robert L. Black, "Disposition of intra-articularly injected cortisone and hydrocortisone," *Arthritis Rheum*, vol. 2, pp. 433–439, 1959.

[39] H. Johal, T. Devji, E. H. Schemitsch, and M. Bhandari, "Viscosupplementation in knee osteoarthritis: Evidence revisited," *JBJS Reviews*, vol. 4, no. 4, pp. 1–11, 2016.

[40] P. David Jevsevar, MD, MBA, Patrick Donnelly, MA, Gregory A. Brown, MD, PhD, and Deborah S. Cummins, "Viscosupplementation for osteoarthritis of the knee: A Systematic Review of the Evidence," *The Journal of Bone and Joint Surgery*, vol. 97, pp. 2047–2060, 2015.

[41] E. Thienpont, "Viscosupplementation for osteoarthritis of the knee," *New England Journal of Medicine*, vol. 372, no. 26, pp. 2569–2570, 2015.

[42] G. M. Pontes-Quero, L. García-Fernández, M. R. Aguilar, J. San Román, J. Pérez Cano, and B. Vázquez-Lasa, "Active viscosupplements for osteoarthritis treatment," *Seminars in Arthritis and Rheumatism*, vol. 49, no. 2, pp. 171–183, 2019.

[43] M. B. Goldring and F. Berenbaum, "Emerging Targets in Osteoarthritis Therapy," *Current Opinion in Pharmacology*, vol. 22, pp. 51–63, 2015.

[44] X. Chevalier, F. Eymard, and P. Richette, "Biologic agents in osteoarthritis: Hopes and disappointments," *Nature Reviews Rheumatology*, vol. 9, no. 7, pp. 400–410, 2013.

[45] K. Grothe, K. Flechsenhar, T. Paehler, O. Ritzeler, J. Beninga, J. Saas, M. Herrmann, and K. Rudolphi, "IκB kinase inhibition as a potential treatment of osteoarthritis – results of a clinical proof-of-concept study," *Osteoarthritis and Cartilage*, vol. 25, pp. 46–52, 2017.

[46] L. S. Lohmander, S. Hellot, D. Dreher, E. F. Krantz, D. S. Kruger, A. Guermazi, and F. Eckstein, "Intraarticular sprifermin (recombinant human fibroblast growth factor 18) in knee osteoarthritis: A randomized, double-blind, placebo-controlled trial," *Arthritis and Rheumatology*, vol. 66, no. 7, pp. 1820–1831, 2014.

[47] M. L. Kang, J.-Y. Ko, J. E. Kim, and G.-I. Im, “Intra-articular delivery of kartogenin-conjugated chitosan nano/ microparticles for cartilage regeneration,” *Biomaterials*, vol. 35, pp. 9984–9994, 2014.

[48] G. Mohan, S. Magnitsky, G. Melkus, K. Subburaj, G. Kazakia, A. J. Burghardt, A. Dang, N. E. Lane, and S. Majumdar, “Kartogenin treatment prevented joint degeneration in a rodent model of osteoarthritis: A pilot study,” *Journal of Orthopaedic Research*, vol. 34, no. 10, pp. 1780–1789, 2016.

[49] Y. Ono, S. Ishizuka, C. B. Knudson, and W. Knudson, “Chondroprotective Effect of Kartogenin on CD44-Mediated Functions in Articular Cartilage and Chondrocytes,” *Cartilage*, vol. 5, no. 3, pp. 172–180, 2014.

[50] W. H. Robinson, C. M. Lepus, Q. Wang, H. Raghu, R. Mao, T. M. Lindstrom, and J. Sokolove, “Low-grade inflammation as a key mediator of the pathogenesis of osteoarthritis,” *Nat Rev Rheumatol*, vol. 12, no. 10, pp. 580–592, 2016.

[51] M. S. M. Persson, A. Sarmanova, M. Doherty, and W. Zhang, “Meta-analysis Conventional and biologic disease-modifying anti-rheumatic drugs for osteoarthritis: a meta-analysis of randomized controlled trials,” *Rheumatology*, vol. 57, pp. 1830–1837, 2018.

[52] X. Chevalier, F. Eymard, and P. Richette, “Biologic agents in osteoarthritis: hopes and disappointments,” *Nat. Rev. Rheumatol*, vol. 9, pp. 400–410, 2013.

[53] T. E. Kavanaugh, T. A. Werfel, H. Cho, K. A. Hasty, and C. L. Duvall, “Particle Based Technologies for Osteoarthritis Detection and Therapy,” *Drug Deliv Transl Res.*, vol. 6, no. 2, pp. 132–147, 2016.

[54] S. Owen, H. Francis, and M. Roberts, “Disappearance kinetics of solutes from synovial fluid after intra- articular injection.,” *British Journal of Clinical Pharmacology*, vol. 38, no. 4, pp. 349–355, 1994.

[55] R. J. S. W. F. Elmquist, K. K. H. Chan, “Synovial mean transit time of diclofenac and other nonsteroidal antiinflammatory drugs,” *Pharmaceutical Research*, vol. 11, no. 12, pp. 1689–1697, 1994.

[56] P. A. Simkin, M. P. Wu, and D. M. Foster, “Articular Pharmacokinetics of Protein-Bound Antirheumatic Agents,” *Clinical Pharmacokinetics*, vol. 25, no. 4, pp. 342–350, 1993.

[57] S. M. Wigginton, B. C. Chu, M. H. Weisman, and S. B. Howell, “Methotrexate pharmacokinetics after intraarticular injection in patients with rheumatoid arthritis,” *Arthritis & Rheumatism*, vol. 23, no. 1, pp. 119–122, 1980.

[58] R. E. Whitmire, D. S. Wilson, A. Singh, M. E. Levenston, N. Murthy, and A. J. García, “Self-assembling nanoparticles for intra-articular delivery of anti-inflammatory proteins,” *Biomaterials*, vol. 33, no. 30, pp. 7665–7675, 2012.

[59] A. Singh, R. Agarwal, C. A. Diaz-Ruiz, N. J. Willett, P. Wang, L Andrew Lee, Q. Wang, R. E. Guldberg, and A. J. García, “Nano-engineered particles for enhanced intra-articular retention and delivery of proteins,” *Adv Healthc Mater*, vol. 3, no. 10, pp. 1562–1567, 2014.

[60] B. Palmieri, V. Rottigni, and T. Iannitti, “Preliminary study of highly cross-linked hyaluronic acid-based combination therapy for management of knee osteoarthritis-related pain,” *Drug Design, Development and Therapy*, vol. 7, pp. 7–12, 2013.

[61] M. J. K. Chan Woong Park , Kyung Wan Ma , Sun Woo Jang, Miwon Son, “Comparison of Piroxicam Pharmacokinetics and Anti-Inflammatory Effect in Rats after intra-Articular and Intramuscular Administration,” *Biomolecules & Therapeutics*, vol. 22, no. 3, pp. 260–266, 2014.

[62] K. Yoshioka, Y. Yasuda, T. Kisukeda, R. Nodera, Y. Tanaka, and K. Miyamoto, “Pharmacological effects of novel cross-linked hyaluronate, Gel-200, in experimental animal models of osteoarthritis and human cell lines,” *Osteoarthritis and Cartilage*, vol. 22, no. 6, pp. 879–887, 2014.

[63] A. Petit, E. M. Redout, C. H. Van De Lest, J. C. De Grauw, B. Müller, R. Meyboom, P. Van Midwoud, T. Vermonden, W. E. Hennink, and P Ren E Van Weeren, “Sustained intra-articular release of celecoxib from in situ forming gels made of acetyl-capped PCLA-PEG-PCLA triblock copolymers in horses,” *Biomaterials*, vol. 53, pp. 426–436, 2015.

[64] A. Samad, Y. Sultana, M. Aqil, Y Sultana, and M Aqil, “Liposomal Drug Delivery Systems: An Update Review,” *Current Drug Delivery*, vol. 4, pp. 297–305, 2007.

[65] X. Xu, A. K. Jha, D. A. Harrington, M. C. Farach-Carson, and X. Jia, “Hyaluronic Acid-Based Hydrogels: from a Natural Polysaccharide to Complex Networks,” *Soft Matter*, vol. 8, no. 12, pp. 3280–3294, 2012.

[66] A. Akbarzadeh, R. Rezaei-Sadabady, S. Davaran, S. Woo Joo, N. Zarghami, Y. Hanifehpour, M. Samiei, M. Kouhi, and K. Nejati-Koshki, “Liposome: clas-

sification, preparation, and applications," *Nanoscale Research Letters*, vol. 8, no. 102, pp. 1–9, 2013.

[67] S. H. R. Edwards, M. A. Cake, G. Spoelstra, and R. A. Read, "Biodistribution and Clearance of Intra-articular Liposomes in a Large Animal Model Using a Radiographic Marker," *Journal of Liposome Research*, vol. 17, pp. 249–261, 2007.

[68] N. Kamaly, Z. Xiao, P. M. Valencia, A. F. Radovic-Moreno, and O. C. Farokhzad, "Targeter polymeric therapeutic nanoparticles: design, development and clinical translation," *Chem Soc Rev*, vol. 29, no. 10, pp. 1883–1889, 2012. arXiv: NIHMS150003.

[69] J. Pradal, P. Maudens, C. Gabay, C. A. Seemayer, O. Jordan, and E. Allémann, "Effect of particle size on the biodistribution of nano- and microparticles following intra-articular injection in mice," *International Journal of Pharmaceutics*, vol. 498, pp. 119–129, 2016.

[70] A. Singh, R. Agarwal, C. A. Diaz-Ruiz, N. J. Willett, P. Wang, L Andrew Lee, Q. Wang, R. E. Guldberg, and A. J. García, "Nano-engineered particles for enhanced intra-articular retention and delivery of proteins," *Adv Health Mater*, vol. 3, no. 10, pp. 1562–1567, 2014.

[71] M. Morgen, D. Tung, B. Boras, W. Miller, A.-M. Malfait, M. Tortorella, M Morgen, W Miller, D Tung, B Boras, A.-M Malfait, and M Tortorella, "Nanoparticles for Improved Local Retention after Intra-Articular Injection into the Knee Joint," *Pharm Res*, vol. 30, pp. 257–268, 2013.

[72] P Arunkumar, S Indulekha, S Vijayalakshmi, and R Srivastava, "Synthesis, characterizations, in vitro and in vivo evaluation of Etoricoxib-loaded Poly (Caprolactone) microparticles-a potential Intra-articular drug delivery system for the treatment of Osteoarthritis," *Journal of Biomaterials science*, vol. 27, no. 4, pp. 303–316, 2016.

[73] P. J. E. Maarten Janssen, Ufuk Tan Timur, Nina Woike, Tim J.M. Welting, Guy Draaisma, Marion Gijbels, Lodewijk W. van Rhijn, George Mihov, Jens Thies, "Celecoxib-loaded PEA microspheres as an auto regulatory drug-delivery system after intra-articular injection," *Journal of Controlled Release*, vol. 244, pp. 30–40, 2016.

[74] Flexion Therapeutics, *ZILRETTA® (triamcinolone acetonide extended-release injectable suspension)*.

[75] P. G. Conaghan, D. J. Hunter, S. B. Cohen, V. B. Kraus, F. Berenbaum, J. R. Lieberman, D. G. Jones, A. I. Spitzer, D. S. Jevsevar, N. P. Katz,

D. J. Burgess, J. Lufkin, J. R. Johnson, and N. Bodick, “Effects of a Single Intra-Articular Injection of a Microsphere Formulation of Triamcinolone Acetonide on Knee Osteoarthritis Pain,” *The Journal of Bone and Joint Surgery*, vol. 100, no. 8, pp. 666–677, 2018.

[76] M. C. Hochberg, L. A. Tive, S. B. Abramson, E. Vignon, K. M. Verburg, C. R. West, M. D. Smith, and D. S. Hungerford, “When Is Osteonecrosis Not Osteonecrosis?: Adjudication of Reported Serious Adverse Joint Events in the Tanezumab Clinical Development Program,” *Arthritis and Rheumatology*, vol. 68, no. 2, pp. 382–391, 2016.

[77] J. Zhang and J. H. Wang, “Kartogenin induces cartilage-like tissue formation in tendon-bone junction,” *Bone Research*, vol. 2, no. January, pp. 12–17, 2014. arXiv: NIHMS150003.

[78] D. Shi, X. Xu, Y. Ye, K. Song, Y. Cheng, J. Di, Q. Hu, J. Li, H. Ju, Q. Jiang, and Z. Gu, “Photo-Cross-Linked Scaffold with Kartogenin- Encapsulated Nanoparticles for Cartilage Regeneration,” *ACS NANO*, vol. 10, pp. 1292–1299, 2016.

[79] M.-L. Kang, S.-Y. Jeong, and G.-I. Im, “Hyaluronic Acid Hydrogel Functionalized with Self-Assembled Micelles of Amphiphilic PEGylated Kartogenin for the Treatment of Osteoarthritis,” *Tissue Engineering Part A*, vol. 23, no. 13-14, pp. 630–639, 2017.

[80] X. Li, J. Ding, Z. Zhang, M. Yang, J. Yu, J. Wang, F. Chang, and X. Chen, “Kartogenin-Incorporated Thermogel Supports Stem Cells for Significant Cartilage Regeneration,” *ACS Applied Materials & Interfaces*, vol. 8, pp. 5148–5159, 2016.

[81] C. Hughes, B. Faurholm, F. Dell’Accio, A. Manzo, M. Seed, N. Eltawil, A. Marrelli, D. Gould, C. Subang, A. Al-Kashi, C. De Bari, P. Winyard, Y. Chernajovsky, and A. Nissim, “Human single-chain variable fragment that specifically targets arthritic cartilage,” *Arthritis and Rheumatism*, vol. 62, no. 4, pp. 1007–1016, 2010.

[82] H. Cho, E. Pinkhassik, V. David, J. M. Stuart, and K. A. Hasty, “Detection of early cartilage damage using targeted nanosomes in a post-traumatic osteoarthritis mouse model,” *Nanomedicine: Nanotechnology, Biology, and Medicine*, vol. 11, pp. 939–946, 2015.

[83] B.-H. M. Hongsik Cho, Byoung Ju Kim, Sang-Hyug Park, Karen A Hasty, “Noninvasive visualization of early osteoarthritic cartilage using targeted nanosomes in a destabilization of the medial meniscus mouse model,” *International Journal of Nanomedicine*, vol. 13, pp. 1215 –1224, 2018.

[84] Y. Pi, X. Zhang, J. Shi, J. Zhu, W. Chen, C. Zhang, W. Gao, C. Zhou, and Y. Ao, "Targeted delivery of non-viral vectors to cartilage in vivo using a chondrocyte-homing peptide identified by phage display," *Biomaterials*, vol. 32, no. 26, pp. 6324–6332, 2011.

[85] C. S. F. Cheung, J. C. Lui, and J. Baron, "Identification of Chondrocyte-Binding Peptides by Phage Display," *J Orthop Res*, vol. 31, no. 7, 2013.

[86] D. A. Rothenfluh, H. Bermudez, C. P. O 'neil, and J. A. Hubbell, "Biofunctional polymer nanoparticles for intra-articular targeting and retention in cartilage," *Nature Materials*, vol. 7, pp. 248–254, 2008.

[87] S. B. Brown, L. Wang, R. R. Jungels, and B. Sharma, "Effects of cartilage-targeting moieties on nanoparticle biodistribution in healthy and osteoarthritic joints," *Acta Biomaterialia*, vol. 101, pp. 469–483, 2020.

[88] H.-Y. Hu, N.-H. Lim, H.-P. Juretschke, D. Ding-Pfennigdorff, P. Florian, M. Kohlmann, A. Kandira, J. Peter Von Kries, J. Saas, K. A. Rudolphi, K. U. Wendt, H. Nagase, O. Plettenburg, M. Nazare, and C. Schultz, "In vivo visualization of osteoarthritic hypertrophic lesions," *Chem. Sci.*, vol. 6, 2015.

[89] H. Chen, Z. Qin, J. Zhao, Y. He, E. Ren, Y. Zhu, G. Liu, C. Mao, and L. Zheng, "Cartilage-targeting and dual MMP-13/pH responsive theranostic nanoprobes for osteoarthritis imaging and precision therapy," *Biomaterials*, vol. 225, 2019.

[90] W. Yi, H. Zhou, A. Li, Y. Yuan, Y. Guo, P. Li, B. Qi, Y. Xiao, A. Yu, and X. Hu, "A NIR-II fluorescent probe for articular cartilage degeneration imaging and osteoarthritis detection," *Biomater. Sci*, vol. 7, p. 1043, 2019.

[91] L. Lee, C. Buckley, M. C. Blades, G. Panayi, and A. J. T. George, "Identification of Synovium-Specific Homing Peptides by In Vivo Phage Display Selection," vol. 46, no. 8, pp. 2109–2120, 2002.

[92] Y.-H. Yang, R. Rajaiah, E. Ruoslahti, and K. D. Moudgil, "Peptides targeting inflamed synovial vasculature attenuate autoimmune arthritis.," *Proceedings of the National Academy of Sciences of the United States of America*, vol. 108, no. 31, pp. 12 857–62, 2011.

[93] S. E. Wythe, D. Dicara, T. E. I. Taher, C. M. Finucane, R. Jones, M. Bombardieri, Y. K. S. Man, A. Nissim, S. J. Mather, Y. Chernajovsky, and C. Pitzalis, "Targeted delivery of cytokine therapy to rheumatoid tissue by a synovial targeting peptide," *Ann Rheum Dis*, vol. 72, pp. 129–135, 2013.

[94] R. R. Meka, S. H. Venkatesha, and K. D. Moudgil, "Peptide-directed liposomal delivery improves the therapeutic index of an immunomodulatory cytokine in controlling autoimmune arthritis," *Journal of Controlled Release*, vol. 286, pp. 279–288, 2018.

[95] Z. Mi, X. Lu, J. C. Mai, B. G. Ng, G. Wang, E. R. Lechman, S. C. Watkins, H. Rabinowich, and P. D. Robbins, "Identification of a synovial fibroblast-specific protein transduction domain for delivery of apoptotic agents to hyperplastic synovium," *Molecular Therapy*, vol. 8, no. 2, pp. 295–305, 2003.

[96] A. S. Vanniasinghe, N. Manolios, S. Schibeci, C. Lakhiani, E. Kamali-Sarvestani, R. Sharma, V. Kumar, M. Moghaddam, M. Ali, and V. Bender, "Targeting fibroblast-like synovial cells at sites of inflammation with peptide targeted liposomes results in inhibition of experimental arthritis," *Clinical Immunology*, vol. 151, no. 1, pp. 43–54, 2014.

[97] C. You, J. Zu, X. Liu, P. Kong, C. Song, R. Wei, C. Zhou, Y. Wang, and J. Yan, "Synovial fibroblast-targeting liposomes encapsulating an NF-κB-blocking peptide ameliorates zymosan-induced synovial inflammation.," *Journal of cellular and molecular medicine*, vol. 22, no. 4, pp. 2449–2457, 2018.

[98] S. C. Rizzi and J. A. Hubbell, "Articles Recombinant Protein-co-PEG Networks as Cell-Adhesive and Proteolytically Degradable Hydrogel Matrixes. Part I: Development and Physicochemical Characteristics," *Biomacromolecules*, vol. 6, pp. 1226–1238, 2005.

[99] S. C. Rizzi, M. Ehrbar, S. Halstenberg, G. P. Raeber, H. G. Schmoekel, H. Hagenmü, R. Mü, F. E. Weber, and J. A. Hubbell, "Recombinant Protein-co-PEG Networks as Cell-Adhesive and Proteolytically Degradable Hydrogel Matrixes. Part II: Biofunctional Characteristics," *Biomacromolecules*, vol. 7, pp. 3019–3029, 2006.

[100] E. A. Phelps, N. O. Enemchukwu, V. F. Fiore, J. C. Sy, N. Murthy, T. A. Sulchek, T. H. Barker, and A. J. García, "Maleimide cross-linked bioactive PEG hydrogel exhibits improved reaction kinetics and cross-linking for cell encapsulation and in situ delivery," *Advanced Materials*, vol. 24, pp. 64–70, 2012. arXiv: NIHMS150003.

[101] D. M. Headen, G. Aubry, H. Lu, and A. J. García, "Microfluidic-based generation of size-controlled, biofunctionalized synthetic polymer microgels for cell encapsulation," *Advanced Materials*, vol. 26, no. 19, pp. 3003–3008, 2014. arXiv: 15334406.

[102] D. M. Headen, J. R. García, and A. J. García, "Parallel droplet microfluidics for high throughput cell encapsulation and synthetic microgel generation," *Microsystems & Nanoengineering*, vol. 4, p. 17 076, 2018.

[103] G. A. Foster, D. M. Headen, C. González-García, M. Salmerón-Sánchez, H. Shirwan, and A. J. García, "Protease-degradable microgels for protein delivery for vascularization," *Biomaterials*, vol. 113, pp. 170–175, 2017.

[104] A. M. Bendele, "Animal models of osteoarthritis," Tech. Rep. 4, 2001, pp. 363–376.

[105] M. J. Janusz, A. M. Bendele, K. K. Brown, Y. O. Taiwo, L Hsieh, and S. A. Heitmeyer, "Induction of osteoarthritis in the rat by surgical tear of the meniscus: Inhibition of joint damage by a matrix metalloproteinase inhibitor," *Osteoarthritis and Cartilage*, vol. 10, pp. 785–791, 2002.

[106] T Wei, N. H. Kulkarni, Q. Q. Zeng, L. M. Helvering, X Lin, F Lawrence, L Hale, M. G. Chambers, C Lin, A Harvey, Y. L. Ma, R. L. Cain, J Oskins, M. A. Carozza, D. D. Edmondson, T Hu, R. R. Miles, T. P. Ryan, J. E. Onyia, and P. G. Mitchell, "Analysis of early changes in the articular cartilage transcriptisome in the rat meniscal tear model of osteoarthritis: pathway comparisons with the rat anterior cruciate transection model and with human osteoarthritic cartilage," *Osteoarthritis and Cartilage*, vol. 18, pp. 992–1000, 2010.

[107] S. Ashraf, P. I. Mapp, and D. A. Walsh, "Contributions of angiogenesis to inflammation, joint damage, and pain in a rat model of osteoarthritis," *Arthritis and Rheumatism*, vol. 63, no. 9, pp. 2700–2710, 2011.

[108] T Thote, A. S. P. Lin, Y Raji, S Moran, H. Y. Stevens, M Hart, R. V. Kamath, R. E. Guldberg, N. J. Willett Z Y, and W. H. Coulter, "Localized 3D analysis of cartilage composition and morphology in small animal models of joint degeneration," *Osteoarthritis and Cartilage*, vol. 21, pp. 1132–1141, 2013.

[109] L. Bédouet, F. Pascale, L. Moine, M. Wassef, S. H. Ghegediban, V.-N. Nguyen, M. Bonneau, D. Labarre, and A. Laurent, "Intra-articular fate of degradable poly(ethyleneglycol)-hydrogel microspheres as carriers for sustained drug delivery," *International Journal of Pharmaceutics*, vol. 456, pp. 536–544, 2013.

[110] M. J. P. Thomas J. Dougherty, *Antibiotic Discovery and Development*. 2012, pp. 800–805.

[111] I. Bala, S. Hariharan, and M. N. Kumar, *PLGA nanoparticles in drug delivery: The state of the art*, 2004.

[112] S. Fredenberg, M. Wahlgren, M. Reslow, and A. Axelsson, *The mechanisms of drug release in poly(lactic-co-glycolic acid)-based drug delivery systems - A review*, 2011.

[113] Y. Fu and W. J. Kao, "Drug Release Kinetics and Transport Mechanisms of Non-degradable and Degradable Polymeric Delivery Systems," *Expert Opin Drug Devil*, vol. 7, no. 4, pp. 429–444, 2010.

[114] Y. P. Li, Y. Y. Pei, X. Y. Zhang, Z. H. Gu, Z. H. Zhou, W. F. Yuan, J. J. Zhou, J. H. Zhu, and X. J. Gao, "PEGylated PLGA nanoparticles as protein carriers: Synthesis, preparation and biodistribution in rats," *Journal of Controlled Release*, vol. 71, no. 2, pp. 203–211, 2001.

[115] M. K. D.K. Sahana, G. Mittal, V. Bhardwaj, "PLGA Nanoparticles for Oral Delivery of Hydrophobic Drugs: Influence of Organic Solvent on Nanoparticle Formation and Release Behavior In Vitro and In Vivo Using Estradiol as a Model Drug," *Journal of pharmaceutical sciences*, vol. 97, no. 4, pp. 1530–1542, 2008.

[116] W. Gao, Y. Zhang, Q. Zhang, and L. Zhang, "Nanoparticle-Hydrogel: A Hybrid Biomaterial System for Localized Drug Delivery," *Annals of biomedical engineering*, vol. 44, no. 6, pp. 2049–2061, 2016.

[117] W. Wu, J. Shen, P. Banerjee, and S. Zhou, "Chitosan-based responsive hybrid nanogels for integration of optical pH-sensing, tumor cell imaging and controlled drug delivery," *Biomaterials*, vol. 31, no. 32, pp. 8371–8381, 2010.

[118] W. Wu, T. Zhou, A. Berliner, P. Banerjee, and S. Zhou, "Smart core-shell hybrid nanogels with ag nanoparticle core for cancer cell imaging and gel shell for pH-regulated drug delivery," *Chemistry of Materials*, vol. 22, no. 6, pp. 1966–1976, 2010.

[119] X. Zhou, F. Chen, H. Lu, L. Kong, S. Zhang, W. Zhang, J. Nie, B. Du, and X. Wang, "Ionic Microgel Loaded with Gold Nanoparticles for the Synergistic Dual-Drug Delivery of Doxorubicin and Diclofenac Sodium," *Industrial and Engineering Chemistry Research*, 2019.

[120] U. G. Spizzirri, S. Hampel, G. Cirillo, F. P. Nicoletta, A. Hassan, O. Vittorio, N. Picci, and F. Iemma, "Spherical gelatin/CNTs hybrid microgels as electroresponsive drug delivery systems," *International Journal of Pharmaceutics*, vol. 448, no. 1, pp. 115–122, 2013.

[121] R. Regmi, S. R. Bhattarai, C. Sudakar, A. S. Wani, R. Cunningham, P. P. Vaishnava, R. Naik, D. Oupicky, and G. Lawes, "Hyperthermia controlled

rapid drug release from thermosensitive magnetic microgels," *Journal of Materials Chemistry*, vol. 20, no. 29, pp. 6158–6163, 2010.

[122] B. Sung, S. Shaffer, M. Sittek, T. Alboslemy, C. Kim, and M. H. Kim, "Alternating magnetic field-responsive hybrid gelatin microgels for controlled drug release," *Journal of Visualized Experiments*, vol. 2016, no. 108, 2016.

[123] S. Chai, J. Zhang, T. Yang, J. Yuan, and S. Cheng, "Thermoresponsive microgel decorated with silica nanoparticles in shell: Biomimetic synthesis and drug release application," *Colloids and Surfaces A: Physicochemical and Engineering Aspects*, vol. 356, no. 1-3, pp. 32–39, 2010.

[124] J. Li, D. J. Mooney, and J. A. Paulson, "Designing hydrogels for controlled drug delivery HHS Public Access," *Nat Rev Mater*, vol. 1, no. 12, 2016.

[125] H. M. Shirin Rafieian, Hamid Mirzadeh and M. E. Masoumi, "A review on nanocomposite hydrogels and their biomedical applications," *Sci Eng Compos Mater*, pp. 154–174, 2019.

[126] Y. Y. Liu, X. Y. Liu, J. M. Yang, D. L. Lin, X. Chen, and L. S. Zha, "Investigation of Ag nanoparticles loading temperature responsive hybrid microgels and their temperature controlled catalytic activity," *Colloids and Surfaces A: Physicochemical and Engineering Aspects*, vol. 393, pp. 105–110, 2012.

[127] I. Gorelikov, L. M. Field, and E. Kumacheva, "Hybrid Microgels Photoresponsive in the Near-Infrared Spectral Range," *J. AM. CHEM. SOC*, vol. 126, pp. 15 938–15 939, 2004.

[128] M. N. Hsu, R. Luo, K. Z. Kwek, Y. C. Por, Y. Zhang, and C. H. Chen, "Sustained release of hydrophobic drugs by the microfluidic assembly of multistage microgel/poly (lactic-co-glycolic acid) nanoparticle composites," *Biomicrofluidics*, vol. 9, no. 5, 2015.

[129] E. Ruoslahti, "RGD and other recognition sequences for integrins," *Annual Review of Cell and Developmental Biology*, vol. 12, no. 1, pp. 697–715, 1996.

[130] D. C. Montgomery, *Design and Analysis of Experiments*, 8th. Arizona, 2013, pp. 642–679, ISBN: 9781119113478.

[131] A. G. Bajpayee and A. J. Grodzinsky, "Cartilage-targeting drug delivery: can electrostatic interactions help?" Tech. Rep., 2017.

[132] A. Vedadghavami, E. K. Wagner, S. Mehta, T. He, C. Zhang, and A. G. Bajpayee, "Cartilage Penetrating Cationic Peptide Carriers for Applications in

Drug Delivery to Avascular Negatively Charged Tissues," *Acta Biomaterialia*, vol. 93, pp. 258–269, 2019.

[133] Y. Dong, Y. Dong, Q. Xu, G. Hu, and W. Dong, "The effect of varying degrees of radial meniscal tears on the knee contact stresses: A finite element analysis," *Advanced Materials Research*, vol. 304, no. July 2011, pp. 135–141, 2011.

[134] L. C. Tsai, E. S. Cooper, K. M. Hetzendorfer, G. L. Warren, Y. H. Chang, and N. J. Willett, "Effects of treadmill running and limb immobilization on knee cartilage degeneration and locomotor joint kinematics in rats following knee meniscal transection," *Osteoarthritis and Cartilage*, vol. 27, no. 12, pp. 1851–1859, 2019.

[135] N. J. Willett, T. Thote, A. S. Lin, S. Moran, Y. Raji, S. Sridaran, H. Y. Stevens, and R. E. Guldberg, "Intra-articular injection of micronized dehydrated human amnion/chorion membrane attenuates osteoarthritis development," *Arthritis Research and Therapy*, vol. 16, no. 1, 2014.

[136] L. Kou, S. Xiao, R. Sun, S. Bao, Q. Yao, and R. Chen, "Drug Delivery Biomaterial-engineered intra-articular drug delivery systems for osteoarthritis therapy Biomaterial-engineered intra-articular drug delivery systems for osteoarthritis therapy," 2019.

[137] E. Horisawa, K. Kubota, I. Tuboi, K. Sato, H. Yamamoto, H. Takeuchi, and Y. Kawashima, "Size-Dependency of DL-Lactide/ Glycolide Copolymer Particulates for Intra-Articular Delivery System on Phagocytosis in Rat Synovium," *Pharma*, vol. 19, no. 2, 2002.

[138] R. Liggins, W. L. H. , T. Cruz, W.Min, L. Liang, and H. M. Burt, "Intra-articular treatment of arthritis with microsphere formulations of paclitaxel: biocompatibility and efficacy determinations in rabbits," *Inflammation Research*, vol. 53, pp. 365–372, 2004.

[139] D. Y. Park, B. H. Min, D. W. Kim, B. R. Song, M. Kim, and Y. J. Kim, "Polyethylene wear particles play a role in development of osteoarthritis via detrimental effects on cartilage, meniscus, and synovium," *Osteoarthritis and Cartilage*, vol. 21, no. 12, pp. 2021–2029, 2013.

[140] H. E. Kloefkorn and K. D. Allen, "Quantitative histological grading methods to assess subchondral bone and synovium changes subsequent to medial meniscus transection in the rat," *Connective Tissue Research*, vol. 58, no. 3-4, pp. 373–385, 2017.

[141] P. P. Srinivasan, S. Y. Mccoy, A. K. Jha, W. Yang, X. Jia, M. C. Farach-Carson, C. B. Kirn-Safran, and C. Kirn-Safran, "Injectable Perlecan Domain 1-Hyaluronan Microgels Potentiate the Cartilage Repair Effect of BMP2 in a Murine Model of Early Osteoarthritis," *Biomed Materials*, vol. 7, no. 2, p. 24 109, 2012.

[142] M. Saravanan, K. Bhaskar, G. Maharajan, & Kalathil, and S. Pillai, "Development of gelatin microspheres loaded with diclofenac sodium for intra-articular administration," *Journal of Drug Targeting*, vol. 19, no. 2, pp. 96–103, 2011.

[143] S. E. A. Gratton, P. A. Ropp, P. D. Pohlhaus, J. C. Luft, V. J. Madden, M. E. Napier, and J. M. Desimone, "The effect of particle design on cellular internalization pathways," *PNAS*, vol. 105, no. 33, pp. 11 613–11 618, 2008.

[144] L. C. Zanetti-Domingues, C. J. Tynan, D. J. Rolfe, D. T. Clarke, and M Martin-Fernandez, "Hydrophobic Fluorescent Probes Introduce Artifacts into Single Molecule Tracking Experiments Due to Non-Specific Binding) Hydrophobic Fluorescent Probes Introduce Artifacts into Single Molecule Tracking Experiments Due to Non-Specific Binding," *PLoS ONE*, vol. 8, no. 9, p. 74 200, 2013.

[145] D. Miranda, J. F. Lovell, and C. F. Jonathan Lovell, "Mechanisms of light-induced liposome permeabilization," *Bioengineering and Translational Medicine*, vol. 1, pp. 267–276, 2016.

[146] U. D. o. H. U.S. National Library of Medicine, U.S. National Institutes of Health and H. Services, *ClinicalTrials.gov*.

[147] L. S. Liang, W. Wong, and H. M. Burt, "Pharmacokinetic study of methotrexate following intra-articular injection of methotrexate loaded poly(L-lactic acid) microspheres in rabbits," *Journal of Pharmaceutical Sciences*, vol. 94, no. 6, pp. 1204–1215, 2005.

[148] L. Bédouet, L. Moine, F. Pascale, V. N. Nguyen, D. Labarre, and A. Laurent, "Synthesis of hydrophilic intra-articular microspheres conjugated to ibuprofen and evaluation of anti-inflammatory activity on articular explants," *International Journal of Pharmaceutics*, vol. 459, no. 1-2, pp. 51–61, 2014.

[149] M. L. Kang, J. E. Kim, and G. I. Im, "Thermoresponsive nanospheres with independent dual drug release profiles for the treatment of osteoarthritis," *Acta Biomaterialia*, vol. 39, pp. 65–78, 2016.

[150] E. Teeple, G. D. Jay, K. A. Elsaid, and B. C. Fleming, “Animal models of osteoarthritis: Challenges of model selection and analysis,” *AAPS Journal*, vol. 15, no. 2, pp. 438–446, 2013.

[151] T. Thote, A. S. Lin, Y. Raji, S. Moran, H. Y. Stevens, M. Hart, R. V. Kamath, R. E. Guldberg, and N. J. Willett, “Localized 3D analysis of cartilage composition and morphology in small animal models of joint degeneration,” *Osteoarthritis and Cartilage*, vol. 21, no. 8, pp. 1132–1141, 2013.

[152] G. E. Salazar-Noratto, C. C. Nations, H. Y. Stevens, and R. E. Guldberg, “Localized Osteoarthritis Disease-Modifying Changes due to Intra-articular Injection of Micronized Dehydrated Human Amnion/Chorion Membrane,” *Regenerative Engineering and Translational Medicine*, vol. 5, no. 2, pp. 210–219, 2019.

[153] B. Shoelson, *createCirclesMask.m*, 2020.

[154] N. G. Zhegalova, S. He, H. Zhou, D. M. Kim, and M. Y. Berezin, “Minimization of self-quenching fluorescence on dyes conjugated to biomolecules with multiple labeling sites via asymmetrically charged NIR fluorophores,” *Contrast Media and Molecular Imaging*, vol. 9, no. 5, pp. 355–362, 2014.